
Electronic Thesis and Dissertation Repository

12-3-2021 2:00 PM

Endothelial Dysfunction in Hindlimb Arteries of Old Sprague Dawley rats, and the Type 2 Diabetic Zucker Diabetic Sprague Dawley strain.

Andrea N. Wang, *The University of Western Ontario*

Supervisor: McGuire, John J., *The University of Western Ontario*

A thesis submitted in partial fulfillment of the requirements for the Master of Science degree in Medical Biophysics

© Andrea N. Wang 2021

Follow this and additional works at: <https://ir.lib.uwo.ca/etd>



Part of the [Circulatory and Respiratory Physiology Commons](#)

Recommended Citation

Wang, Andrea N., "Endothelial Dysfunction in Hindlimb Arteries of Old Sprague Dawley rats, and the Type 2 Diabetic Zucker Diabetic Sprague Dawley strain." (2021). *Electronic Thesis and Dissertation Repository*. 8275.

<https://ir.lib.uwo.ca/etd/8275>

This Dissertation/Thesis is brought to you for free and open access by Scholarship@Western. It has been accepted for inclusion in Electronic Thesis and Dissertation Repository by an authorized administrator of Scholarship@Western. For more information, please contact wlsadmin@uwo.ca.

Abstract

Ageing, and type 2 diabetes are associated with cardiovascular diseases and endothelial dysfunction. Endothelial dysfunction is characterized by a decline in endothelium-mediated vasodilation. In this thesis, we determined the vascular function of hindlimb arteries supplying skeletal muscle and extremities using isolated arteries and wire myography. For ageing studies, we used Sprague Dawley rats and for type 2 diabetes we used the Zucker Diabetic Sprague Dawley strain. Vasodilation of hindlimb arteries with acetylcholine were impaired in both models. However, protease-activated receptor 2 mediated vasodilation was upregulated in arteries. Evidence of non-nitric oxide mechanisms were also found in peripheral vasculature. These data suggest heterogenous mechanisms of endothelium-mediated vasodilation in hindlimb vasculature which differ between models of endothelial dysfunction.

Keywords

ageing, Type 2 diabetes, skeletal muscle, vascular tone regulation, endothelial function, protease-activated receptor 2

Summary for Lay Audience

The endothelium is a layer of cells that line the inside of our blood vessels and produces vasoactive compounds, that regulate the diameter of the vessels and blood flow. With ageing or diseases like type 2 diabetes, the endothelium undergoes a state of “endothelial dysfunction” which is characterized by a change in the production or response to vasoactive compounds. Endothelial dysfunction has been well-characterized in large arteries but has yet to be characterized in smaller blood vessels that feed the skeletal muscles of the leg or the feet. The first part of our study measured tension produced by live blood vessels in response to different drugs from old and young rats. The second part of our study compared the tension produced from blood vessels in healthy compared to a type 2 diabetic rats. This is the first study to employ the use of a new animal model of type 2 diabetes using this technique. We found that certain areas of the leg exhibit a lower magnitude of response to dilation inducing compounds. This warrants consideration in future studies on endothelial dysfunction in the hindlimb and could be beneficial to therapy development in the future.

Co-Authorship Statement

Andrea Wang conducted all experiments, data collection and analyses unless otherwise noted below.

Chapter 1.4 is derived from a summary of early and revised drafts of a manuscript describing a systematic review of the ZDSD model. This revised manuscript with minor revisions pending, is currently (Nov. 2021) being considered for publication in *Experimental Physiology*. The details of this co-authored manuscript are:

The Zucker Diabetic Sprague Dawley (ZDSD) rat: an animal model for the study of type 2 diabetes by Andrea Wang, Joselia Carlos, Graham Fraser, and John McGuire. EP-REV-2020-089947 50 pages and 72 references.

Dr. John McGuire conceived the research projects outlined in this thesis, advised, and supervised Andrea Wang on experimental design, conducting experiments, analyses and interpretation of data, the presentation of results, and the writing, editing, revising of drafts of this entire thesis.

Joselia Carlos provided technical assistance with the blood glucose monitoring, and blood vessel preparations described in the studies of Chapter 3.

Dr. Graham Fraser (Memorial University) was instrumental in the design, and conception of research questions, particularly with respect to the ZDSD model in Chapter 3.

Dr. Krishna Singh was instrumental in advising experimental design, technical assistance, data analyses and interpretation of the PCR endothelial cell gene expression array studies in Chapter 3.

Acknowledgments

I would to thank my supervisor Dr. John McGuire for recruiting me into the lab, and acting as an incredible mentor and supervisor. Your support has been invaluable, and I appreciate the multiple avenues and opportunities you have provided for me to develop as a graduate student. I am also very thankful for the members of my lab who have made this experience very fun and memorable especially during the COVID-19 pandemic. I am especially thankful for my lab mate Joselia Carlos who braved the Friday mornings to help me with blood collection and played a tremendous role in helping with experiments.

I am very thankful to have learned some molecular biology skills from Dr. Krishna Singh's lab with the help of his students, Dr. Lynn Wang, and Dr. Singh himself. I would also like to thank the technicians and caretakers from Animal Care and Veterinary Services who aided with animal husbandry and procurement of supplies. Thank you to my advisory committee of Dr. Graham Fraser, Dr. Mamadou Diop, and Dr. Krishna Singh for your continuous guidance and enthusiasm towards my research.

This thesis was supported by a Project Grant awarded to Drs. Fraser and McGuire from the Canadian Institutes of Health Research (CIHR). Technical assistance to the project was supported by a Discovery Grant awarded to Dr. McGuire by the Natural Sciences and Engineering Research Council of Canada (NSERC). Andrea Wang was a recipient of a Western Graduate Research Scholarship.

Table of Contents

Abstract.....	ii
Summary for Lay Audience.....	iii
Co-Authorship Statement.....	iv
Acknowledgments.....	v
Table of Contents.....	vi
Abbreviations and Glossary.....	ix
List of Tables.....	xi
List of Figures.....	xiii
List of Appendices.....	xv
Chapter 1.....	1
1 Introduction and Literature Review.....	1
1.1 General overview.....	1
1.1.1 Organization of the Cardiovascular system.....	1
1.1.2 Skeletal muscle perfusion and peripheral arterial disease.....	1
1.1.3 Type 2 diabetes.....	2
1.2 Endothelial function and dysfunction.....	3
1.2.1 The vascular endothelium and characterization of endothelial dysfunction.....	3
1.2.2 Endothelial dysfunction with age.....	4
1.2.3 Endothelial dysfunction with type 2 diabetes.....	5
1.3 Pharmacological pathways of interest.....	6
1.3.1 Vasoconstriction.....	6
1.3.2 Vasodilation.....	8
1.3.3 Protease-activated receptor 2.....	9
1.4 Zucker Diabetic Sprague Dawley.....	10
1.5 Thesis statement.....	14
1.5.1 Ageing study rationale.....	14
1.5.2 T2D study rationale.....	15

Chapter 2.....	17
2 The effects of ageing on endothelium function in isolated hindlimb arteries from Sprague Dawley rats	17
2.1 Abstract.....	17
2.2 Introduction.....	18
2.3 Materials and Methods.....	20
2.3.1 Animals.....	20
2.3.2 Drugs and chemicals.....	20
2.3.3 Isolation of hindlimb arteries	21
2.3.4 Isometric tension measurements with isolated rings	22
2.3.5 Data analysis	24
2.4 Results.....	25
2.4.1 Physical characteristics of rat hindlimb arterial ring segments	25
2.4.2 Selective increases in PE and U46619-mediated contractions by location of arterial segment with baseline NOS inhibition in young animals.....	26
2.4.3 Increased concentration response curves to U46619 in aged animals.....	26
2.4.4 Effects of ageing on endothelium-dependent relaxations by acetylcholine and PAR2-AP	30
2.5 Discussion.....	34
2.6 Conclusion	38
Chapter 3.....	39
3 The effects of type 2 diabetes on endothelium function in the Zucker Diabetic Sprague Dawley rat.....	39
3.1 Abstract.....	39
3.2 Introduction.....	40
3.3 Materials and Methods.....	42
3.3.1 Experimental Design.....	42
3.3.2 Wire myography experiments.....	45
3.3.3 Gene expression	48
3.3.4 Data analysis	49
3.4 Results.....	51

3.4.1	Blood glucose levels	51
3.4.2	Body mass, abdominal circumference, and heart size	53
3.4.3	Relaxations of ZDSD and SD hindlimb arteries by the endothelium-dependent agonist ACh	55
3.4.4	Relaxations of ZDSD and SD hindlimb arteries by the PAR2 activating peptide 2fLIGRLO.....	57
3.4.5	Relaxations of ZDSD and SD hindlimb by the endothelium-independent agonist SNP.....	59
3.4.6	Contraction of ZDSD and SD hindlimb by the TP receptor agonist U46619	60
3.4.7	Effects of the nonselective cyclooxygenase inhibitor indomethacin and the thromboxane A ₂ synthase inhibitor ozagrel on ZDSD and SD hindlimb arteries relaxations	64
3.4.8	Endothelial cell gene expression in ZDSD and SD aortas.....	77
3.5	Discussion.....	79
3.5.1	Endothelium-dependent response to muscarinic agonist.....	79
3.5.2	Nitric oxide pathways	80
3.5.3	PAR2 function in T2D.....	81
3.5.4	COX and thromboxane synthase inhibition.....	83
3.5.5	Aortic endothelial cell gene expression	84
3.5.6	Development of T2D and obesity	86
3.5.7	Significance of study.....	88
3.6	Conclusion	88
Chapter 4	90
4	Summary of thesis.....	90
4.1	Significance.....	91
4.2	Future work.....	92
References	95
Appendices	122
Curriculum Vitae	124

Abbreviations and Glossary

2fLIGRLO	2-furoyl-LIGRLO 2-furoyl-leucine-isoleucine-glycine-arginine-leucine-ornithine-amide
ACh	acetylcholine a muscarinic receptor ligand used to test endothelium function
AGE	advanced glycation end products
ANOVA	analysis of variance
ApoE	apolipoprotein E
AT1	angiotensin II receptor 1
BH ₄	tetrahydrobiopterin
cAMP	cyclic adenosine monophosphate
cGMP	cyclic guanosine monophosphate
Col18a1	collagen type XVIII alpha 1 chain
COX	cyclooxygenases
CRC	concentration-response curve
DAG	diacylglycerol
EDHF	endothelium-derived hyperpolarizing factors
eNOS	endothelial nitric oxide synthase in this thesis refers to NOS3 isoform
GPCR	G-protein coupled receptor
GTP	guanosine triphosphate
HbA1c	glycated hemoglobin
HFD	high fat diet in this thesis, HFD refers to diets fed to ZSD, including Purina 5SCA, Research Diet D12468, and Research Diet D12079B
IP ₃	inositol triphosphate
KIT	KIT proto-oncogene receptor tyrosine kinase
L-NAME	N(ω)-nitro-L-arginine methyl ester a substrate inhibitor of NO synthases
NADPH	nicotinamide adenine dinucleotide phosphate
NO	Nitric oxide free radical gas also referred in this thesis as NO•
PAR2	protease-activated receptor 2 proteinase-activated receptor 2
PAR2-AP	PAR2 activating peptides in this thesis, the standard single letter abbreviation for amino acids in peptide sequence are used to refer to amidated peptides unless otherwise specified
PCR	polymerase chain reaction
PDGF	platelet derived growth factor
PGF	placental growth factor
PGI ₂	prostaglandin I ₂ prostacyclin
PKA	protein kinase A
PKC	protein kinase C
Plau	plasminogen activator, urokinase
PLC	phospholipase C

RAGE	advanced end glycation receptors
SD	Sprague Dawley rat(s)
SEM	standard error of mean
sGC	soluble guanylyl cyclase
SHRSP.ZF	SHRSP.Z- <i>Lepr^{fa}</i> /IzmDmcr rat(s)
SNP	sodium nitroprusside
T2D	type 2 diabetes
TP receptor	thomboxane receptor
TXA2	thromboxane A ₂
U46619	thromboxane A ₂ mimetic
VEGF	vascular endothelial growth factor
Xdh	xanthine dehydrogenase
XO	xanthine oxidase
ZDF	Zucker Diabetic Fatty rat(s)
	obese ZDF have homozygous mutation (<i>fa/fa</i>) of the leptin receptor
ZDSD	Zucker Diabetic Sprague Dawley rat(s)

List of Tables

Table 1.1 The development of hyperglycemia in ZDSD	13
Table 2.1 Baseline blood vessel diameters, resting tension, and K ⁺ contractions in young and old rats.....	25
Table 2.2 The effects of NOS inhibition on PE and U46619 concentration-response curves in hindlimb arteries of young and old rats.	29
Table 2.3 Age-dependent effects on concentration-response curves of agonists of endothelium dependent relaxation with rat saphenous arteries and the caudal branch.	33
Table 3.1 Diet transition period of ZDSD and SD.....	43
Table 3.2 Blood glucose levels (mM) of individual SD and ZDSD rats between 15 to experimental endpoint (between 20-21 weeks of age).	52
Table 3.3 Measurements of body mass, abdominal circumference, and heart mass at the experimental endpoint (20-21 weeks of age).....	54
Table 3.4 Baseline blood vessel diameters, resting tension, and K ⁺ contractions in ZDSD and SD.	55
Table 3.5 Concentration-response curves of ACh with L-NAME in hindlimb arteries of SD and ZDSD rats.....	57
Table 3.6 Concentration-response curves of SNP with L-NAME in hindlimb arteries of SD and ZDSD rats.....	60
Table 3.7 Concentration-response curves of U46619 with L-NAME in hindlimb arteries of SD and ZDSD rats.	63
Table 3.8 Effects of indomethacin and ozagrel on 2fLIGRLO CRC in SD and ZDSD	66
Table 3.9 Effects of indomethacin and ozagrel on ACh CRC in SD and ZDSD	69
Table 3.10 Effects of indomethacin and ozagrel on SNP CRC in SD and ZDSD.....	72

Table 3.11 Endothelial cell gene expressions in ZDSD relative to SD thoracic aortas using
PCR microarray 77

List of Figures

Figure 1.1 Direct proposed mechanism of U46619-mediated contraction.	7
Figure 1.2 Mechanisms of endothelial nitric oxide production.	8
Figure 2.1 Anatomical representation of hindlimb arteries of rat.	21
Figure 2.2 Representative isometric tension recordings of arterial rings.	23
Figure 2.3 The effects of NOS inhibition on PE vasoconstriction in young SD rats.	27
Figure 2.4 The effects of NOS inhibition on U46619 vasoconstriction in young and old SD rats.	28
Figure 2.5 ACh concentration-response curves in young and old rats.	30
Figure 2.6 2fLIGRLO concentration-response curves in young and old rats.	31
Figure 2.7 The effects of NOS inhibition on ACh concentration-response curves in the distal saphenous artery and caudal branch in young rats.	32
Figure 2.8 The effects of NOS inhibition on 2fLIGRLO concentration-response curves in the distal saphenous artery and caudal branch in young rats.	32
Figure 3.1 Representation of diet protocol for ZDSD and SD.	44
Figure 3.2 Protocol for substudy 2 following KCl concentration-response curve.	47
Figure 3.3 Blood glucose of ZDSD and SD.	51
Figure 3.4 Body weight of ZDSD and SD.	53
Figure 3.5 ACh concentration-response curves in hindlimb arteries of ZDSD and SD.	56
Figure 3.6 2fLIGRLO concentration-response curves in hindlimb arteries of ZDSD and SD.	58

Figure 3.7 SNP concentration-response curves in hindlimb arteries of ZDSD and SD.	59
Figure 3.8 Normalized U46619 concentration-response curves in hindlimb arteries of ZDSD and SD.....	61
Figure 3.9 Non-normalized U46619 concentration-response curves in hindlimb arteries of ZDSD and SD.	62
Figure 3.10 2fLIGRLO concentration-response curves with indomethacin and ozagrel treatment in ZDSD and SD.....	65
Figure 3.11 ACh concentration-response curves with indomethacin and ozagrel treatment in ZDSD and SD.	68
Figure 3.12 SNP concentration-response curves with indomethacin and ozagrel treatment in ZDSD and SD.	71
Figure 3.13 Maximum ACh relaxation with indomethacin and L-NAME treatment.....	73
Figure 3.14 Maximum ACh relaxation with ozagrel and L-NAME treatment.....	74
Figure 3.15 Maximum ACh relaxation in denuded arteries.	75
Figure 3.16 Representative isometric tension recordings of ACh CRC in the saphenous artery with intact and denuded endothelium.	76
Figure 3.17 Aortic endothelial cell gene expression of ZDSD and SD.....	78
Figure 4.1 Summary of thesis	91

List of Appendices

Appendix A Targets from Endothelial Cell Biology (SAB Target List) R384	122
Appendix B Animal use protocol	123

Chapter 1

1 Introduction and Literature Review

Cardiovascular diseases are the leading cause of death globally and the World Health Organization estimates that 17.9 million people died from cardiovascular disease in 2019 (World Health Organization, 2021). Understanding how risk factors impact cardiovascular health is essential for prevention of disease and for the development of therapies. This chapter will present a description of the mechanisms involved in the regulation of vascular tone in the skeletal muscle, how they can be compromised in disease and with ageing, and rationale to measure these impairments.

1.1 General overview

1.1.1 Organization of the Cardiovascular system

The cardiovascular system is comprised of the heart and blood vessels which transport blood to different tissues of the body. Blood contains nutrients and oxygen which are supplied to different tissues within the body. Dynamic regulation of blood flow occurs through homeostatic adjustments of resistance and thereby diameter/area of vasculature. Most vasculature are comprised of multiple layers: tunica intima, tunica media and tunica adventitia; capillaries are an exception since their vessel wall is composed of a single layer of endothelial cells (endothelium) to allow for more rapid diffusion of oxygen and nutrients into adjacent tissue. The structures of blood vessels differ depending on the physiological role, the aorta for example, has a high content of elastic fibres in the tunica media to enable recoil and propagation of blood to the system. Arterioles have a large proportion smooth muscle cells in the tunica media. The adventitia is comprised of various cells such as fibroblasts, macrophages, progenitor cells, and nerves (Majesky et al., 2011).

1.1.2 Skeletal muscle perfusion and peripheral arterial disease

In healthy persons, blood is perfused to the limbs and skeletal muscles to enable mobility. The blood flow to the skeletal muscle can change in response to the tissue's needs for

oxygen (Bliss, 1998; Mackie & Terjung, 1983; Sarelius & Pohl, 2010). Skeletal muscles such as the gracilis or gastrocnemius receive more oxygen when the muscle is under active use (Bockman, 1983; Mohrman & Regal, 1988). This phenomenon has been described in humans, where skeletal muscles have higher levels of perfusion during exercise to meet the increased demand of oxygen (Hellsten et al., 2012; Saltin et al., 1998). Mechanisms of matching skeletal muscle oxygen demand during exercise are impaired in diseases such as type 2 diabetes (T2D) (Kingwell et al., 2003; Lalande et al., 2008). Decreases in oxygen perfusion are also associated with a decline in mobility with age (Adelina et al., 2019), which may lead to disability or fragility (Ferrucci et al., 2016). Another example of decline in perfusion to the limbs of the body is peripheral arterial disease. Peripheral arterial disease occurs when there is insufficient perfusion to the extremities of the body due to occlusion by atherosclerosis and increases in prevalence with age (Aronow, 2007). Plaques that develop in atherosclerosis obstruct the arterial lumen which decreases the vessel area to decrease blood flow to the extremities (Aronow, 2012; Sontheimer, 2006). Peripheral arterial disease is accompanied by pain, paresthesia, paralysis (Sontheimer, 2006), and in severe cases of critical limb ischemia may lead to lower extremity amputation (Swaminathan et al., 2014). Peripheral arterial disease increases the risk of other cardiovascular disorders such as myocardial infarction (Rossi et al., 2002) and stroke (Banerjee et al., 2010). Understanding the pathophysiological mechanisms by which the limbs are perfused is necessary to prevent comorbidities that may occur with cardiovascular disorders.

1.1.3 Type 2 diabetes

Type 2 diabetes (T2D) is a chronic and prevalent disease with characteristics of hyperglycemia, hyperinsulinemia, insulin resistance, and pancreatic beta cell failure. The estimated prevalence of type 2 diabetes worldwide is 417 million persons, representing 90% of all the adults living with diabetes, and including ~232 million undiagnosed cases (S. Chatterjee et al., 2017; International Diabetes Federation, 2019). In the United States of America, 10.5% of the population is living with diabetes and 34.5% of the adult population have clinical signs of prediabetes, a condition characterized by elevated blood glucose levels with sustained sensitivity to regulation by insulin (Centers for Disease

Control and Prevention, 2020). Under euglycemic conditions, glucose homeostasis is maintained such that 80% of glucose uptake occurs in the skeletal muscle (Thiebaud et al., 1982). Therefore, the skeletal muscle is a principle determinant site of insulin sensitivity. Insulin resistance in skeletal muscle is a primary step that has been found to precede the development of hyperglycemia or pancreatic beta cell failure (DeFronzo & Tripathy, 2009; Lillioja et al., 1988; Warram, 1990). Primary prevention is one priority strategy to reduce morbidity and mortality associated with T2D (Blaslov et al., 2018). Determining the mechanistic impacts of hyperglycemia on blood flow to skeletal muscles will help to identify therapeutic targets for the comorbidities found in T2D.

1.2 Endothelial function and dysfunction

1.2.1 The vascular endothelium and characterization of endothelial dysfunction

The vascular endothelium is comprised of a single layer of endothelial cells and constitutes the innermost lining of all vasculature. The normal endothelium has several roles in homeostasis, from control of thrombosis and thrombolysis, platelet interaction, and regulation of cell proliferation and angiogenesis (Galley & Webster, 2004).

Quiescent endothelial cells generate an anti-thrombotic surface for blood to transit through the vascular system (Rajendran et al., 2013). The endothelium also plays a major physiological role in the regulation of blood flow. In 1980, Robert F. Furchgott and John V. Zawadzki found that isolated preparations of rabbit aorta required the presence of endothelial cells in order to induce vasodilation of the vessel (Furchgott & Zawadzki, 1980). Numerous vasoactive factors and mechanisms have since been identified involving the vascular endothelium (Sandoo et al., 2015; Triggle et al., 2012).

Dysfunction of the endothelium is present in cardiovascular and metabolic disorders (Galley & Webster, 2004; Rajendran et al., 2013) from atherosclerosis (Davignon & Ganz, 2004; Gimbrone & García-Cardena, 2016), hypertension (Brandes, 2014; Schulz et al., 2011), type 1 and 2 diabetes (De Vriese et al., 2000a; Ding & Triggle, 2005; Hadi & Al Suwaidi, 2007) among others. In all cases, the physiological roles of a healthy endothelium are reduced or undergo dysfunction, thus termed “endothelial dysfunction”.

A loss of normal endothelial function has several consequences and predisposes atherogenesis and thrombosis (Davignon & Ganz, 2004; Rajendran et al., 2013). Endothelial dysfunction is characterized by an imbalance of factors which produce vasoconstriction and vasodilation (Rachel L. Matz & Andriantsitohaina, 2003; Tang & Vanhoutte, 2010). For example, endothelial dysfunction is often described with a decrease in the bioavailability of nitric oxide (NO) (Incalza et al., 2018; Tang & Vanhoutte, 2010; Versari et al., 2009). Nitric oxide is produced by endothelial nitric oxide synthase (eNOS aka NOS3) in the endothelium and diffuses to the adjacent smooth muscle to induce smooth muscle relaxation (Ignarro et al., 1987; Sandoo et al., 2015). Endothelial function is often quantified by the measurement of vasodilation where reduced vasodilation of a vessel indicates endothelial dysfunction (Bonetti et al., 2003).

1.2.2 Endothelial dysfunction with age

Ageing increases the risk of developing vascular disease and is associated with impaired endothelial function (Lakatta & Levy, 2003; North & Sinclair, 2012; Triggle et al., 2012). Reduced endothelial-dependent vasodilation has been found in humans with *in vivo* (Egashira et al., 1993) and *ex vivo* techniques (Hatake et al., 1990). Furthermore, several animal models have demonstrated reduced endothelial-mediated vasodilation with age (Brandes et al., 2005); arteries in mice (Blackwell et al., 2004; Donato et al., 2011; Lesniewski et al., 2009), pigs (Murohara et al., 1991), rabbits (Chinellato et al., 1991), conduit arteries (Barton et al., 1997; Luttrell et al., 2020), and resistance arteries of rats (Arribas et al., 1997; Muller-Delp et al., 2002; Woodman et al., 2002). Subsequently, studies have reported decreased eNOS expression and NO production with age (Barton et al., 1997; Csiszar et al., 2002; Tschudi et al., 1996), and decreased NO bioavailability has been proposed as a potential mechanism for endothelial dysfunction with age. However, an increase in eNOS expression has also been found (Van Der Loo et al., 2000), albeit it is suggested as a compensatory mechanism. Increase in oxidative stress is another potential contributing factor in ageing. Increases in a reactive oxygen species, specifically superoxide anion, can interact with NO to form peroxynitrite and uncouple eNOS (Csiszar et al., 2002; Van Der Loo et al., 2000). Other potential mechanisms of endothelial dysfunction with ageing have been reviewed and detailed (Brandes et al.,

2005). *Ex vivo* techniques have also been used to assess the reversal of endothelial dysfunction in ageing animals with physical activity or pharmacological intervention (Durrant et al., 2009; Gaertner et al., 2020; Gómez-Zamudio et al., 2015; M. B. Harris et al., 2010; Wong et al., 2006). Given this evidence, the endothelium is a potential target site to ameliorate cardiovascular risk with ageing (Versari et al., 2009).

1.2.3 Endothelial dysfunction with type 2 diabetes

Cardiovascular disease is the largest cause of morbidity and mortality for people living with T2D (S. Chatterjee et al., 2017; Hudspeth, 2018; Sowers, 2013). Hyperglycemia, an excessive level of glucose in the bloodstream (e.g. levels greater than 13.3mM, (American Diabetes Association, 2021)) affects vascular health in T2D. Reduced endothelial-mediated vasodilation has been observed in rats (Oltman et al., 2008; Pereira et al., 2017; Sakamoto et al., 1998), mice (Lagaud et al., 2001; Pannirselvam et al., 2006; Park et al., 2008), and humans (Johnstone et al., 1993; Mokhtar et al., 2016; O'Driscoll et al., 1999) presenting with T2D. However, preserved endothelial function has also been reported in T2D rats (Zucker Diabetic Fatty rats) (Bohlen and Lash 1995), and T1D (Enderle et al., 1998) and T2D patients (Szerafin et al. 2006). Like ageing, T2D commonly presents with increased levels of reactive oxygen species or increased oxidative stress which is the primary mechanisms proposed for endothelial dysfunction with hyperglycemia (Hadi and Al Suwaidi 2007; De Vriese et al. 2000). Oxidative stress in T2D is associated with an increase in the expression of cyclooxygenases (COX) which are increased in coronary arterioles of T2D patients (Szerafin et al., 2006). COX modulate vascular tone by producing prostacyclin (PGI₂, vasodilation) and thromboxane A₂ (TXA₂, vasoconstriction) (Matsumoto et al., 2007; Vanhoutte et al., 2005). Heterogeneity in the production of these vasoactive factors may underlie the heterogeneity observed in endothelial function with T2D. Another mechanism of endothelial dysfunction in T2D is through the formation of advanced glycation end (AGE) products. AGEs are a heterogenous group of products from nonenzymatic reaction between reducing sugars and proteins, lipids, or nucleic acids (Negre-Salvayre et al., 2009; Vlassara, 1997). AGE can influence vascular homeostasis in a number of a different ways (Stirban et al., 2014) however, most notably they may bind to receptors for

AGE (RAGE) which can induce proinflammatory signalling with increased oxidative stress (Bierhaus et al., 2005). Vascular endothelial cells incubated with AGE or AGE modified proteins have demonstrated suppression of eNOS function (Xu et al., 2005) and endothelial intracellular Ca^{2+} storage (Naser et al., 2013). Circulating levels of glycosylated hemoglobin (HbA1C) is a surrogate biomarker for AGE production and is used as an early marker for a prediabetic state (Guo et al., 2014; Lyons & Basu, 2012).

Insulin has demonstrated vasodilatory effects in the brachial artery (Scherrer et al., 1994) and lower limbs of humans primarily in microcirculation (Baron & Brechtel, 1993; Calles-Escandon & Cipolla, 2001). Mechanisms of insulin-induced vasodilation have been primarily attributed to NO (Muniyappa & Sowers, 2013) as NO-suppression reduces muscle blood flow with hyperinsulinemia (Scherrer et al., 1994). The magnitude of vasodilation by insulin may be linked to the rate of glucose metabolism (Aljada & Dandona, 2000) and insulin resistant mice models have shown reduced NO activity (Kubota et al., 2003). Therefore, aside from hyperglycemia and other metabolic effects of insulin resistance in T2D, another consequence of insulin resistance may thereby be a decrease in endothelial mediated vasodilation.

1.3 Pharmacological pathways of interest

1.3.1 Vasoconstriction

Thromboxane A_2 (TXA₂) is a product of arachidonic acid that activates the thromboxane (TP) receptor, which is a G-protein coupled receptor (GPCR) (Tosun et al., 1998; Wilson et al., 2005) expressed in endothelial (Kent et al., 1993) and vascular smooth muscle cells (Morinelli et al., 1990). U46619 is a stable analogue of thromboxane A_2 and is the most potent agonist of TP receptor (Félétou et al., 2009). Activating the TP receptor contracts vascular smooth muscle via two GPCR pathways, G_q or $\text{G}_{12/13}$ (Ozen et al., 2020). The G_q pathway involves the increase of inositol triphosphate (IP_3) and diacylglycerol (DAG) which induces Ca^{2+} influx and activates protein kinase C (PKC) to induce contraction (Berridge, 2016). Binding of $\text{G}_{12/13}$ activates Rho/Rho-kinase to induce vasoconstriction by myosin light chain phosphorylation (Geraldès & King, 2010; Siehler, 2009). U46619 may also decrease NO production which indirectly leads to vasoconstriction (Liu et al.,

2009). However, the mechanisms of U46619-mediated vasoconstriction have shown heterogeneity depending on the species and vasculature of interest (Ozen et al., 2020; Wilson et al., 2005) (Figure 1.1).

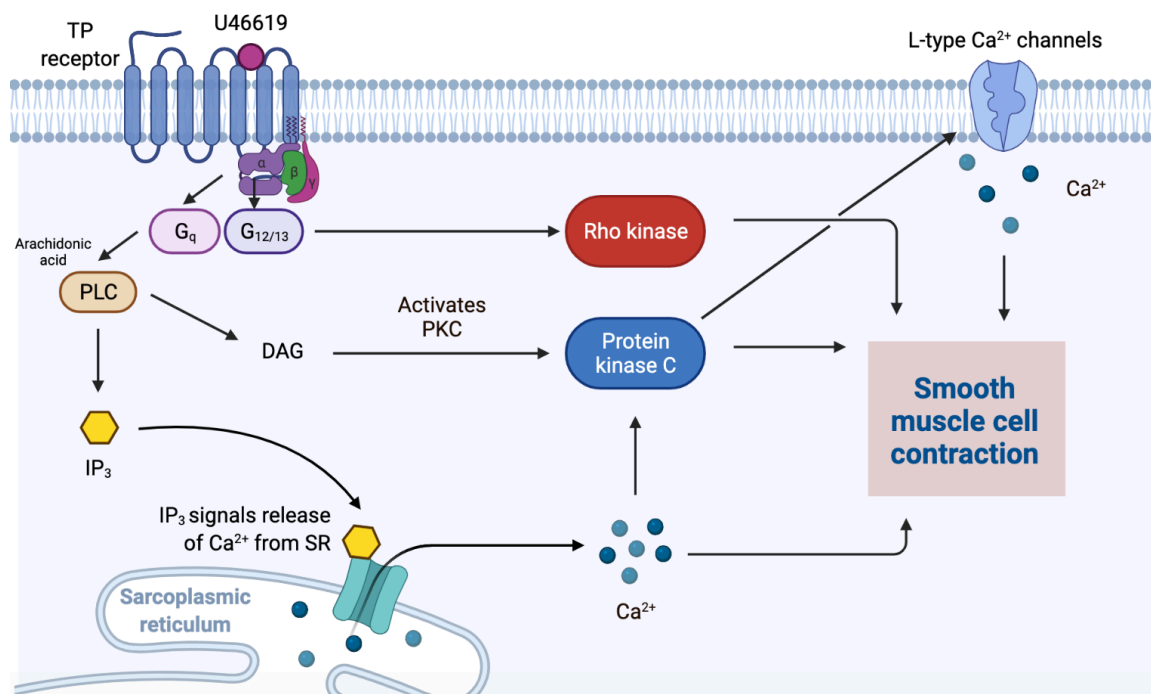


Figure 1.1 Direct proposed mechanism of U46619-mediated contraction.

Adapted from (Jiang et al., 2021; Ozen et al., 2020), image generated from Biorender.

Abbreviations: DAG, diacylglycerol; IP₃, inositol triphosphate; NO, nitric oxide; PLC, phospholipase C; PKC, Protein kinase C; SR, sarcoplasmic reticulum; TP receptor, thromboxane receptor.

1.3.2 Vasodilation

Nitric oxide protects vascular health by inhibiting the activation of platelets, decreasing adhesion of leukocytes, and modulating of vascular tone (Gimbrone & García-Cardeña, 2016). Acetylcholine, bradykinin, adenosine tri-phosphate, substance P, or thrombin can activate GPCR to activate NOS and NO production (Figure 1.2).

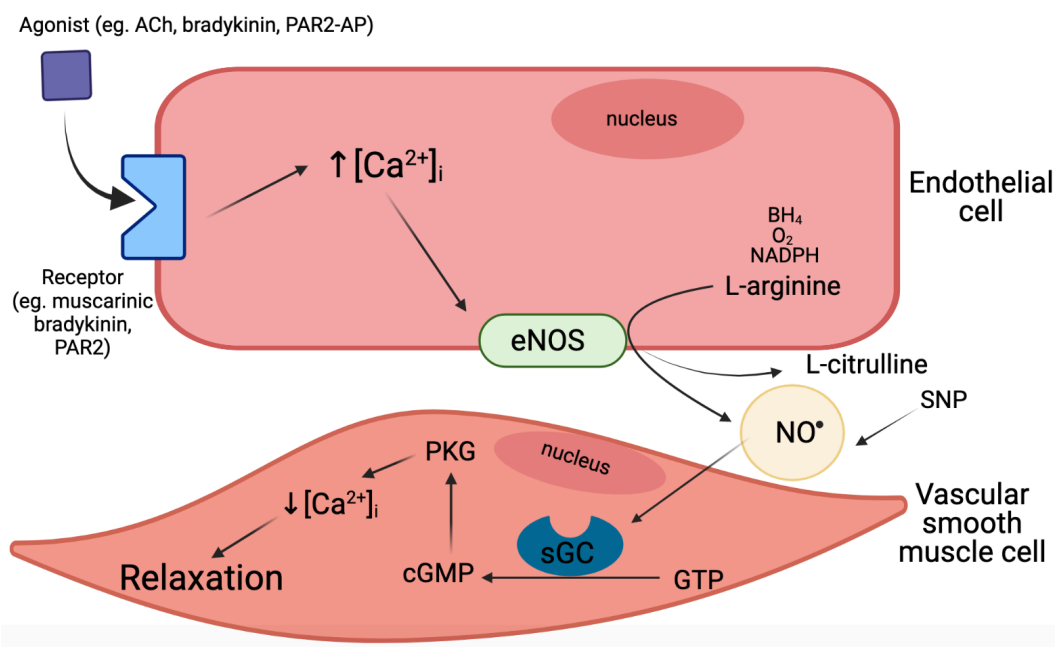


Figure 1.2 Mechanisms of endothelial nitric oxide production.

Nitric oxide production can occur by agonist-induced production such as acetylcholine (ACh), bradykinin, adenosine tri-phosphate, substance P, or thrombin (Moncada & Higgs, 2006). Signal transduction increases intracellular levels of Ca^{2+} which activate eNOS (Bucci et al., 2000). Activated eNOS converts L-arginine to NO (Palmer et al., 1988). NO diffuses to the smooth muscle cell where it binds to the enzyme soluble guanylate cyclase (sGC) (Ignarro et al., 1986). sGC converts guanosine triphosphate (GTP) to cyclic guanosine monophosphate (cGMP) which decreases cytoplasmic levels of Ca^{2+} and induces smooth muscle relaxation (Collins et al., 1986). Adapted from (Sandoo et al., 2015), image generated with Biorender.

Abbreviations: BH_4 , tetrahydrobiopterin; NADPH, nicotinamide adenine dinucleotide phosphate; SNP, sodium nitroprusside.

Prostacyclin or prostaglandin I₂ (PGI₂) is a metabolite of arachidonic acid produced at the endothelium (Félétou & Vanhoutte, 2007). The key mechanisms involve PGI₂ acting on the prostacyclin receptor (IP), which is a GPCR. G_s increases the levels of cyclic adenosine monophosphate (cAMP) and protein kinase A (PKA). Elevated levels of PKA lead to decreased [Ca²⁺] in the smooth muscle or inhibition of Rho kinase, which leads to smooth muscle relaxation and downstream vasodilation (Majed & Khalil, 2012).

Non-NO and non-prostacyclin endothelial-mediated vasodilation are attributed to endothelium-derived hyperpolarizing factors (EDHF) (Burnham et al., 2006). EDHF are a group of factors and mechanisms produced at the endothelium (epoxyeicosatrienoic acids, hydrogen peroxide, potassium ions) that hyperpolarize vascular smooth muscle cells (Luksha, Agewall, and Kublickiene 2009). The key mechanisms involve Ca²⁺-activated K⁺ channels (SK_{Ca} and IK_{Ca}) in the endothelium (Edwards et al., 2010; Luksha et al., 2009) and voltage-gated Ca²⁺ channels (McGuire et al., 2001). As a mechanism of vasodilation, EDHF increases in prominence from proximal to distal vasculature (Hill, Phillips, and Sandow 2001). EDHF as a mechanism of vasodilation may thereby be examined in smaller resistance arteries, which have a prominent role in the regulation of vascular tone.

1.3.3 Protease-activated receptor 2

Protease-activated receptor 2 (PAR2) is a GPCR found in the cell membrane of vascular endothelium (Saifeddine et al., 1996). PAR2 is endogenously activated by serine proteases, such as trypsin, and by PAR2 activating peptides (PAR2-AP), such as SLIGRL and 2-furoyl-LIGRLO (2fLIGRLO) (Al-Ani et al., 1995; McGuire et al., 2004). Serine proteases cleave PAR2 at the N-terminus to expose a tethered ligand. The tethered ligand interacts with the second extracellular loop of PAR2 to induce the activated state of the receptor (Cottrell et al., 2003; Kagota et al., 2016). PAR2 mechanisms of vascular smooth muscle relaxation involve NO and EDHF pathways (Kagota et al., 2011; McGuire et al., 2002a, 2004; Robin et al., 2003). Furthering the understanding of PAR2 in the vascular endothelium and the mechanisms by which it functions will provide insight on PAR2 as a potential therapeutic target of vascular disease.

1.4 Zucker Diabetic Sprague Dawley

The Zucker Diabetic Sprague Dawley rat (ZDSD) is an animal model developed for preclinical experimental research on T2D. Obese Sprague Dawley rats (strain CrI/CD; obese SD) were crossbred with lean Zucker Diabetic Fatty rats (ZDF) homozygous wild type for the leptin receptor (*Lepr* +/+). Selective inbreeding of the resulting offspring for more than 30 generations established the ZDSD model (Peterson et al., 2015). Male ZDSD spontaneously develop T2D (hyperglycemia where blood glucose >250 mg/dL or 13.9 mM) while fed a diet of Purina 5008 or Formulab diet consisting of 27% protein, 16% fat, and 57% carbohydrates by kcal (Table 1.1). However, when ZDSD are fed Purina 5008 alone, there is a marked heterogeneity in the time necessary to develop hyperglycemia and T2D. These reports include hyperglycemia developing later in subsets of ZDSD cohorts (Peterson et al., 2015) and a study where the majority of ZDSD fed only Purina 5008 (n=44) had not reached the threshold for significant hyperglycemia by 26 weeks, and thus were considered still prediabetic (Hutter, 2019). The age at which ZDSD develop diabetic phenotypes can be decreased by using a high fat diet (HFD) (Purina 5SCA; calories provided by 9% protein, 48.5% fat, 42.7% carbohydrate or Research Diet D12468; calories provided by: 10% protein, 48% fat, 42% carbohydrate), often referred to as a 'Western Diet' (Table 1.1). Feeding with HFD periods as short as 2 weeks can accelerate the increase of ZDSD blood glucose levels to >13.9 mM at 18 weeks of age (Davis et al., 2013; Suckow et al., 2017).

ZDSD demonstrate evidence of T2D characteristics, including hyperglycemia, hyperinsulinemia, insulin resistance, and pancreatic beta-cell failure. Insulin and glucose tolerance tests revealed that ZDSD demonstrate decreased glucose disposal and increased insulin resistance with age (L. Han et al., 2020; Peterson et al., 2015). With age, ZDSD also demonstrate significantly increased levels of glycated hemoglobin (HbA1c) (Peterson et al., 2015; Reinwald et al., 2009) which shows strong positive correlation with blood glucose concentration and reflects red blood cell exposure to glucose (Makris & Spanou, 2011; Nitin, 2010). ZDSD also present with attenuation of pancreatic beta-cell function, with lower levels of glucagon and insulin staining (L. Han et al., 2020), and

increased pancreatic mass, which may be compensatory to restore euglycemia (Reinwald et al., 2009).

ZDSD demonstrate phenotypes and comorbidities associated with T2D. Obesity is closely associated with T2D in humans and has been reported in the ZDSD at younger ages (S. Chatterjee, Khunti, and Davies 2017; Peterson et al. 2015). Body masses of ZDSD steadily increase from 7 to 21 weeks of age and reach a plateau at 23 weeks before beginning a decline (Choy et al., 2016; Davidson et al., 2014; Peterson et al., 2015). The decrease in body mass in older animals has been interpreted as evidence of T2D disease progression such as dehydration due to polyuria, muscle breakdown, and cell apoptosis (Choy et al., 2016). Visceral fat and organ weights have been compared in studies examining the obesity phenotype. Kidney, liver, heart, peritoneal, and retroperitoneal fat depot weights (normalized to body mass) were larger in ZDSD and ZDF compared to controls (nondiabetic or lean control groups) (Han et al., 2020; Reinwald et al., 2009). Other clinical deteriorations associated with human T2D and observed in the ZDSD rat include delayed wound healing, cardiomyopathy, nephropathy, and neuropathy (Davidson et al., 2014; Peterson et al., 2015; Suckow et al., 2017; Sun et al., 2018). While these impairments are closely linked to vascular and endothelial dysfunction, to this date, only one study has directly assessed endothelial function in the ZDSD; ZDSD demonstrated decreased endothelium-dependent vasodilation with ACh and calcitonin gene-related peptide in pressurized (40 mmHg) epineurial arterioles with *in vitro* video microscopy (Davidson et al., 2014).

In principle, the phenotypic and genotypic characteristics of the ZDSD model may be more advantageous for translation of preclinical findings to the clinic than the ZDF strain. Firstly, ZDSD show age-dependent and reproducible progression that qualitatively resembles prediabetic changes of blood glucose concentration and insulin sensitivity that occur in humans (Choy, de Winter, Karlsson, & Kjellsson, 2016; Han et al., 2020; Peterson et al., 2015); albeit in human T2D this progression can span decades (Bertram & Vos, 2010). In contrast, prediabetes in the ZDF strain may take place in a short time period between 5-7 weeks of age (Pick et al., 1998) since ZDF present with a rapid onset of hyperglycemia at 8-10 weeks of age (King, 2012; Shiota & Printz, 2012). Unlike the

ZDF strain ZDSD also do not carry the leptin receptor mutation (*fa/fa*). Thus, the mechanisms underlying the T2D in ZDSD may be more akin to those in humans as leptin receptor mutations are rare in humans (Davidson et al., 2014). The effects of the leptin receptor mutation are apparent in circulating concentrations of leptin. Diabetic ZDSD have fifteen-fold less circulating leptin concentrations and a 70% less insulin compared to SD rats. In contrast, ZDF have a two-fold higher leptin concentration and 44% less insulin than controls (lean ZDF) (Reinwald et al., 2009). Additionally, the leptin mutation in the ZDF model is associated with congenital skeletal defects, which may confound studies on skeletal development (Fajardo, Karim, Calley, & Bouxsein, 2014; Reinwald et al., 2009). The prediabetic condition, extended period of development of T2D, and lack of leptin mutation in the ZDSD are advantageous for studies on developmental changes with T2D such as bone turnover and skeletal development (Reinwald, Peterson, Allen, & Burr, 2009). One area of interest that has yet to be explored in the ZDSD strain is skeletal muscle glucose uptake. ZDF rats have demonstrated reduced skeletal muscle uptake with a hyperinsulinemic-glucose clamp technique (Fujimoto et al., 2004; Torres et al., 2011). The extended window of time to study prediabetes in the ZDSD merits its utilization for insight on vascular function and glucose metabolism in the skeletal muscle with T2D.

Control	Sex	HFD	Diabetic age (weeks)	Sample size (n)	Notes	Citation
SD	Male	Yes	20	12		(Bhamb et al., 2019)
None	Male	No	23	23		(Choy et al., 2016)
SD	Male	Yes	32	18		(Creecy et al., 2016)
SD	Male	Yes	34	9	Blood glucose measured at experimental endpoint	(Davidson et al., 2014)
Control diet ZDSD	Male	Yes	18	6	Blood glucose measured at experimental endpoint. Only HFD study to use Research Diet D12468.	(Davis et al., 2013)
SD	Male	Yes	13	20		(Glaeser et al., 2020)
SD	Female	Yes	32	4	Only 4/5 of the ZDSD rats became diabetic.	(Gonzalez et al., 2014)
SD	Male	Yes	30	9	Blood glucose measured at experimental endpoint.	(Hammond et al., 2014)
SD	Male	No	25	9		(Hutter, 2019)
ZDSD	Female	Yes	32	4		(Gallant et al., 2014)
SD	Male	No	21	23		(Peterson et al., 2015)
SD	Male	No	24	16		(Peterson et al., 2017)
ZDF and SD	Male	No	15	6		(Reinwald et al., 2009)
SD	Male	Yes	18	-	Unclear sample size.	(Suckow et al., 2017)
SD	Male	No	30	8		(Sun et al., 2018)

Diabetic age is the earliest age indicated by the studies when blood glucose (mean) >250 mg/dL or 13.9 mM of (n) animals. Studies that only measured blood glucose at experimental endpoint are noted.

1.5 Thesis statement

1.5.1 Ageing study rationale

Ageing is associated with increased cardiovascular risk and endothelial dysfunction (Chapter 1.2.2). In animal models, age-dependent endothelial dysfunction is well-characterized in large diameter conduit arteries such as the femoral artery. Decreased NO bioavailability has been proposed as a potential mechanism for endothelial dysfunction with age (Chapter 1.2.2). The saphenous artery and its branches feed the feet and skeletal muscle in the hindlimb; the effects of ageing on endothelium function in these vessels have yet to be elucidated. Understanding the mechanisms of endothelial function in the vasculature that supplies skeletal muscle and the periphery is essential to prevent comorbidities that occur with cardiovascular disorders (Chapter 1.1.2). To assess the endothelial function in vasculature we used various GPCR agonists to measure the vasoreactivity of the saphenous arteries and branches from aged rats (Chapter 1.2.1, Chapter 1.3). We investigated NO and non-NO mechanisms (EDHF) using a NOS inhibitor (Chapter 1.3.2). As the prominence of EDHF increases distally along the vascular tree, we also measured vasodilation in separate arterial segments in a proximal to distal fashion (Chapter 1.3.2).

Hypotheses:

The hindlimb arteries of aged Sprague Dawley (SD) rats exhibit endothelial dysfunction.

1. Vasoconstriction responses to agonists are enhanced in old animals.
2. Vasodilation responses to agonists are reduced in old animals.
3. NOS inhibition will have less potentiating effect on vasoconstrictors in old than in young animals. Agonist-stimulated NO mechanisms contribute more to the vasodilation responses of proximal arteries than the distal saphenous artery and its branches.

Aim

To characterize the vascular function of hindlimb arteries in ageing rats, where groups were young (n=32, 10-12 weeks of age) and old (n=6, 27-29 weeks of age).

1. We assessed contractility using phenylephrine (alpha-1-adrenergic receptor agonist) and U46619 (TP receptor agonist).
2. We examined endothelium-dependent mechanisms of relaxation using GPCR agonists acetylcholine (muscarinic receptor agonist) and 2fLIGRLO (PAR2-AP).
3. We assessed basal GPCR-activated and NOS contribution to vascular tone using NOS inhibitor (L-NAME).

1.5.2 T2D study rationale

T2D is characterized by hyperglycemia and higher risk of cardiovascular disease (Chapter 1.2.3). While endothelial dysfunction is well-characterized in conduit arteries and several models of T2D, the mechanisms of blood flow regulation to the skeletal muscle vasculature in T2D have not been well-studied. The skeletal muscle is the primary location for glucose uptake and a principle determinant site of insulin sensitivity and T2D disease severity (Chapter 1.1.2). Investigating the pathophysiological mechanisms of T2D on vasculature perfusing the skeletal muscle will provide insight on therapies to reduce cardiovascular risk. This is the first study focused on endothelial function in the ZDSD, a model of T2D (Chapter 1.4). To assess the endothelial function in vasculature we used various GPCR agonists to measure the vasoreactivity of the femoral, saphenous arteries, and distal branches from ZDSD (Chapter 1.2.1, Chapter 1.3). We also used inhibitors of COX and thromboxane synthase to examine the mechanisms of vasodilation in T2D and to see if impairments in vasodilation could be reversed (Chapter 1.2.3). Finally, we assessed endothelial gene expression in aortas to confirm our wire myography studies and assess endothelial functions at the genetic level.

Hypotheses

The hindlimb arteries of ZDSD rats exhibit endothelial dysfunction.

1. ACh-induced endothelium-dependent vasodilation will be reduced in ZDSD compared to age-matched controls. PAR2-dependent vasodilation will be preserved in ZDSD.
2. Endothelial-independent vasodilation capacity will not differ between ZDSD and SD.

3. The inhibition of thromboxane synthase and COX will improve agonist-elicited vasodilation in ZDSD. NOS inhibition will reduce vasodilation of arteries; NO-mediated vasodilation decreases from most proximal to distal arteries.
4. Gene expression in aorta of ZDSD will differ from controls. PAR2 gene expression will be increased in ZDSD.

Aims

To characterize the vascular function of hindlimb arteries in T2D and examine gene expression in vasculature. ZDSD (T2D group) were fed a HFD and the development of hyperglycemia was assessed. The control strain was age-matched SD (20-21 weeks of age). The study was executed as two separate cohorts of animals. These cohorts were run between January to March 2021 (substudy 1; ZDSD n=5, SD n=6) and March to June 2021 (substudy 2; ZDSD n=5, SD n=5).

1. We assessed endothelium-dependent mechanisms of relaxation using GPCR agonists ACh and 2fLIGRLO.
2. We examined endothelium-independent mechanisms of relaxation with the NO donor sodium nitroprusside (SNP).
3. We assessed the agonist-elicited vasodilation with thromboxane synthase, COX, and NOS inhibitor treatments.
4. We examined endothelial cell gene expression in aortas using a PCR microarray and quantitative real-time PCR.

Chapter 2

2 The effects of ageing on endothelium function in isolated hindlimb arteries from Sprague Dawley rats

2.1 Abstract

Ageing is associated with impaired endothelial function. Age-dependent endothelial dysfunction is well-characterized in large diameter conduit arteries such as the femoral artery. However, ageing effects on endothelial function in the connected distal blood vessels such as the saphenous artery and its branches in the hindlimb have yet to be elucidated. Our study characterizes endothelial function of rat hindlimb vasculature in young and old Sprague Dawley using GPCR agonists and nitric oxide synthase inhibition.

We isolated saphenous arteries and its caudal branches from young male (10-12 weeks of age) and old Sprague Dawley (27-29 weeks of age). We treated arterial rings with phenylephrine, U46619, acetylcholine, PAR2 agonist 2-furoyl-LIGRLO (2fLIGRLO), and nitric oxide synthase inhibitor (N(ω)-nitro-L-arginine methyl ester, L-NAME), and measured isometric tension responses by wire myography. All artery segments showed attenuated agonist-induced endothelium-dependent smooth muscle relaxation responses in old compared to young rats with one exception. L-NAME treatment increased PE and U46619-induced contractions in the more proximal saphenous arterial segments of young animals but not the distal segments.

We conclude that endothelium-mediated vasodilation of the saphenous artery and its branches were reduced in older compared to younger Sprague Dawley. However, the change in endothelium function is dependent on GPCR. Basal nitric oxide modulation of vasoconstrictor tone was decreased in old versus young groups in the saphenous artery but was not affected in its caudal branches. Our data suggest that the mechanisms underlying endothelium function of the distal segments and branches of the saphenous arteries differ from the more proximal segments.

2.2 Introduction

Ageing is associated with functional changes in the vascular endothelium of humans (North & Sinclair, 2012; Seals et al., 2011; Triggle et al., 2012). The endothelium plays an important physiological role in cardiovascular health through the regulation of thrombosis, platelet adhesion, and modulation of vascular tone and blood flow (Galley & Webster, 2004). Dysfunction of the endothelium and impairment of its homeostatic roles may occur in cardiovascular diseases such as atherosclerosis, hypertension, or naturally with age (Brandes et al., 2005; Galley & Webster, 2004). The imbalance of vasoactive agents in the endothelium and smooth muscle is a well-known characteristic of endothelial dysfunction (Rachel L. Matz & Andriantsitohaina, 2003; Tang & Vanhoutte, 2010). Indeed, ageing studies in human forearm blood vessels demonstrated impaired endothelial-mediated vasodilation with muscarinic receptor activation (DeSouza et al., 2002; Gerhard et al., 1996). Animal models of cardiovascular disease have also shown endothelial dysfunction and reduced vasodilation with ageing (Barton et al., 1997; Gragasin & Davidge, 2009; Prisby et al., 2007).

Ageing is a contributing factor to endothelial dysfunction, although the pathways underlying this dysfunction are not completely clear (Gómez-Zamudio et al., 2015). Endothelial-mediated vasodilation can be broadly categorized into NO and non-NO pathways (Hill et al., 2001). NO pathways involve the activation of eNOS. As previously described, NO• (nitric oxide free radical) produced in the endothelium diffuses from the endothelium to the adjacent vascular smooth muscle to cause vasodilation (Chapter 1.3.2). Implications of the eNOS pathway (e.g. lower eNOS expression) and decreased NO bioavailability are regarded as key processes of vasodilation which are impaired with age (Barton et al., 1997; Chennupati et al., 2013; R. L. Matz et al., 2000; Yang et al., 2009). As described in Chapter 1, the presence of NO-independent relaxation has been attributed to prostacyclin and EDHF (Duprez, 2010; Féletou & Vanhoutte, 2007). The prominence of EDHF as a mechanism of vasodilation increases in more distal or in smaller arteries (Hill et al., 2001). EDHF have been found to be either impaired or sustained in cardiovascular disorders such as hypertension, atherosclerosis, and diabetes (Luksha et al., 2009).

The hindlimb vasculature of primary interest in this study are the femoral and saphenous artery and its caudal branches. The femoral artery is a conduit artery which supplies the vascular tree of the hindlimb and therefore the skeletal muscle of the hindlimb (Kochi et al., 2013; Luttrell et al., 2020). In rodents, the femoral artery bifurcates into the popliteal and saphenous artery (Hellingman et al., 2010). The saphenous artery feeds the foot and also has branches which feed the medial thigh muscles (Kochi et al., 2013). The femoral artery has demonstrated evidence of impaired vasodilation with age in rat (Gaertner et al., 2020; M. B. Harris et al., 2010; Shi et al., 2008; Soltis, 1987) and mice (Donato et al., 2011; Lesniewski et al., 2009). Conversely, evidence of preserved vasodilation in the femoral artery with age has also been found in rats (Barton et al., 1997; Luttrell et al., 2020), dogs (Haidet et al., 1995; Kaiser & Ptui, 1992), and humans (Newcomer et al., 2005). These effects have not been explored in detail in distal hindlimb vasculature of a healthy ageing rat model (Gaertner et al., 2020; M. B. Harris et al., 2010). Similarly, the vasoreactivity of vasculature such as the saphenous artery and branches have not been explored in detail (Chennupati et al., 2013).

Protease-activated receptor 2 is a GPCR expressed by the endothelium (Al-Ani et al., 1995; Cicala, 2002). The activation of PAR2 causes endothelial-dependent relaxation of the smooth muscle and subsequent vasodilation (Cicala, 2002; Heuberger & Schuepbach, 2019; McGuire et al., 2002b). PAR2 is activated by serine proteases or by PAR2-activating peptides (PAR2-AP) such as 2-furoyl-LIGRLO-amide (2fLIGRLO) and elicits vasodilation through both nitric oxide and non-nitric oxide pathways (McGuire et al., 2004). Previous *ex vivo* studies have shown both impaired or sustained PAR2 function in vascular and metabolic disorders (Ando et al., 2018; El-Daly et al., 2018; Kagota et al., 2011). For age-related changes, PAR2-mediated responses were preserved in SHRSP.Z-Lep^{fa}/IzmDmcr (SHRSP.ZF) rat aortas with metabolic syndrome but were later shown to decrease with age (Maruyama et al., 2016, 2017). Similar decreases in PAR2-mediated responses using 2fLIGRLO were also observed in the renal arteries of SHRSP.ZF rats (Maruyama-Fumoto et al., 2021).

The aim of this study was to assess the endothelium function of hindlimb blood vessels that supply the skeletal muscle in aged Sprague Dawley. Different GPCRs of endothelial-

mediated vasodilation (ACh and 2fLIGRLO) were examined. Nitric oxide and non-nitric oxide mechanisms were examined during vasodilation and vasoconstriction with NOS inhibition. We also measured vasodilation in separate arterial segments of the saphenous artery and its branches.

2.3 Materials and Methods

2.3.1 Animals

All procedures involving animals were approved by the Institutional Animal Care Committee of Western University in accordance with guidelines and principles by the Canadian Council on Animal Care. Male Sprague Dawley rats were purchased from Charles River Laboratory (PQ). Rats were fed a standard chow diet of Prolab 3000 and provided water *ad libitum*. Housing rooms were set for 12 hr light (7 am to 7 pm) and 12 hr dark cycle (7 pm to 7 am) with a constant room temperature (20-24°C) in the Animal Care Health Sciences Facility at Western University. Animals were assigned to treatment groups: young (n=32, 10-12 weeks of age) and old (n=6, 27-29 weeks of age). On the morning of experiments, the rat was weighed and euthanized by cervical dislocation under isofluorane anaesthesia.

2.3.2 Drugs and chemicals

Unless stated otherwise, all drugs and reagents were purchased from Sigma Aldrich Canada (Oakville, ON, Canada). 2-furoyl-leu-ile-gly-arg-leu-orn (2fLIGRLO) was purchased from GenScript (Piscataway, NJ). A stock solution of 2fLIGRLO was prepared in 25 mM HEPES pH 7.4 and stored at -20 °C. U46619 was purchased from the Cayman Chemical Company (Ann Arbor, MI). The stock solution was prepared in distilled water and stored at -20 °C. Dilutions of stock drug solutions were freshly prepared the day of use or 1-4 days prior and stored in -20 °C.

2.3.3 Isolation of hindlimb arteries

As shown in Figure 2.1, the skeletal muscle of the hindlimb containing the blood vessels of interest were dissected *in situ* and immediately placed into ice-cooled Krebs buffer (114 mM NaCl, 4.7 mM KCl, 0.8 mM KH₂PO₄, 1.2 mM MgCl₂ • 6H₂O, 2.5 mM CaCl₂ • 2H₂O, 11.0 mM D-Glucose, 20 mM NaHCO₃, and 5 mM HEPES hemisodium salt). The femoral, saphenous, and caudal branch of saphenous artery were isolated from the hindlimb skeletal muscle and cleaned of surrounding fat, the femoral and saphenous nerves and veins. Each blood vessel was cut into 1-2 mm length rings and the saphenous artery was subdivided according to the distance from femoral artery into proximal, middle, and distal segments.

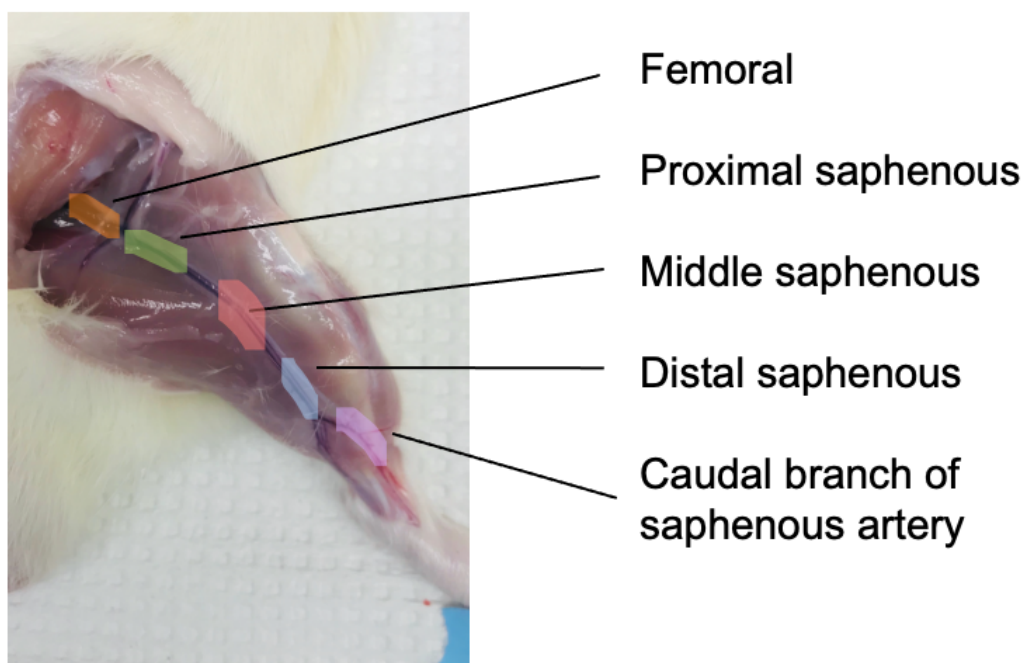


Figure 2.1 Anatomical representation of hindlimb arteries of rat.

The femoral artery (orange) is identified as the artery prior to bifurcation into popliteal and epigastric arteries. The saphenous arteries were separated into proximal (green), middle (red), and distal (blue) segments based on distance to the femoral artery. The caudal branch of the saphenous artery (purple) is one of the arteries that bifurcates off of the saphenous artery.

2.3.4 Isometric tension measurements with isolated rings

We inserted two 40 μm silver-plated tungsten wires through the lumen of each ring and mounted rings between two jaws of the myograph while suspended in chambers (DMT 620M) containing Krebs buffer (pH 7.4). One jaw was connected to a micropositioner and the other was connected to a force transducer. The chambers were filled with Krebs buffer that was continuously bubbled with 95% O_2 /5% CO_2 at 37 °C throughout the duration of the experiment. The initial resting tension of blood vessels was determined for each artery segment such that the vessels were stretched to 90% of the circumference expected to produce wall tension of 13.3 kPa (100 mmHg); this was modified from (Mulvany & Halpern, 1977). Blood vessels were held at resting tension to equilibrate for 30 min prior to the addition of any drugs. Isometric tensions of the blood vessels were recorded continuously while drugs were added directly to the baths. Cumulative concentration-response curves (CRC) were constructed for phenylephrine (PE, 1nM–10 μM), U46619 (1nM–1 μM), ACh (1nM–10 μM), and 2fLIGRLO (1nM–3 μM) in untreated (controls), and NOS inhibitor-treated arteries (L-NAME, 100 μM for 10 min prior to contraction of the arterial rings) (Barton et al., 1997; Kagota et al., 2011; Luttrell et al., 2020) (Figure 2.2). We used U46619 to produce submaximal contraction (80% of maximum) in all vessels. Specifically, we used the following concentrations of U46619: femoral artery, 0.5 μM ; proximal and middle saphenous arteries, 0.1 μM ; distal and caudal branches of saphenous artery, 0.2 μM . Following each CRC that was conducted, a 30-min washout period was applied wherein the chambers were rinsed with Krebs buffer 5 consecutive times.

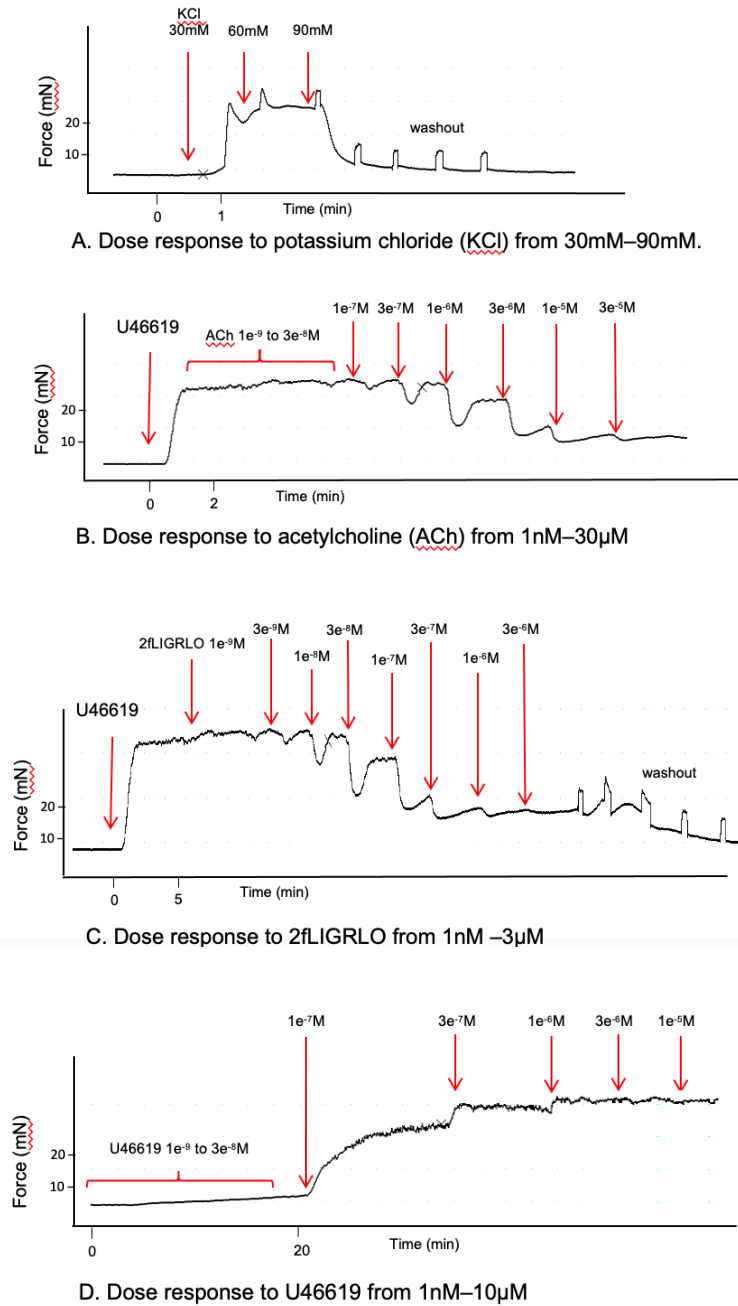


Figure 2.2 Representative isometric tension recordings of arterial rings.

Acetylcholine (B) and 2fLIGRLO (C) relaxation curves were preceded by dosing with a submaximal contraction to U46619. The five peaks following the dose response curve (seen in A,C) are the washout periods where chambers were rinsed with Krebs buffer 5 consecutive times with a 1 min waiting period in-between.

2.3.5 Data analysis

Data are reported as the mean \pm standard error of mean (SEM) unless otherwise indicated, n=number of independent experiments (rats), each with two to three replicates for each type of vessel. On the graphs (Figure 2.3 and onwards) the lines are the concentration-response curves determined by nonlinear regression curve fitting using best fit Sigmoidal dose response equations calculated with GraphPad Prism (version 9, GraphPad). For each drug, the maximum effects (E_{max}) for contraction or % relaxation were calculated directly from the responses of each arterial ring and averaged for each rat. Drug potency ($-\log EC_{50}$ where EC_{50} is the effective drug concentration (M) producing 50% of E_{max}) and Hill slope (nH) were determined from the best-fit curves for each group. E_{max} for U46619 and PE are expressed as a percentage of the contractions elicited by 90 mM KCl in the same artery.

$$\text{Contraction (\%)} = \frac{\text{tension with U46619 or PE (mN)} - \text{resting tension (mN)}}{\text{tension with 90 mM KCl (mN)} - \text{resting tension (mN)}}$$

E_{max} for relaxation by ACh and 2fLIGRLO are calculated from the reversal of the precontraction tone where 100% relaxation is a complete reversal of agonist-induced contraction.

$$\text{Relaxation (\%)} = \frac{\text{tension with U46619 (mN)} - \text{tension with ACh or 2fLIGRLO (mN)}}{\text{tension with U46619 (mN)} - \text{resting tension (mN)}}$$

Unpaired Student's *t*-test was used to compare two groups. One-way analysis of variance (ANOVA) or two-way ANOVA were used to compare more than two groups and followed by multiple comparison testing using Bonferroni post hoc tests. $p < 0.05$ were considered statistically significant.

2.4 Results

2.4.1 Physical characteristics of rat hindlimb arterial ring segments

Old (27-29 weeks) Sprague Dawley rats (663 ± 104 g, $n=32$) weighed almost two times the younger (10-12 weeks) rats (376 ± 80 g, $n=6$). Femoral arteries were almost two times greater in diameter than the caudal branches ($p<0.0001$). Interestingly, the distal portion of the saphenous artery had a diameter 1.0 to 1.1 times greater than other sections of the saphenous artery ($p<0.001$). The resting tension of the arterial rings did not differ between age groups for each vessel (Table 2.1). The contractions of arteries by 90 mM KCl were 1.1 to 1.3 times greater in old rats than young rats ($p<0.05$) with the exception of the caudal branch ($p>0.05$).

Table 2.1 Baseline blood vessel diameters, resting tension, and K⁺ contractions in young and old rats.

Artery type	Group	Vessel diameter (μm)	Resting tension (mN)	K ⁺ 90 mM contraction (mN)
Femoral	young	936 ± 93	10.7 ± 2.2	15.4 ± 3.9
Proximal	young	535 ± 70	6.9 ± 2.7	15.0 ± 4.4
	old	$609 \pm 50^*$	6.0 ± 0.8	$19.1 \pm 5.5^*$
Middle	young	559 ± 81	7.5 ± 2.7	18.4 ± 4.4
	old	$645 \pm 59^*$	6.3 ± 0.9	$21.1 \pm 3.5^*$
Distal	young	600 ± 74	6.3 ± 1.2	19.8 ± 5.0
	old	$690 \pm 76^*$	6.5 ± 0.7	$24.8 \pm 5.0^*$
Caudal branch	young	516 ± 54	4.6 ± 0.8	12.4 ± 3.3
	old	$588 \pm 41^*$	5.0 ± 0.9	12.9 ± 4.3

Data are mean \pm standard deviation of young (10-12 weeks old, $n=32$) and old (27-29 weeks old, $n=6$) Sprague Dawley rats with 1 to 2 arteries of each type from each animal. Vessel diameters are determined under conditions of baseline resting tension. Resting tension is recorded after normalization of artery rings to 0.9 IC₁₀₀ for 100 mmHg. Artery rings were 1.0-2.0 mm long. K⁺ contractions are the increase in tension by addition of 90 mM K⁺ from resting tension. * $p<0.05$ with Student's *t*-test between young and old animals.

2.4.2 Selective increases in PE and U46619-mediated contractions by location of arterial segment with baseline NOS inhibition in young animals

At baseline tension in young animals, the inhibition of NO synthase activity by L-NAME was more effective in enhancing contractions of femoral and proximal saphenous arteries than the other regions (Figure 2.3). NOS inhibition increased the maximal contractions (E_{max}) induced by PE in the femoral and proximal saphenous artery (20-40% increase in contraction as $\%K^+ 90$ mM) (Figure 2.3). U46619-mediated contractions showed similar increased maximal contractions in the proximal saphenous and middle saphenous artery (Figure 2.4). The sensitivity of these blood vessel segments ($-\log EC_{50}$) differed in the femoral and middle saphenous segments with PE and the proximal saphenous segment with U46619 (Table 2.2). The hill slopes did not differ between treatment groups ($p > 0.05$) except for in the caudal branch of the saphenous artery when contracted with U46619 ($p < 0.05$).

2.4.3 Increased concentration response curves to U46619 in aged animals

All arteries from old animals demonstrated an increased sensitivity to U46619-mediated contraction (2 to 4 times increase in EC_{50}) (Figure 2.4). Proximal saphenous arterial segments were the only segment to show an increase in maximal contractions in old animals (30% increase in contraction as $\%K^+ 90$ mM). All arteries (both NOS inhibitor treated and untreated) from old animals showed increased sensitivity to U46619-mediated contractions compared to control young animals (Table 2.2). Within the old animal group, NOS inhibition did not change any of CRC in any of the vessel segments.

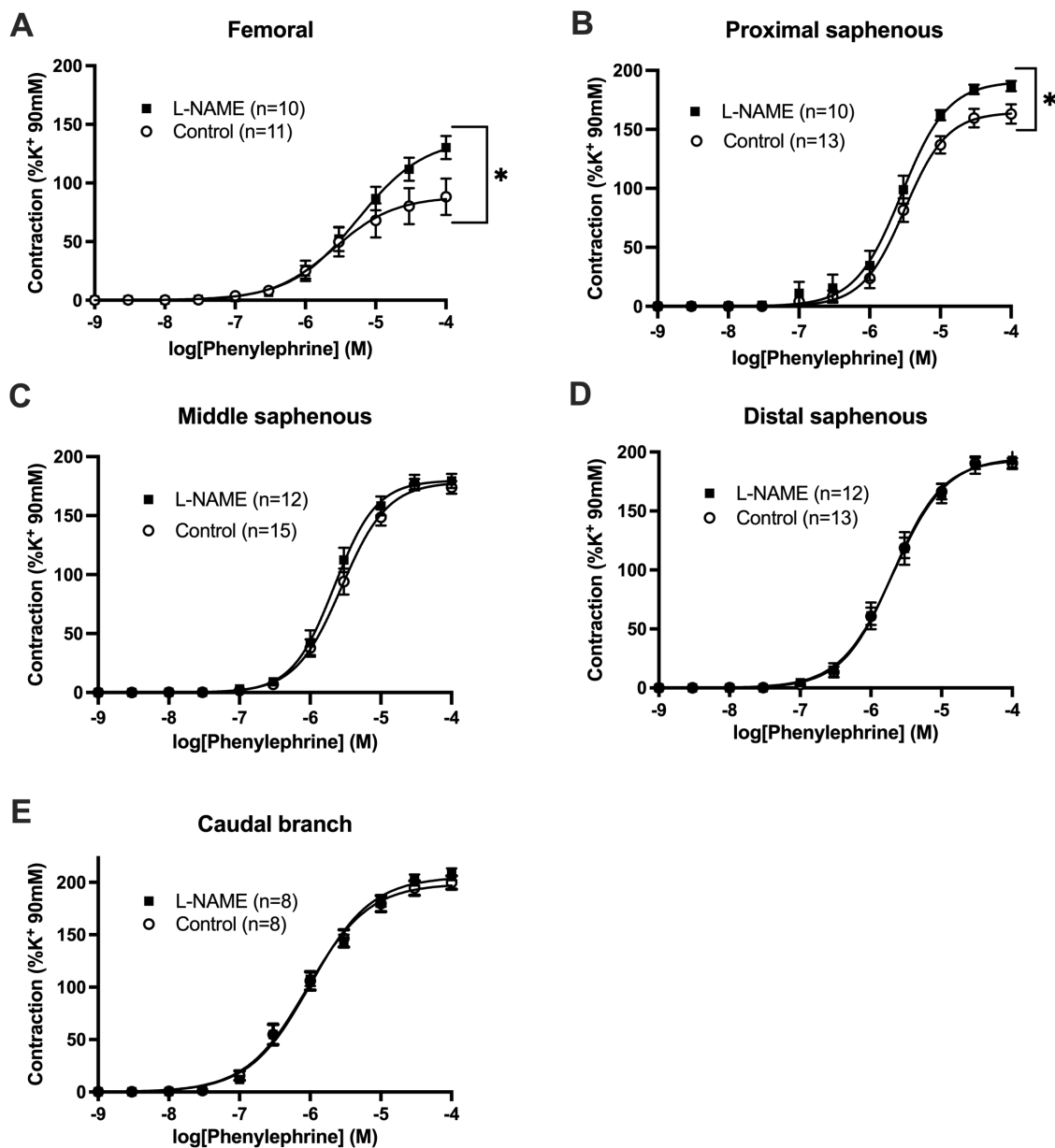


Figure 2.3 The effects of NOS inhibition on PE vasoconstriction in young SD rats. Results are expressed as mean \pm SEM of (n) animals. Lines represent best-fit four parameter Sigmoidal dose response curves. $*p < 0.05$ E_{max} with Student's *t*-test between L-NAME and control.

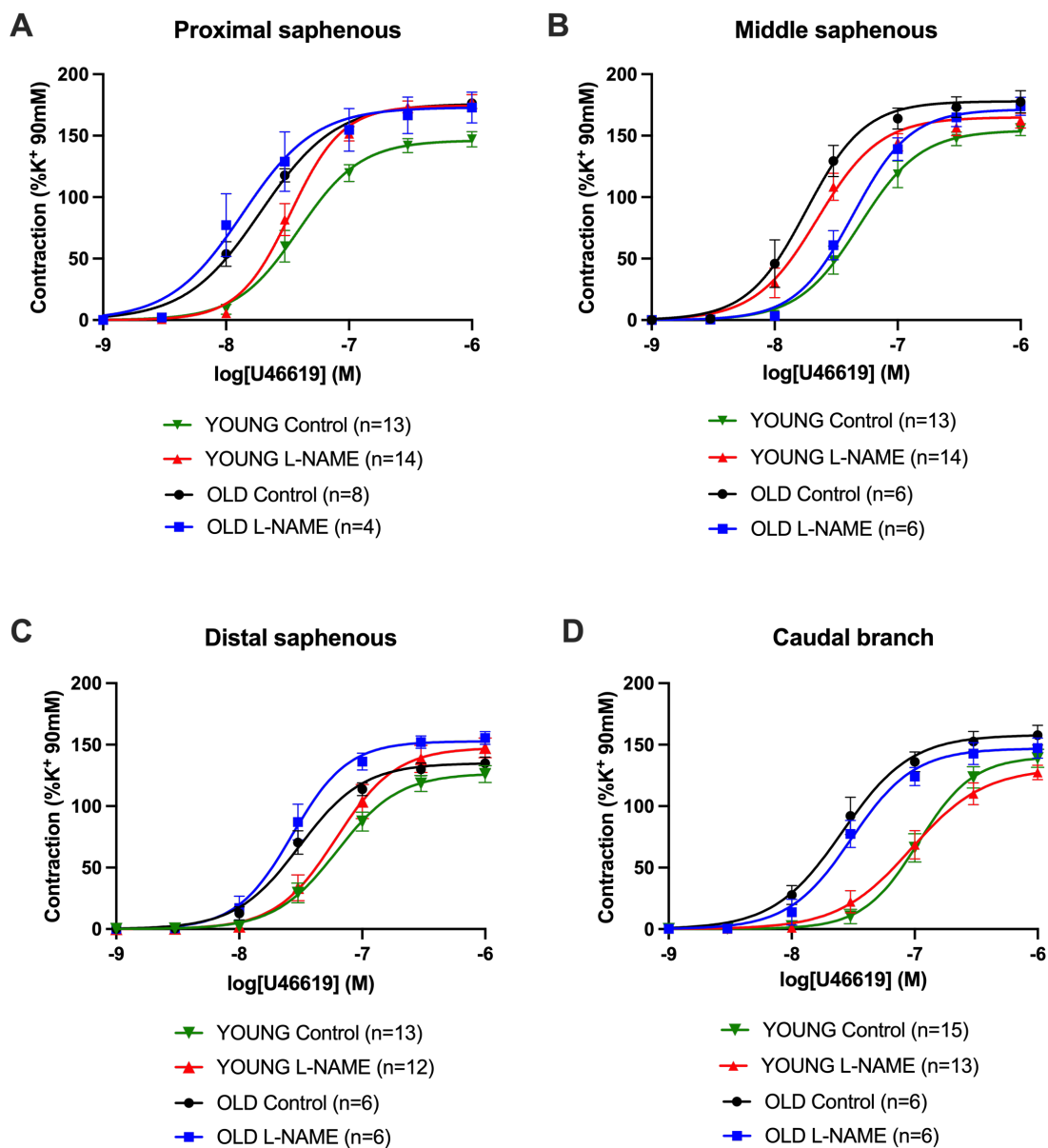


Figure 2.4 The effects of NOS inhibition on U46619 vasoconstriction in young and old SD rats.

Results are expressed as mean \pm SEM of (n) animals. Lines represent best-fit four parameter Sigmoidal dose response curves.

Table 2.2 The effects of NOS inhibition on PE and U46619 concentration-response curves in hindlimb arteries of young and old rats.

Agonist	Artery	Age group	Treatment (n)	E_{max} (%K ⁺ 90 mM)	Hill slope	$-\log EC_{50}$ (M)	
PE	femoral	young	Control (11)	88 ± 16	0.96 ± 0.05	5.58 ± 0.03	
			L-NAME (10)	130 ± 10*	0.91 ± 0.03	5.26 ± 0.03*	
	proximal	young	Control (13)	163 ± 8	1.44 ± 0.06	5.51 ± 0.02	
			L-NAME (10)	187 ± 4*	1.36 ± 0.10	5.54 ± 0.03	
	middle	young	Control (15)	176 ± 5	1.33 ± 0.06	5.56 ± 0.02	
			L-NAME (12)	179 ± 6	1.45 ± 0.05	5.66 ± 0.01*	
	distal	young	Control (13)	191 ± 4	1.22 ± 0.05	5.69 ± 0.02	
			L-NAME (12)	192 ± 7	1.16 ± 0.04	5.68 ± 0.02	
	caudal branch	young	Control (8)	200 ± 6	1.00	6.04 ± 0.03	
			L-NAME (8)	209 ± 5	1.00	6.00 ± 0.04	
	U46619	proximal	young	Control (13)	147 ± 6	1.72 ± 0.13	7.41 ± 0.02
				L-NAME (14)	178 ± 6*	2.06 ± 0.29	7.48 ± 0.03*
old			Control (4)	176 ± 2*	1.42 ± 0.15	7.72 ± 0.03*	
			L-NAME (4)	173 ± 13	1.49 ± 0.23	7.87 ± 0.05*	
middle		young	Control (13)	155 ± 5	1.74 ± 0.12	7.31 ± 0.02	
			L-NAME (14)	174 ± 7 [#]	1.86 ± 0.18	7.36 ± 0.03	
		old	Control (6)	162 ± 6	1.71 ± 0.19	7.65 ± 0.03*	
			L-NAME (6)	178 ± 9	1.82 ± 0.13	7.74 ± 0.02*	
distal		young	Control (13)	126 ± 7	1.72 ± 0.08	7.21 ± 0.02	
			L-NAME (12)	148 ± 8	1.78 ± 0.08	7.21 ± 0.02	
		old	Control (6)	135 ± 5	1.68 ± 0.15	7.51 ± 0.03*	
			L-NAME (6)	155 ± 5	1.92 ± 0.18	7.57 ± 0.02*	
caudal branch		young	Control (15)	139 ± 7	1.94 ± 0.04	6.97 ± 0.01	
			L-NAME (13)	127 ± 6	1.47 ± 0.09*	7.03 ± 0.02	
		old	Control (6)	158 ± 8	1.56 ± 0.11*	7.59 ± 0.02*	
			L-NAME (6)	147 ± 8	1.70 ± 0.16	7.52 ± 0.03*	

Data are the mean ± SEM of (n) young and old rats. E_{max} , maximum contraction response by phenylephrine or U46619; EC_{50} , molar concentration of drug producing 50% of E_{max} . EC_{50} and Hill slope are determined by nonlinear regression analyses of group data using sigmoidal dose-curve equation. * p <0.05 with ANOVA and Bonferroni post hoc test to young Control, [#] p <0.05 with unpaired Student's t-test between Control and L-NAME in same age group.

2.4.4 Effects of ageing on endothelium-dependent relaxations by acetylcholine and PAR2-AP

In aged animals, the acetylcholine induced vasodilation of hindlimb arteries decreased (E_{max}) within all examined hindlimb vasculature (Figure 2.5). The caudal branch of the saphenous artery also showed a rightward shift in ACh CRC in old animals, indicating a decrease in sensitivity (1.6 times) to ACh with age (Table 2.3, Figure 2.5D). The caudal branch of the saphenous artery showed a decline in vasodilation when relaxing with PAR2-AP 2fLIGRLO (Figure 2.6D) and the proximal segment showed a trending decline but not significant ($p>0.05$) (Figure 2.6A). The other segments (middle and distal saphenous) showed a rightward shift in the CRC (Figure 2.6B-C, Table 2.3).

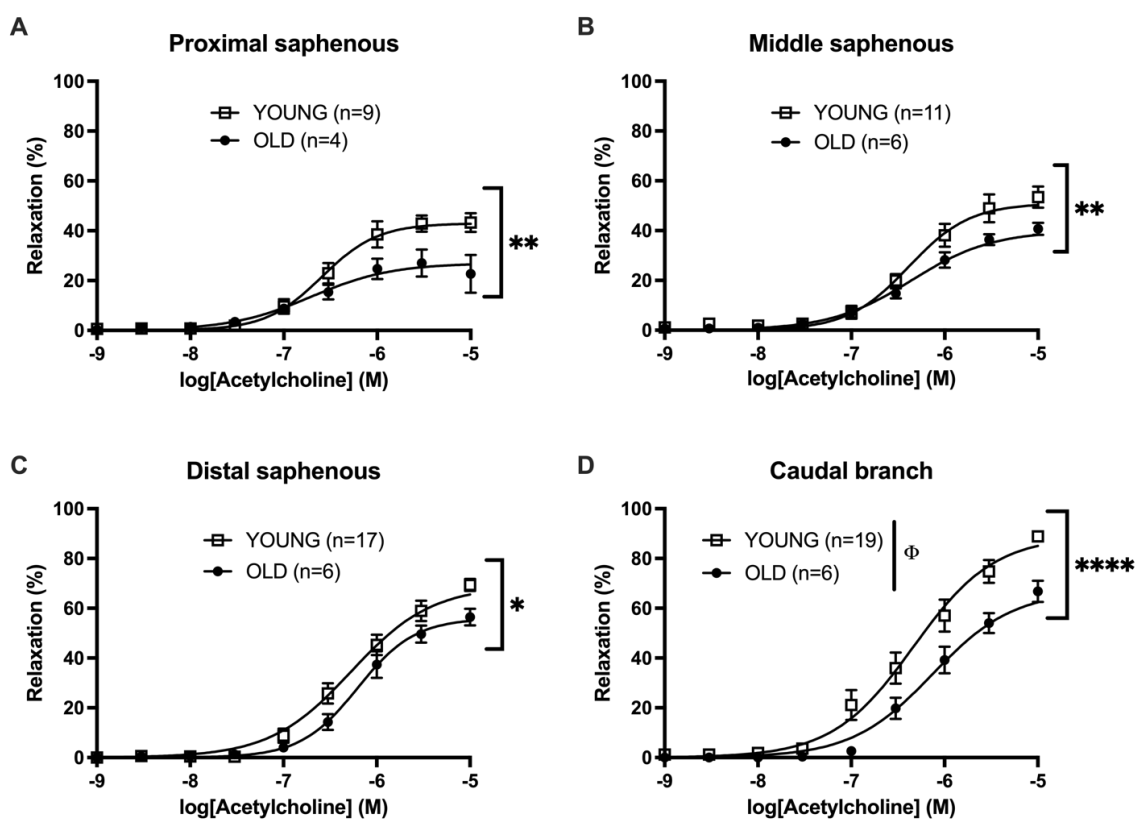


Figure 2.5 ACh concentration-response curves in young and old rats.

Results are expressed as mean \pm SEM of (n) animals. Lines represent best-fit four parameter Sigmoidal dose response curves. E_{max} and $-\log EC_{50}$ were compared between groups by Student's *t*-test. * $p<0.05$, ** $p<0.01$, **** $p<0.0001$ E_{max} ; Φ $p<0.05$ $-\log EC_{50}$.

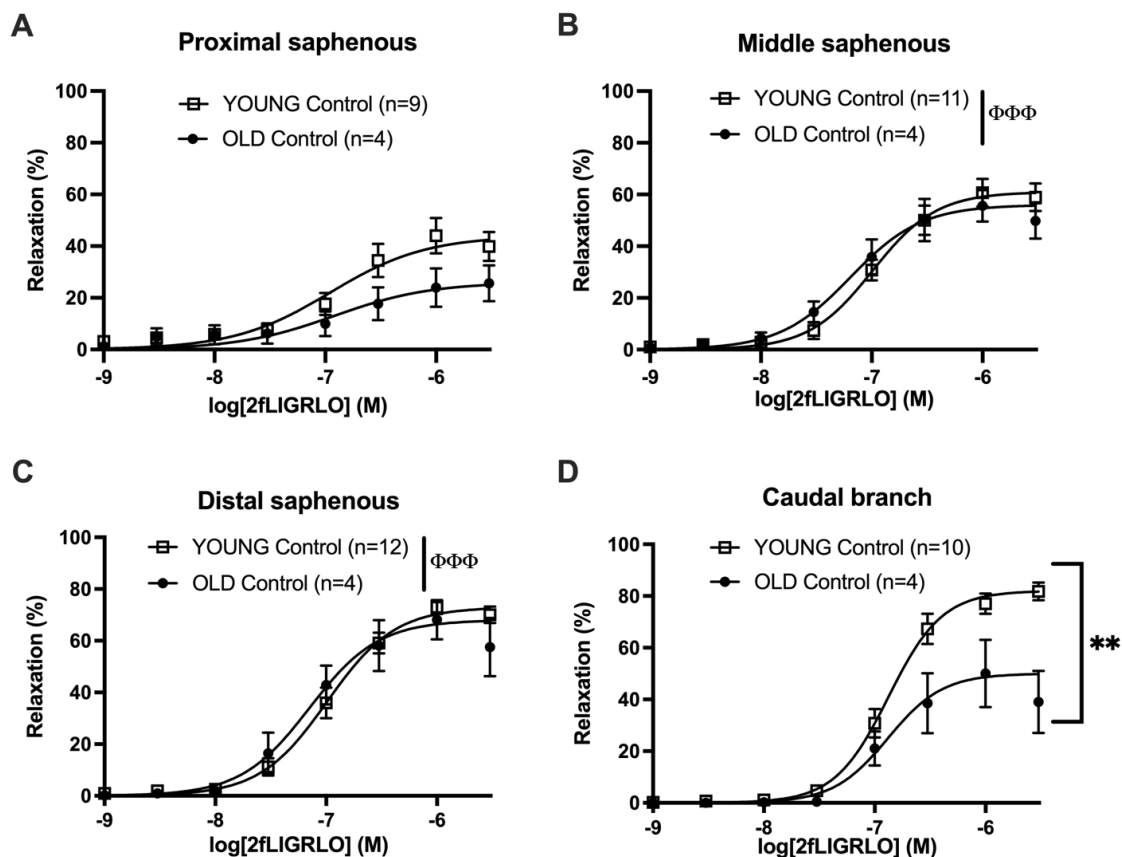


Figure 2.6 2fLIGRLO concentration-response curves in young and old rats.

Results are expressed as mean \pm SEM of (n) animals. Lines represent best-fit four parameter Sigmoidal dose response curves. E_{max} and $-\log EC_{50}$ were compared between groups by Student's *t*-test. $**p < 0.01$ E_{max} ; $\Phi\Phi\Phi p < 0.001$ $-\log EC_{50}$.

Treating the arterial segments with L-NAME abolished all ACh and 2fLIGRLO induced vasodilation in old animals (not shown). Younger animals showed residual relaxation in distal saphenous and caudal branch of the saphenous artery when treated with L-NAME prior to ACh and 2fLIGRLO relaxations. The distal saphenous artery showed reduced but residual relaxations of $28 \pm 6\%$ (n=11) and $42 \pm 5\%$ (n=9) when relaxed with the highest dose of ACh (10 μ M) and 2fLIGRLO (3 μ M) respectively (Figure 2.7A, Figure 2.8A). The caudal branch of the saphenous artery showed residual relaxations of $56 \pm 5\%$ (n=18) and $33 \pm 9\%$ (n=11) with the highest dose of ACh and 2fLIGRLO respectively (Figure 2.7B, Figure 2.8B).

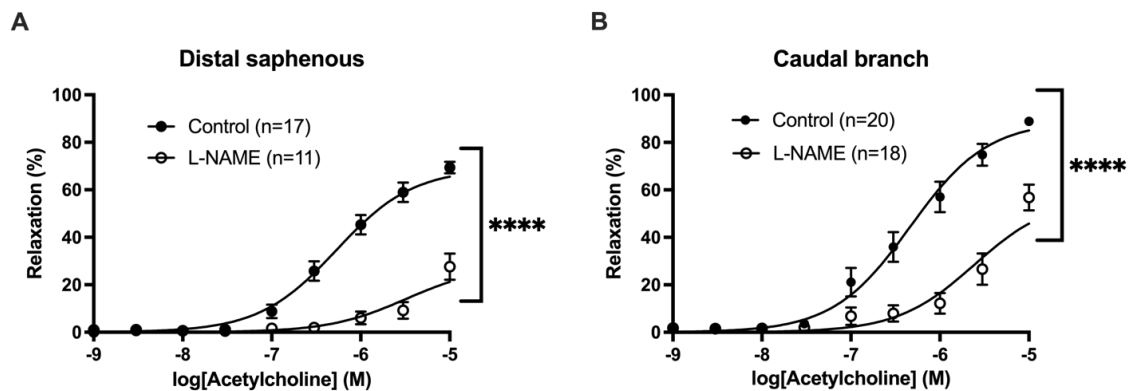


Figure 2.7 The effects of NOS inhibition on ACh concentration-response curves in the distal saphenous artery and caudal branch in young rats.

Results are expressed as mean \pm SEM of (n) animals. Lines represent best-fit four parameter Sigmoidal dose response curves. **** $p < 0.0001$ E_{max} with Student's *t*-test.

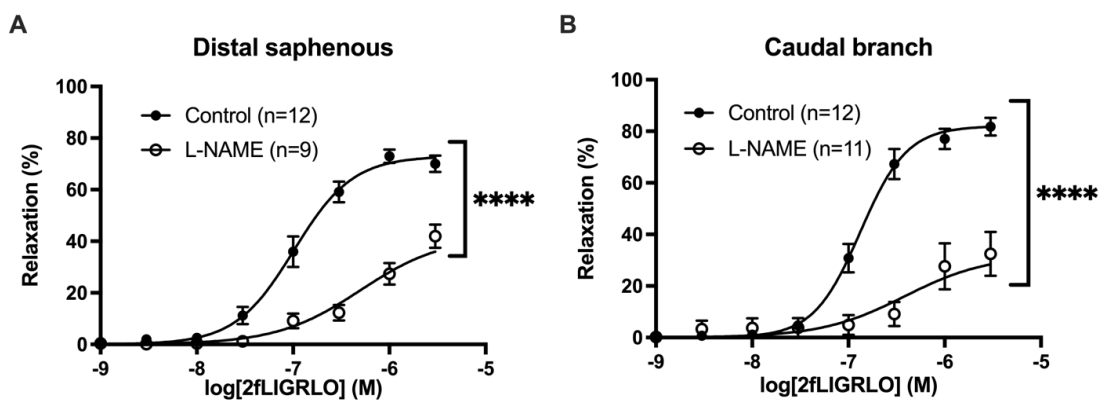


Figure 2.8 The effects of NOS inhibition on 2fLIGRLO concentration-response curves in the distal saphenous artery and caudal branch in young rats.

Results are expressed as mean \pm SEM of (n) animals. Lines represent best-fit four parameter Sigmoidal dose response curves. **** $p < 0.0001$ E_{max} with Student's *t*-test.

Table 2.3 Age-dependent effects on concentration-response curves of agonists of endothelium dependent relaxation with rat saphenous arteries and the caudal branch.

Acetylcholine					
Age group	Saphenous artery segment	n	E_{max} (%)	-logEC₅₀	Hill slope
Young	proximal	9	43 ± 4	6.59 ± 0.02	1.45 ± 0.08
	middle	11	53 ± 4	6.39 ± 0.04	1.33 ± 0.13
	distal	17	69 ± 2	6.28 ± 0.03	1.12 ± 0.07
	caudal branch	19	89 ± 2	6.33 ± 0.04	1.00
Old	proximal	4	27 ± 5*	6.71 ± 0.07	1.09 ± 0.18
	middle	6	41 ± 2*	6.35 ± 0.03	1.12 ± 0.07
	distal	6	56 ± 3*	6.20 ± 0.01	1.42 ± 0.05*
	caudal branch	6	67 ± 4*	6.13 ± 0.04*	1.00
2fLIGRLO					
Age group	Saphenous artery segment	n	E_{max} (%)	-logEC₅₀	Hill slope
Young	proximal	9	44 ± 7	6.96 ± 0.08	1.00
	middle	11	61 ± 5	6.99 ± 0.02	1.50 ± 0.10
	distal	12	73 ± 3	6.99 ± 0.02	1.42 ± 0.08
	caudal branch	10	81 ± 3	6.88 ± 0.01	1.79 ± 0.08
Old	proximal	4	26 ± 7	6.92 ± 0.10	1.00
	middle	4	56 ± 6	7.19 ± 0.01*	1.36 ± 0.05
	distal	4	68 ± 8	7.15 ± 0.02*	1.40 ± 0.09
	caudal branch	4	50 ± 13*	6.88 ± 0.03	1.76 ± 0.21

Data are the mean ± SEM of n young and old rats. E_{max}, maximum relaxation response by agonist; EC₅₀, molar concentration of drug producing 50% of E_{max}. EC₅₀ and Hill slope are determined by nonlinear regression analyses of group data using sigmoidal dose-curve equation. **p*<0.05 with unpaired Student's *t*-test between old and young.

2.5 Discussion

The main finding of this study is that ACh- and PAR2-mediated vascular smooth muscle relaxations are decreased in the hindlimb vasculature of ageing male Sprague Dawley rats (Figure 2.5, Figure 2.6). The appearance of these impaired relaxations varied depending on the GPCR and the segment vasculature. In the middle and distal saphenous arterial segments we found preserved endothelial function in response to the PAR2-AP 2fLIGRLO. We also identified non-NO pathways present in the distal hindlimb arteries of young animals based on residual relaxation in NOS inhibitor-treated vessels (Figure 2.7, Figure 2.8). Finally, this study identified that NOS inhibition increased PE- and U46619-mediated contractions in the more proximal arteries of the hindlimb (Figure 2.3, Figure 2.4).

Ageing has been demonstrated to affect endothelial function across several different levels of vasculature. Reduced endothelial-dependent vasodilation has been found in rat aorta (Barton et al., 1997; Luttrell et al., 2020), mesenteric arteries (Zhou et al., 2010), basilar arteries (Arribas et al., 1997), and feed arteries and arterioles of the soleus muscle (Muller-Delp et al., 2002; Woodman et al., 2002) when ACh or bradykinin target GPCRs. While ageing studies on hindlimb vasculature have primarily been done on the femoral artery (Gaertner et al., 2020; M. B. Harris et al., 2010), our current study is the first to demonstrate decreased vasodilation and differences in vasoreactivity within the more distal saphenous artery and its branches in the Sprague Dawley. In a previous study examining the vasoreactivity of the saphenous artery from normal ageing male and female C57BL/6 mice, the ACh-induced vasodilation did not differ between age groups (12, 34, and 64 weeks) (Chennupati et al., 2013). Differences between Chennupati et al. and our study is likely due to differences in study design; Chennupati et al. did not distinguish between segments of the saphenous artery and used phenylephrine to induce contraction prior to measuring relative relaxation.

We have also demonstrated changes in vascular reactivity with an age difference as little as 4 months. Rats reach adulthood around 10 weeks of age, during which time skeletal development continues until reaching maturity at around 7-8 months (Sengupta, 2013). Decreases in vasodilation with age has primarily been presented with a 10 to 20 month

age difference between young and old cohorts (Gómez-Zamudio et al., 2015; M. I. Harris et al., 1992; Luttrell et al., 2020; Rachel L. Matz & Andriantsitohaina, 2003; Woodman et al., 2002). The present study has primarily focused on endothelial function between a young (10-12 weeks of age) and “middle-aged” age group (27-29 weeks of age) consistent with Gaertner et al.’s age group. Our data using Sprague Dawley, a commonly used control strain in biomedical research studies, contributes to the evidence of evolving vascular pharmacology with age and variable vasoreactivity along the vascular tree, suggesting these factors are important considerations for experimental design.

The present study also demonstrates that vascular dysfunction with ageing is dependent on the GPCR. Decreased vasodilation has been associated with various disease states and attributed to endothelial dysfunction (Fujii et al., 1993; Kagota et al., 2014). PAR2-mediated vasodilation has been examined in rat models of hypertension (Ando et al., 2018; Sobey et al., 1999), diabetes (El-Daly et al., 2018; Matsumoto, Ishida, et al., 2009), obesity (Howitt et al., 2014), and other metabolic disorders (Kagota et al., 2014). In the normally ageing rat of the present study, all hindlimb vasculature showed decreased maximal response to ACh-induced vasodilation with age (Figure 2.5). However, only the caudal branch of the saphenous artery showed decreased maximal response to the PAR2 activating peptide 2fLIGRLO (Figure 2.6D). Vasodilation by PAR2 pathways and PAR2 mRNA levels are negatively correlated with serum levels of thiobarbituric acid reactive substances and thereby oxidative stress in the SHRSP.ZF, a rat model of metabolic syndrome (Maruyama et al., 2017). Increase in oxidative stress has traditionally been linked to ageing, which may attenuate PAR2-mediated vasodilation. This proposed mechanism was found in a model of metabolic disorder and to better understand PAR2 function with ageing further exploration is necessary without the influence of comorbidities.

This study also identified that the middle and distal saphenous vessel segments demonstrated increased sensitivity to PAR2 activation in the old animal (Figure 2.6B, 2.6C). Preserved function to PAR2 agonists have been previously described in the mesenteric arteries of type 2 diabetic mice (Kagota et al., 2011). In a type 2 diabetic Goto-Kakizaki rat, superior rat mesenteric arteries demonstrated upregulated vasodilation

in response to PAR2 activating peptide (SLIGRL) but downregulated response to ACh (Matsumoto, Ishida, et al., 2009). With regards to age-related changes, PAR2-mediated responses were preserved in SHRSP.ZF rat aortas with metabolic syndrome but eventually deteriorated with age (Maruyama et al., 2016, 2017). Other study designs which implemented ageing found increased sensitivity to PAR2 with the progression of the metabolic disorders (Kagota et al., 2016; Roviezzo et al., 2005). PAR2-mediated responses appear to differ according to location of vasculature of interest; in this case the responses appear to even differ within separate areas of a single vessel type. We speculate that the different responses to PAR2 activation in our ageing model may be attributed to differing physiological roles based on the location of the vessel. Depending on PAR2 agonist, biased signalling may cause selectivity of different pathways (Ca^{2+} -dependent or Ca^{2+} -independent) to induce vasodilation (P. Zhao et al., 2014). Better understanding the physiological role of PAR2 with age and cardiovascular disorders will give insight on the potential of PAR2 targeted therapies in the future.

There are many pathways (nitric oxide, EDHF, prostacyclin) by which the endothelium modulates vascular tone (Félétou & Vanhoutte, 2007; Triggle et al., 2012). In the present study, all relaxation was abolished in the femoral arteries of our study with NOS inhibition. We identified contributions of non-NO mediated relaxations in the distal saphenous and caudal branch of the saphenous artery with both muscarinic and PAR2 activation (Figure 2.7, Figure 2.8). Non-NO pathways have greater contribution to vasodilation in the smaller diameter resistance arteries with ACh and PAR2 agonists (De Vriese et al., 2000b; Huang et al., 2000; Pires et al., 2012; Shimokawa et al., 1996; Trottier et al., 2002). Non-NO mechanisms such as EDHF which occur via Ca^{2+} -activated K^+ channels, are especially apparent when NO pathways are compromised (De Vriese et al., 2000b; Duprez, 2010; Félétou & Vanhoutte, 2007; Park et al., 2008). Our data indicate contributions of non-NO pathways have a greater contribution to vasodilation in the distal vasculature of the hindlimb or peripheral vasculature. However, a handful of studies have also identified non-NO pathways in larger caliber arteries such as the aorta and main pulmonary artery in albino rats (Chen et al., 1988). There is also evidence of endothelial dysfunction in the femoral arteries of hypertensive rats occurring through loss of NO-independent pathways (Púzserová et al., 2013). There may be shifts in the balance

between non-NO and NO pathways in vasodilation dependent on disease state or animal strain, which would require further investigation.

We found the basal contribution of nitric oxide during contraction differs depending on the segment of hindlimb vasculature. Our study demonstrates that NO pathways have a greater contribution to modulation of tone during vasoconstriction with agonists of alpha-1-adrenergic and thromboxane A₂ receptors in the femoral artery and more proximal hindlimb arterial segments. The effects of NOS inhibition are not apparent in caudal branches of young animals with PE or U46619 contraction indicating lower basal contribution of NO (Figure 2.3E, Figure 2.4D). A decrease of NO function was observed when moving distally along the saphenous artery. We also found similarities in contractility to U46619 in the proximal saphenous arterial segment between old and young animals with NOS inhibition (Figure 2.4A). This similarity in maximal response to U46619 is indicative of declining NO modulation with age. When functioning normally, shear stress or agonist-induced activation causes the endothelium to release NO (Hill et al., 2001; Rubanyi et al., 1986; Tousoulis et al., 2011). Ageing is associated with an increase in reactive oxygen species which can decrease the bioavailability of NO (Finkel & Holbrook, 2000; Incalza et al., 2018; Schulz et al., 2011; Triggle et al., 2012). A previous study demonstrated a decrease in endothelial modulation of aortas during PE-mediated contractions due to ageing (Gómez-Zamudio et al., 2015). In our study, all saphenous arterial segments and the caudal branch also show increased sensitivity to U46619-mediated contractions with age. These data are consistent with previous studies which found increased U46619-mediated contractions in denuded rat pulmonary arteries (McKenzie et al., 2009) and ageing female mice (Novella et al., 2013). These data combined with the abolishment of NO-dependent relaxation in the femoral artery and proximal segments of the saphenous artery indicate a tendency for a decline in physiological contribution of NO from proximal to distal vasculature. Given the evidence of non-NO influence in peripheral vasculature, these pathways are promising targets of pharmacological interventions for cardiovascular disorders, particularly concerning peripheral arterial disease (Luksha et al., 2009).

2.6 Conclusion

The mechanisms underlying endothelium function of the distal segments and branches of the saphenous arteries differ from the more proximal segments. In spite of evidence of endothelial dysfunction in an ageing model, sections of the saphenous artery show increased sensitivity to PAR2-mediated vasodilation. Contributions of NO during both vasodilation and vasoconstriction were found to decrease in the hindlimb vasculature in a proximo-distal fashion. These findings warrant consideration for the design of future studies to understand the mechanisms underlying endothelium dysfunction.

Chapter 3

3 The effects of type 2 diabetes on endothelium function in the Zucker Diabetic Sprague Dawley rat

3.1 Abstract

Type 2 diabetes (T2D) is a prevalent disease characterized by hyperglycemia, hyperinsulinemia, insulin resistance, and pancreatic beta cell failure. Hyperglycemia can affect vascular health and specifically impair endothelial function. The skeletal muscle is the primary location for glucose uptake and a principle determinant site of insulin sensitivity and T2D disease severity. The goal of this study was to determine the effects of T2D on the endothelial function of arteries feeding hindlimb skeletal muscle and peripheral vasculature feeding the extremities.

Rat femoral, saphenous arteries, and their caudal branches were isolated from male ZDSD and age-matched Sprague Dawley (SD) (20-21 weeks of age). Isometric tension of isolated arterial rings were assessed with U46619, ACh, sodium nitroprusside (SNP), and PAR2 agonist 2-furoyl-LIGRLO-amide (2fLIGRLO) in untreated, indomethacin, and ozagrel treated vessels. We also measured endothelial cell gene expression in aorta using a PCR microarray. All arterial segments of ZDSD rats showed attenuated vasodilation to ACh but showed increased sensitivity to 2fLIGRLO-mediated vasodilation. Indomethacin and ozagrel treatments did not reverse the endothelial dysfunction in T2D. Distal vasculature exhibited evidence of non-NO mechanisms of vasodilation, and both NO and non-NO mechanisms may be impaired in T2D. Gene expression related to GPCR function, angiogenesis, apoptosis, among other functions differed between ZDSD and SD. PAR2 was upregulated in ZDSD aortas.

We conclude that endothelium-mediated vasodilation is reduced in the vasculature feeding skeletal muscle and extremities of the hindlimb of ZDSD. However, this effect is dependent on the GPCR. Mechanisms underlying endothelial dysfunction in the femoral artery differ from peripheral vasculature feeding the extremities of the hindlimb, which utilize both NO and non-NO mechanisms for relaxation.

3.2 Introduction

Type 2 diabetes (T2D) is a chronic disease with characteristics of hyperglycemia, hyperinsulinemia, and insulin resistance. Hyperglycemia with T2D affects endothelial function. In humans, and many animal models using rats and mice, reduced endothelial-mediated vasodilation is a characteristic of T2D (Lagaud et al., 2001; Mokhtar et al., 2016; O'Driscoll et al., 1999; Oltman et al., 2008; Pannirselvam et al., 2006; Park et al., 2008; Pereira et al., 2017; Sakamoto et al., 1998). The exceptions to such findings are few, but include the Zucker Diabetic Fatty rats where endothelial-mediated vasodilation was preserved (Bohlen & Lash, 1995). Moreover, the effects of hyperglycemia and T2D on the endothelium are dependent on GPCR agonists used for assessment of endothelial function (Kagota et al., 2011; Roviezzo et al., 2005). As discussed in Chapter 1, the Zucker Diabetic Sprague Dawley rat (ZDSD) is an animal model developed for preclinical experimental research on T2D. While the ZDSD strain was selected from the ZDF strain, the lack of *Lepr* deficiency in the ZDSD is distinctive. Endothelium function in the ZDSD has only been investigated in one previous study which found impaired ACh-mediated relaxation in epineurial arterioles (Davidson et al., 2014).

Endothelial dysfunction in T2D is associated with an increase in cyclooxygenases (COX) and thromboxane A₂ (TXA₂) synthase activities as well as oxidative stress (Helmersson et al., 2004; Szerafin et al., 2006). COX produce a number of arachidonic acid metabolites including prostaglandins (PGI₂, PGE₂ as examples), which have opposing vasodilator and vasoconstrictor activities, respectively. It is proposed that pathologies are due to a shift toward higher levels of vasoconstrictors. Thromboxane synthase catalyzes the conversion of intermediate arachidonic acid metabolites to the potent vasoconstrictor thromboxane A₂ (Matsumoto et al., 2007; Vanhoutte et al., 2005). Previous studies have found that the treatments with inhibitors of cyclooxygenase restored endothelial mediated vasodilation in a T2D model (Kagota et al., 2011; Matsumoto et al., 2007; Okon et al., 2003). Ozagrel is a TXA₂ synthase inhibitor that improved vasodilation in T2D in Otsuka Long-Evans Tokushima Fatty rats (Matsumoto, Takaoka, et al., 2009). Intravenous injection of ozagrel has also reduced vasoconstriction of arterioles in the retina which were elevated due to streptozotocin treatments in nonobese hyperglycemic diabetic mice

(Lee & Harris, 2008; Wright & Harris, 2008). These findings suggest ozagrel as potential drug to reverse vascular dysfunction in T2D.

Endothelial dysfunction in T2D is associated with endothelial and vascular smooth muscle gene expression. Studies on the ZDSD have primarily focused on hepatic metabolism (L. Han et al., 2020), diabetic nephropathy (Hutter, 2019; Peterson et al., 2017), obesity (Davis et al., 2013), and bone metabolism (Bhamb et al., 2019).

Endothelial cell gene expression in the ZDSD has not been studied yet.

The purpose of this study was to assess endothelium and vascular smooth muscle function during the development of T2D in the ZDSD. We assessed endothelium and vascular smooth muscle responses using *ex vivo* bioassays to measure isometric tension in isolated hindlimb arteries of male age-matched ZDSD diabetic and SD nondiabetic rats (20 to 21 weeks of age). ACh was less potent or found to cause less endothelium-dependent relaxations of arteries in ZDSD than in nondiabetic controls. Endothelium-dependent relaxation mechanisms differed between vascular segments and were dependent on the GPCR agonist; PAR2-AP 2fLIGRLO was more potent in ZDSD. We observed some changes in endothelial independent vasodilation capacity. Indomethacin and ozagrel treatments in *ex vivo* arteries did not reverse endothelial dysfunction overall, but provided insight on vasodilation pathways impaired in T2D. Endothelial cell specific gene expression in the aortas of ZDSD and SD was explored using a PCR microarray. PAR2, Placental growth factor (PGF), and Collagen type XVIII alpha 1 chain (Col18a1) expression differed between ZDSD and controls. We conclude that ZDSD exhibit endothelium dysfunction of the hindlimb vasculature. The mechanisms underlying the dysfunction warrant further study.

3.3 Materials and Methods

3.3.1 Experimental Design

Animals

All procedures involving animals were approved by the Institutional Animal Care Committee of Western University and conducted in accordance with the guidelines and principles of the Canadian Council on Animal Care. We used 11 SD and 10 ZDSD in this study. 10-week-old male SD and 15-week-old ZDSD were supplied by Charles River Laboratory Canada (PQ). Four of the ZDSD used in this study were provided for evaluation gratis by the supplier. All animals were housed in the Animal Care holding rooms for a 1-week acclimatization period upon arrival. Housing rooms are set for 12 hr light (7 am to 7 pm) and 12 hr dark cycle (7 pm to 7 am) with a constant room temperature (20-24°C) in the Animal Care Health Sciences facilities at Western University. Animals were moved to procedure rooms for blood glucose and body mass measurements and returned to holding rooms afterwards.

ZDSD are fed Purina 5008 diet (27% protein, 16% fat, and 57% carbohydrates by Kcal) (North American Lab Supply, Burlington, ON) from weaning age onwards. At 11 weeks of age, SD were transitioned over a 5-day period from a standard chow diet of Prolab 3000 to Purina 5008. We used a HFD protocol described previously (Hammond et al., 2014; Suckow et al., 2017) (Chapter 1) with modification directed by Western Animal Care Veterinarian Services as follows. At 16 weeks of age, all rats were transitioned over 6-days from Purina 5008 to Research Diet D12079B (HFD, 17% protein, 40% fat, 43% carbohydrate by Kcal) (Research Diets, New Brunswick, New Jersey). Rats were provided Research Diet D12079B from 17 to 19 weeks of age, after which rats were transitioned back to Purina 5008. The diet transition period is outline in the table below (Table 3.1). Diets and water were provided *ad libitum*. The HFD was replaced every 1-2 days as recommended by the supplier to avoid spoilage of the food.

Table 3.1 Diet transition period of ZDSD and SD

Day of transition period	Diet
1-2	75% old food, 25% new food
3-4	50% old food, 50% new food
5-6	25% old food, 75% new food
7	100% new food

ZDSD and SD were transitioned over to a new diet over a 7-day period. Rats fully received the new diet by the 7th day.

This study was executed as two separate cohorts of animals. These cohorts were run between January to March 2021 (substudy 1; ZDSD n=5, SD n=6) and March to June 2021 (substudy 2; ZDSD n=5, SD n=5), respectively. ZDSD and SD experiments were conducted in separate weeks to facilitate project management.

ZDSD and SD were housed in colony cages (2-3 per cage) with soft bedding and monitored for weight, body condition score, appearance, activity/behaviour, and dehydration twice a week. Cage bedding and environmental enrichment were changed 2 times a week in nondiabetic animals and 3-5 times for diabetic animals due to increased urine output.

The experimental endpoint for this study was the earlier date of 20-21 weeks age for diabetic ZDSD or 25 weeks of age for nondiabetic ZDSD if applicable. SD were age-matched to diabetic ZDSD. Tissue harvesting and collections were staggered such that one animal per day was used for blood vessel *in vitro* assays. In brief, on the morning of *in vitro* vessel assays, one rat from the cohort group was randomly selected for use. Body weights and blood glucose were measured as described below. Animals were moved from holding rooms and live animal procedure rooms to a separate laboratory prior to the *in vitro* assays. Abdominal circumference and body length were measured while animals were anaesthetized. Animals were euthanized under anaesthesia by decapitation.

Blood glucose measurements

We measured nonfasted blood glucose using the Contour Next Blood Glucose Meter (Ascensia Diabetes Care, Mississauga, ON) on day 5 of each study week (8:30 am-10:30 am). The procedure was conducted with the assistance of another person. One person restrained the animal and the other person carried out the procedure tasks. Briefly, the

rats in their home cages were placed under a heating lamp for 20 min to increase the visibility of superficial veins for venipuncture. Each animal was restrained in a towel then the posterolateral surface above the hock (ankle) was shaved and swabbed with Vaseline™ for visualization of the vein. The Contour Next glucose strips were inserted into the glucometer to prepare for a blood glucose reading. 25 G needles were used to puncture the lateral saphenous vein resulting in a small blood drop that was directly collected by capillary action into the glucose strip and the blood glucose was recorded. We alternated between using the left and right legs each week for blood collection. The wound was closed by applying light pressure then the area was swabbed with hydrogen peroxide. The animal was monitored for 20 min following the venipuncture procedure.

In our study we defined diabetes by hyperglycemia in the subjects. The criterion for diabetes and therefore, the conditions for meeting the first experimental end point was two consecutive blood glucose measurements >12.5 mM. This blood glucose concentration is approximately 2.5-times higher than the concentrations in ZDSD and SD at baseline as previously described by others (Peterson et al., 2015).

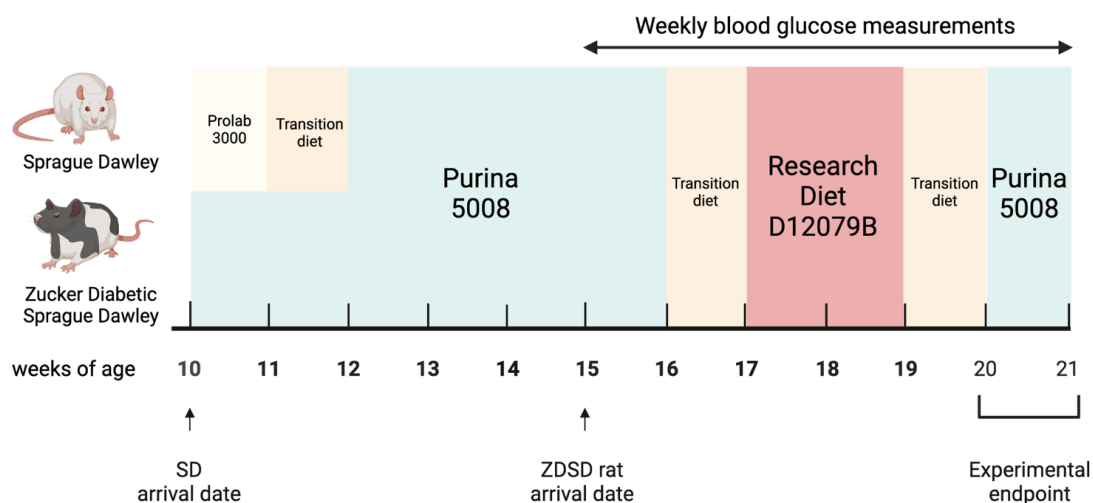


Figure 3.1 Representation of diet protocol for ZDSD and SD.

Rats were gradually transitioned from one diet to a new diet to reduce the risks of gastrointestinal upset and/or refusal to eat a new food. Transition diets took place as such: Day 1-2: 75% old food, 25% new food; Day 3-4: 50% old food, 50% new food; Day 5-6: 25% old food, 75% new food; Day 7: 100% new food. Image generated with Biorender.

Physical characteristics of ZDSD and SD

We measured the body length (cm) from the snout to the base of the tail and abdominal circumference (cm) while the subjects were anaesthetised.

Tissue harvest and collection for in vitro assays

The heart, lungs, kidneys, and descending thoracic aorta and heart were dissected *in situ* and immediately placed into iced-cooled Krebs buffer. Whole hearts were separated from the great vessels and lungs, blotted dry, and weighed. Then the heart atria were removed, and the left and right ventricles, and intraventricular septum isolated and weighed separately. Fat and connective tissues attached to whole aortas were removed by microdissection with the aid of a light microscope. The aorta was opened lengthwise then divided to tubes for protein and RNA. Tissue samples for RNA were placed in RNAlater solution according to manufacturer's instructions (Life Technologies Corporation, Burlington, ON). Heart, lung, kidney, and aorta samples for planned or future use were stored in 1.5 mL tubes in a -80 °C. Samples for future histology were stored in 10% formalin in PBS or Glycofix. The isolation and preparation of the hindlimb vessels was performed using the same methods described in Chapter 2 (Isolation of hindlimb arteries).

3.3.2 Wire myography experiments

Drugs and chemicals for in vitro bioassay studies of hind limb arteries

Similar drugs and reagents were purchased from previously described manufacturers in Chapter 2. Sodium nitroprusside (SNP) was purchased from BioBasic (Markham, ON). Indomethacin (Sigma Aldrich Canada) was dissolved in DMSO for stock solution of 100 mM and subsequent dilutions were all prepared with DMSO. Ozagrel (Sigma Aldrich Canada) was dissolved in water for stock solution of 100mM. Drug dilutions from stocks were freshly prepared the day of use or 1-4 days prior and stored at -20°C.

Buffers

Krebs buffer solution was same as described in Chapter 2.

Isolation of hindlimb arteries

The isolation of hindlimb blood vessels was the same as described in Chapter 2. The middle saphenous arterial segment was not assessed in this study. Extra hindlimb artery samples that were not used in isometric tension studies were stored in 1.5 mL tubes in a -80 °C freezer for future studies.

Isometric tension measurements with isolated rings

The setup of blood vessels was the same as described for Methods in Chapter 2. Isometric tensions of the blood vessels were recorded continuously while drugs agents were added directly to the baths.

Experiment protocol for ZDSD substudies 1 and 2

As described in Chapter 2, we constructed dose response curves for the following chemicals, drugs and agonists: KCl, U46619, ACh, SNP, and 2fLIGRLO. Based on the results of Chapter 2, we used U46619 to produce precontraction tone in the arteries. The selected doses of U46619 produced submaximal contractions of arteries (50 to 90% of E_{max}) in both ZDSD and SD. Specifically, we used the following concentrations of U46619: femoral artery and proximal saphenous artery, 30 nM; distal saphenous artery, 200 nM; caudal branches of saphenous artery, 200 nM (substudy 1) or 100 nM (substudy 2). Following each CRC that was conducted a 30-min washout period was applied wherein the chambers were rinsed with Krebs buffer 5 consecutive times.

Protocol for substudy 1

The femoral, proximal saphenous, distal saphenous, and caudal branch arterial segments were run in triplicates from each animal. One of each vessel segment was treated with L-NAME (10 mM) 10 min prior to each dose response concentration curve. The purpose of treating vessels with L-NAME was to identify the presence of NOS-independent mechanisms of vasodilation. The order of CRC was as follows: KCl (30mM–90mM), ACh (1nM–30μM), 2fLIGRLO (1nM–3μM), SNP (1nM–10μM), and U46619 (1nM–1μM).

Protocol for substudy 2

Samples of each artery type were divided to control (vehicle) and two inhibitor treatment groups (indomethacin 10 μM (Kagota et al., 2000; Vessières et al., 2010); ozagrel 10 μM (Miike et al., 2008)). Tissues were exposed to control and inhibitors for 10 min before determining the dose response curves of agonists. The order of CRC was as follows: KCl (30mM–90mM), 2fLIGRLO (1nM–3 μM), ACh (1nM–30 μM), SNP (0.1nM–10 μM).

In control groups of each artery type, near the end of the experiment, i.e. following the SNP DRC, the arterial rings were removed from the hooks and then a human hair was passed through the lumen and the ring moved along its length to mechanically disrupt the inner surface (denude arteries) before remounting the tissues under the same resting tension conditions. In inhibitor treatment groups, following the SNP DRC, the arterial rings were treated with respective inhibitors and L-NAME 10 min prior to CRC. An ACh CRC was performed in each of these rings using U46619 contracted tissues.

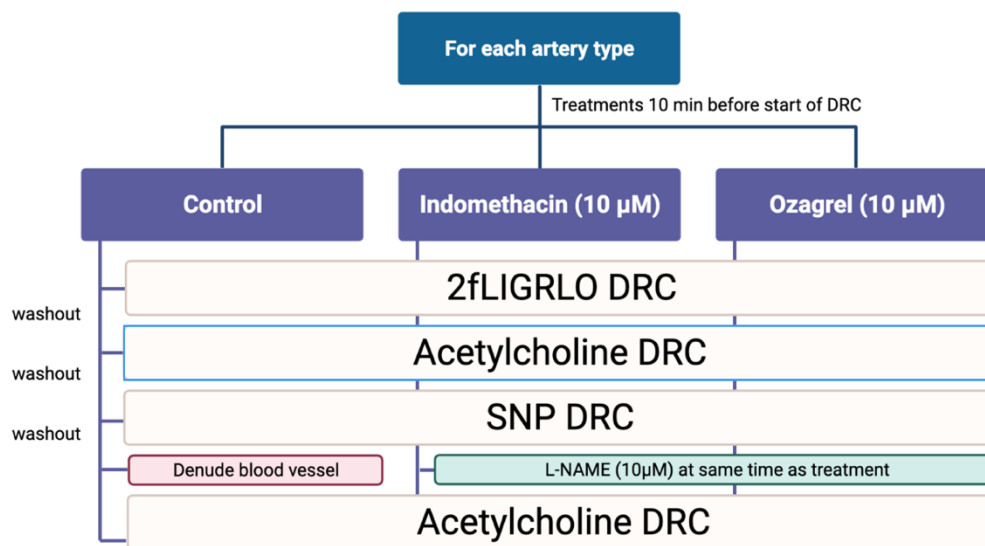


Figure 3.2 Protocol for substudy 2 following KCl concentration-response curve.

3.3.3 Gene expression

RNA isolation from aortas

Rat aortas in RNAlater solution were thawed at room temperature. Tissues were frozen with liquid N₂ and then pulverised with a mortar and pestle. The cell lysis agent TRIzol (1 mL) (Invitrogen, Carlsbad, CA), was added directly to the frozen powder then the mixture was transferred to tubes for extraction of RNA using chloroform. Chloroform (200 µL) was added to each sample which produced three visible layers (aqueous layer containing RNA, middle interphase, lower organic later with DNA and protein) after centrifugation at 4 °C and 12,000 g for 15 min. The supernatant containing the RNA (400 µL) was collected from the upper layer and then mixed with 70% ethanol (v/v) water. We used Qiagen RNeasy Mini Kit spin columns (Qiagen, Toronto, ON) to process this mixture, purifying and concentrating the RNA in 30 µL of molecular biology grade nuclease free water. The quantity and quality of the RNA was determined using 1 µL samples in replicate on a Nanodrop machine, based on optical transmission and the ratios at 260nm and 280nm. The typical yield of RNA was 0.5 to 1.5 µg per aorta with ratios 260/280 >1.8.

PCR microarray

Approximately 550 ng of RNA was used from each sample (SD, n=4; ZDSD, n=4) for cDNA synthesis. cDNA was synthesized using iScript Advanced cDNA Synthesis Kit for RT-qPCR (Bio Rad Laboratories (Mississauga, ON). cDNA synthesis reactions (40 µL volumes) were carried out at 42 °C for 30 min then 95 °C for 3 min. Subsequently, cDNA was used in 10 µL reaction volumes on 384 well PCR microarray plates, containing primers for 88 endothelial specific gene products (Endothelial Cell Biology (SAB Target List) R384 (Bio Rad, Coralville, Iowa)). The amplification protocol was 2 min at 95 °C and 41 cycles of 5 s at 95 °C and 30 s at 60 °C. cDNA was amplified using SsoAdvanced Universal SYBR Green Supermix (Bio Rad Laboratories (Canada), Mississauga, ON) on CFX Opus 384 Real-Time PCR System (Bio Rad). Data were collected from two plates and processed using the CFX Maestro Software for CFX Real-Time PCR Instruments

(Bio Rad Laboratories). PCR plates were run in series on the same day. Each plate contained samples from SD and ZDSD.

Quantitative real-time PCR

Approximately 200 ng of RNA was used to synthesize cDNA to validate the PCR microarray results. We designed qPCR primers for the gene products having the highest fold increase (*PGF*), highest fold decrease (*Col18a1*), and PAR2. Conditions for each primer set were optimized for amplification using cDNA obtained from a male SD rat (not used in study results). A single run qPCR for the selected targets and the housekeeping internal control GAPDH was performed with cDNA of aortas from 5 ZDSD and 6 SD rats with each target-sample pair measured in triplicate. As there was insufficient remaining RNA from the PCR microarray, cDNA were from the remaining ZDSD and SD (n=5 each). The synthesized cDNA was diluted 1:2.5 prior to qPCR. We performed qPCR reactions using cDNA and SsoAdvanced Universal SYBR Green Supermix (Bio Rad Laboratories (Canada), Mississauga, ON). qPCR reactions were run using a QuantStudio™ 3 Real-Time PCR System (Applied Biosystems, Foster City, California). The amplification program was 1 min at 50 °C, 30 s at 95 °C then 40 cycles of 15 s at 95 °C and 1 min at 60 °C. The oligonucleotide primers and their sequences (5'-3') used in qPCR are Rn-PGF-F (CAGCCAACATCACTATGCAG), Rn-PGF-R (TCCTCTGAGTGGCTGGTTA), Rn-Col18a1-F1 (TGAGAGTACGCAAACCCCC), Rn-Col18a1-R1 (AAAATCTCCAGATGCCCGGT), Rn-PAR2-F1 (TGCTGGGAGGTATCACCTT), Rn-PAR2-R1 (CTTTACTGTTGGGTCCCGGT).

3.3.4 Data analysis

Data are reported as the mean \pm standard deviation or standard error of mean (SEM) as applicable. n=number of independent experiments (rats). Blood glucose, basic phenotype characteristics, and baseline characteristics of blood vessels are combined results from substudies 1 and 2.

Student's *t*-test for unpaired data was used to compare phenotype and blood vessel baseline characteristics between ZDSD and SD. Blood vessel data for contraction and

relaxation responses were determined for each vessel type in replicates then averaged for each animal. For K^+ and U46619, contractions (mN) were calculated from isometric tension difference recorded between the presence of drug and baseline. Contractions by U46619 were normalized as a ratio to the contraction by 90 mM K^+ for the same vessel and are reported as (% of 90 mM K^+). Relaxation (%) is the reversal of PE or U46619 induced tension by ACh, SNP, and 2fLIGRLO i.e., 100% relaxation is a complete return to baseline tension. For each vessel type, agonist concentration-response curves were constructed. Data reported on graphs are means (symbols) and SEM (bars) of each group. E_{max} data were obtained directly from the dose responses data sets of each artery type. Dose response data were analyzed using nonlinear regression analysis of the mean data points. The lines on graphs (CRC curves) show the resulting best-fit four parameter Sigmoidal dose response curves (Prism v9, GraphPad) unless otherwise noted in figures. $-\log EC_{50}$ and Hill slope (n_H) were determined from the best-fit curve while keeping the span constant (Top = E_{max} ; Bottom = 0) as described in Chapter 2. We used one-way analysis of variance (ANOVA), or two-way ANOVA repeated measures to compare variables between three or more groups followed by multiple comparison testing using Bonferroni post hoc tests. $*p < 0.05$ were considered statistically significant.

We analyzed the data from the PCR microarray directly using CFX Maestro Software for CFX Real-Time PCR Instruments (Bio Rad Laboratories) and performed a Student's *t*-test to determine the fold-change of endothelial specific gene markers.

Quantitative PCR data were analyzed by the delta-delta Cycle threshold (Ct) method ($2^{-\Delta\Delta Ct}$) with GAPDH as the housekeeping gene (Livak & Schmittgen, 2001). Student's *t*-test for unpaired data was used to compare gene expression between ZDSD and SD.

3.4 Results

3.4.1 Blood glucose levels

ZDSD and SD blood glucose levels did not differ at 15 weeks of age. The diet change to HFD increased blood glucose levels only in ZDSD (Figure 3.3A). Almost all ZDSD rats (9/10) were deemed diabetic according to the study criterion (Table 3.2) at 19 weeks of age. At the experimental endpoint, the blood glucose of ZDSD were 4.36 times higher than controls ($p<0.001$) blood glucose levels from SD rats (Figure 3.3B). A single ZDSD (ID J, Table 3.2) did not exhibit any change in blood glucose levels throughout the study period, even up to 25 weeks of age. Subsequent data collection from ZDSD J have been excluded from the thesis.

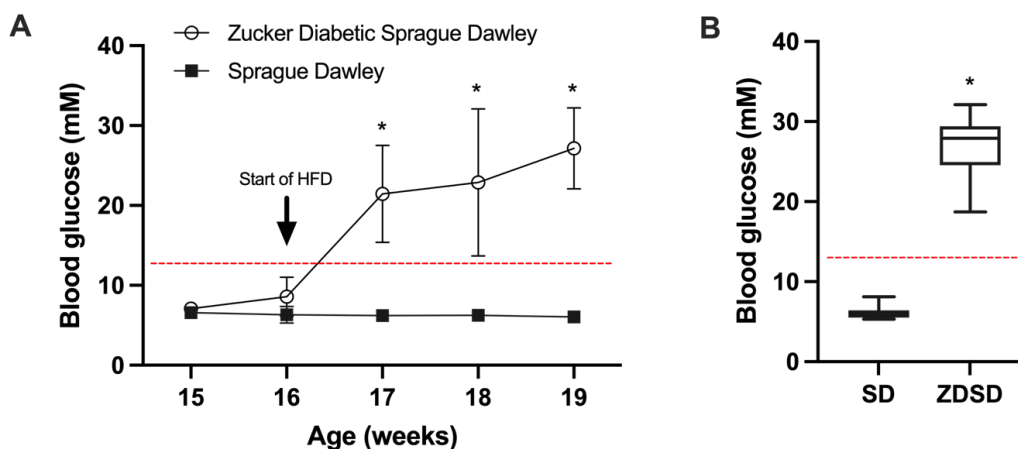


Figure 3.3 Blood glucose of ZDSD and SD.

A) Blood glucose (mean \pm standard deviation) of ZDSD (n=9) and SD (n=11) rats between 15 to 19 weeks of age taken between 8:30-10:30am at the end of the week. Red line indicates hyperglycemia threshold of blood glucose >12.5 mM. $*p<0.05$ 2-way ANOVA between ZDSD and SD at each week of blood glucose measurement. B) Blood glucose levels of ZDSD and SD rats at the time of the blood vessels experiments (20 to 21 weeks of age), box is the lower and upper quartile with median as the line, whiskers are the maximum and minimum. Red line indicates hyperglycemia threshold of blood glucose >12.5 mM. $*p<0.05$ Student's *t*-test between ZDSD and SD.

Table 3.2 Blood glucose levels (mM) of individual SD and ZDSD rats between 15 to experimental endpoint (between 20-21 weeks of age).

Strain	Animal ID	Week 15	Week 16 ^{TD}	Week 17	Week 18	Week 19 ^{TD}	Week 20	Experiment
SD	1	6.2	5.7	6.4	6.4	6.6	-	5.7
	2	6	6.2	5.6	5.3	5.7	-	5.3
	3	6.7	6.4	6.2	6.1	5.7	-	6.3
	4	7.8	8.9	6.3	6.3	5.9	-	8.1
	5	7	5.3	6.5	6.7	5.6	-	6.1
	6	6.7	6.1	6.7	6.7	5.5	-	5.5
	7	6.4	5.8	6.2	5.9	6.1	-	6.4
	8	5.8	5.8	5.6	5.9	6.2	-	5.9
	9	6.8	6.9	6.4	6.9	6.7	-	6.7
	10	7	7	6.6	6.8	6.8	-	6.3
	11	5.9	6.5	6.7	5.9	5.9	-	5.4
ZDSD	A	7.8	13.5	21.1	26	26.4	-	27.9
	C	6.1	8.4	12	9.6	23.8	20.0	24.3
	D	7.5	9.5	25.4	28	23.5	-	32.1
	E	6.6	6.8	25.9	30.8	32.9	-	29.8
	F	6.7	6.6	14.3	7	17.8	15.6	18.7
	G	7.8	7.4	16.1	17.2	28.5	-	28.4
	H	7.2	7.8	22.4	29.5	26.6	-	26.4
	I	6.8	5.9	26.1	27.4	33.3	-	24.8
	J	6.5	6.3	6.9	8	7.7	6.2	6.8
	K	7.2	11.2	29.7	30.3	31.6	27.9	29.0

^{TD} indicates transition diet from Purina 5008 to HFD.

Bold values are glucose levels >12.5 mM.

Nonfasted blood glucose was measured weekly in the morning to noon period (during 12 h light cycle). Subjects were deemed diabetic after two consecutive blood glucose measurements above 12.5 mM. Data from animal J were excluded from further study.

3.4.2 Body mass, abdominal circumference, and heart size

While both ZDSD and SD body weights increased between 15 to 19 weeks of age ($p < 0.001$) (Figure 3.4A), ZDSD and SD body weights did not differ from each other ($p > 0.05$). SD demonstrated significantly higher (1.1 times, $p < 0.05$) body weight than ZDSD at the experimental endpoint (20-21 weeks of age). ZDSD and SD had similar abdominal circumference measurements but ZDSD had shorter body length (snout to base of tail) measurements. Thereby, ZDSD demonstrated greater (1.1 times) abdominal length/body length ratio, an index of abdominal obesity (Table 3.3) (Kagota et al., 2019). ZDSD had similar total, left ventricle, right ventricle, or intraventricular septum mass to SD. However, ZDSD had higher left ventricle/total heart mass ratio (1.2 times) compared to SD (Table 3.3).

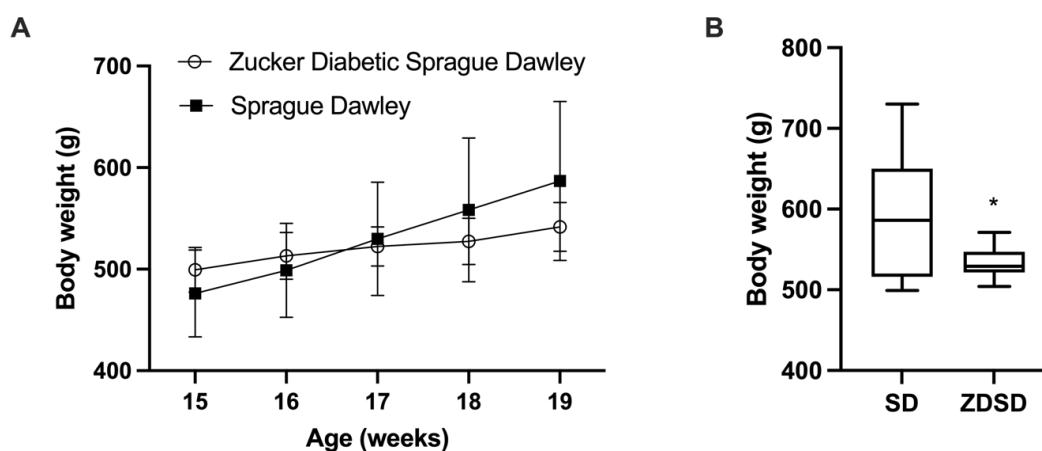


Figure 3.4 Body weight of ZDSD and SD.

A) Body weights (mean \pm standard deviation) of ZDSD (n=9) and SD (n=11) between 15 to 19 weeks of age taken at the end of the week. $*p < 0.05$ 2-way ANOVA between ZDSD and SD at each week of blood glucose measurement. B) Body weights of ZDSD and SD rats at the time of the blood vessels experiments (20 to 21 weeks of age), box is the lower and upper quartile with median as the line, whiskers are the maximum and minimum. $*p < 0.05$ Student's *t*-test between ZDSD and SD.

Table 3.3 Measurements of body mass, abdominal circumference, and heart mass at the experimental endpoint (20-21 weeks of age).

	SD (n=11)	ZDSD (n=9)
Body weight (g)	591.2 ± 76.7	533.4 ± 19.4*
Abdominal circumference (cm)	22.45 ± 2.61	23.38 ± 1.58
Body length (cm)	27.50 ± 1.51	26.00 ± 0.65*
Abdominal length/Body length ratio (cm/cm)	0.82 ± 0.07	0.90 ± 0.07*
Total heart mass (g)	1.91 ± 0.56	1.77 ± 0.16
Left ventricle mass (g)	0.72 ± 0.16	0.83 ± 0.15
Left ventricle/Total heart mass (g/g)	0.39 ± 0.08	0.47 ± 0.07*
Right ventricle mass (g)	0.52 ± 0.09	0.44 ± 0.10
Intraventricular septum mass (g)	0.33 ± 0.11	0.31 ± 0.07

Data reported are mean ± standard deviation for n = number of animals.

Measurements of abdominal circumference, body length, total heart mass, left ventricle mass, right ventricle mass, and intraventricular septum mass had a n=8 in ZDSD rats. * $p < 0.05$ with Student's unpaired *t*-test between ZDSD and SD rats.

Baseline characteristics of blood vessels from ZDSD and SD hindlimb arteries

With the exception of femoral arteries, the inner diameter of arteries at baselines did not differ between ZDSD and SD (Table 3.4). ZDSD femoral arteries were narrower than SD ($797 \pm 121 \mu\text{m}$ vs. $887 \pm 52.5 \mu\text{m}$) and accordingly, the resting tensions of ZDSD femoral rings were less than SD. Interestingly, the resting tensions of the other ZDSD arteries were higher than SD at the same diameters.

Table 3.4 Baseline blood vessel diameters, resting tension, and K⁺ contractions in ZDSD and SD.

Artery type	Strain	Vessel diameter (μm)	Resting tension (mN)	K ⁺ contractions (mN)
Femoral	SD	887 ± 52.5	8.79 ± 1.39	12.21 ± 3.10
	ZDSD	797 ± 121*	7.74 ± 1.81*	11.77 ± 2.36
Proximal saphenous	SD	526 ± 57.3	4.51 ± 1.08	12.67 ± 4.17
	ZDSD	540 ± 49.0	6.06 ± 0.93*	13.39 ± 3.96
Distal saphenous	SD	548 ± 65.4	4.83 ± 0.74	14.14 ± 4.18
	ZDSD	544 ± 47.2	5.98 ± 1.26*	16.61 ± 3.94*
Caudal branch	SD	479 ± 67.0	4.02 ± 0.88	8.07 ± 1.81
	ZDSD	473 ± 42.3	4.87 ± 0.70*	11.15 ± 2.46*

Data are mean ± standard deviation of (n=11) Sprague Dawley and (n=9) Zucker Diabetic Sprague Dawley rats with 1 to 2 arteries of each type from each animal. Vessel diameters are determined under conditions of baseline resting tension. Resting tension is recorded after normalization of artery rings to 0.9 IC₁₀₀ for 100 mmHg. Artery rings were 1.2-2.0 mm long. K⁺ contractions are the increase in tension by addition of 90 mM K⁺ from resting tension. **p*<0.05 with Student's unpaired *t*-test between ZDSD and SD rats.

3.4.3 Relaxations of ZDSD and SD hindlimb arteries by the endothelium-dependent agonist ACh

The ZDSD arteries show evidence of endothelium dysfunction characterized by less relaxation (20-25% less in femoral and caudal branch) and reduced sensitivity (3 to 10 times) to ACh when compared to SD (Figure 3.5, Table 3.5). ACh-induced relaxations of ZDSD arteries were NO-dependent as evidenced by complete inhibition of relaxations by NOS inhibitor L-NAME (Table 3.5; *p*>0.05, E_{max} L-NAME compared to 0 by one-sample *t*-test). In contrast, SD arteries exhibited partially reduced (60 to 80% of control group) relaxations in the presence of L-NAME for the distal saphenous artery (*p*<0.001)

and caudal branches ($p < 0.01$) of the saphenous artery compared to control (Table 3.5).

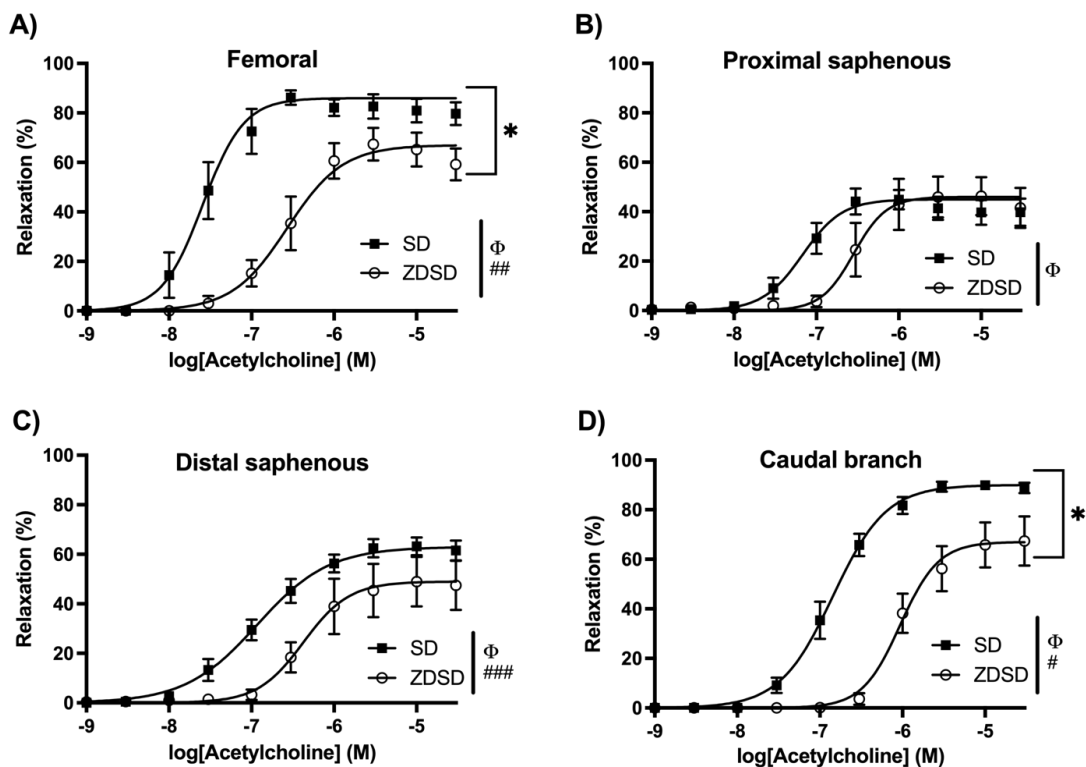


Figure 3.5 ACh concentration-response curves in hindlimb arteries of ZDSD and SD.

Arterial rings were contracted with U46619 and relative relaxation was measured in the femoral (A), proximal (B), distal (C), and caudal branch of the saphenous artery (D).

Data points are mean \pm SEM and lines represent best-fit four parameter Sigmoidal dose response curves. For each vessel type $n=6$ for SD and $n=5$ for ZDSD. E_{max} , $-\log EC_{50}$, and Hill slope were compared between groups by Student's t -test. * $p < 0.05$ E_{max} ; $^{\Phi}p < 0.001$ $-\log EC_{50}$; # $p < 0.05$, ## $p < 0.01$, ### $p < 0.001$ Hill slope.

Table 3.5 Concentration-response curves of ACh with L-NAME in hindlimb arteries of SD and ZDSD rats.

Artery type	Strain	Treatment	E _{max} (%)	Hill slope	-logEC ₅₀ (M)
Femoral	SD	Control	86.2 ± 3.0	1.76 ± 0.12	7.59 ± 0.02
		L-NAME	32.3 ± 15.1	1.00	7.11 ± 0.16
	ZDSD	Control	67.4 ± 6.6 ^a	1.29 ± 0.05 ^b	6.57 ± 0.01 ^c
		L-NAME	0	-	-
Proximal saphenous	SD	Control	39.8 ± 5.5	2.12 ± 0.43	7.25 ± 0.06
		L-NAME	0	-	-
	ZDSD	Control	46.3 ± 7.7	2.19 ± 0.34	6.55 ± 0.03 ^c
		L-NAME	0	-	-
Distal saphenous	SD	Control	63.2 ± 3.7	1.05 ± 0.05	6.93 ± 0.02
		L-NAME	13.3 ± 2.3	2.24 ± 0.30	6.11 ± 0.03
	ZDSD	Control	48.9 ± 10.0	1.56 ± 0.09 ^c	6.37 ± 0.02 ^c
		L-NAME	0	-	-
Caudal branch of saphenous	SD	Control	89.9 ± 1.9	1.34 ± 0.05	6.84 ± 0.01
		L-NAME	32.0 ± 9.2	3.51 ± 0.82	5.92 ± 0.03
	ZDSD	Control	67.4 ± 9.9 ^a	1.88 ± 0.20 ^a	6.03 ± 0.03 ^c
		L-NAME	13.6 ± 10.4	1.00	5.24 ± 0.05

Data are the mean ± SEM in SD (n=6) or ZDSD (n=5) at 20-21 weeks of age. E_{max}, maximum relaxation response by acetylcholine (ACh); EC₅₀, molar concentration of drug producing 50% of E_{max}. EC₅₀ and Hill slope are determined by nonlinear regression analyses of group data using sigmoidal dose-curve equation. Data were analyzed with Student's *t*-test between SD and ZDSD with control treatment. ^a*p*<0.05; ^b*p*<0.01; ^c*p*<0.001

3.4.4 Relaxations of ZDSD and SD hindlimb arteries by the PAR2 activating peptide 2fLIGRLO

2fLIGRLO dose response curves of untreated ZDSD arteries were significantly different than SD arteries (Figure 3.11). All ZDSD arteries demonstrated an increase in 2fLIGRLO

relaxation (15% in caudal branch), increased sensitivity (2 to 4.5 times), or a combination of both.

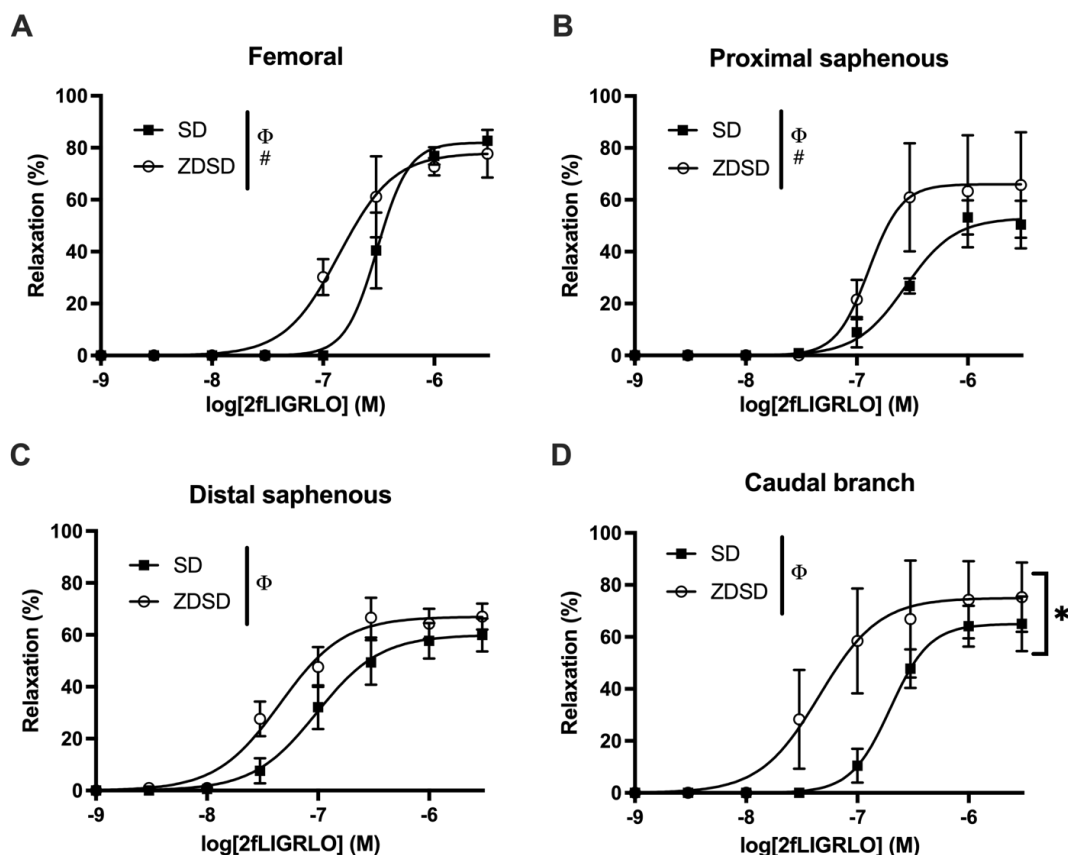


Figure 3.6 2fLIGRLO concentration-response curves in hindlimb arteries of ZDSD and SD.

Arterial rings were contracted with U46619 and relative relaxation was measured in the femoral (A), proximal (B), distal (C), and caudal branch of the saphenous artery (D).

Data points are mean \pm SEM and lines represent best-fit four parameter Sigmoidal dose response curves. For each vessel type $n=5$ for SD and $n=4$ for ZDSD. One SD femoral artery sample was excluded with $<10\%$ relaxation. E_{max} , $-\log EC_{50}$, and Hill slope were compared between groups by 2-way ANOVA with Bonferroni post hoc test. $*p < 0.05$

E_{max} ; $\Phi p < 0.001$ $-\log EC_{50}$; # $p < 0.05$ Hill slope.

3.4.5 Relaxations of ZDSD and SD hindlimb by the endothelium-independent agonist SNP

SNP CRC differed between ZDSD and SD femoral and proximal saphenous arteries (Figure 3.7A, 3.7B). ZDSD femoral arteries were less sensitive to SNP (2.5 times) whereas ZDSD proximal saphenous arteries were more sensitive (2.6 times) to SNP than SD (Figure 3.7B). L-NAME treatment of arteries increased the sensitivity to SNP (1.3 to 4.2 times) of all arteries ($p < 0.0001$, 2-way ANOVA) (Table 3.6).

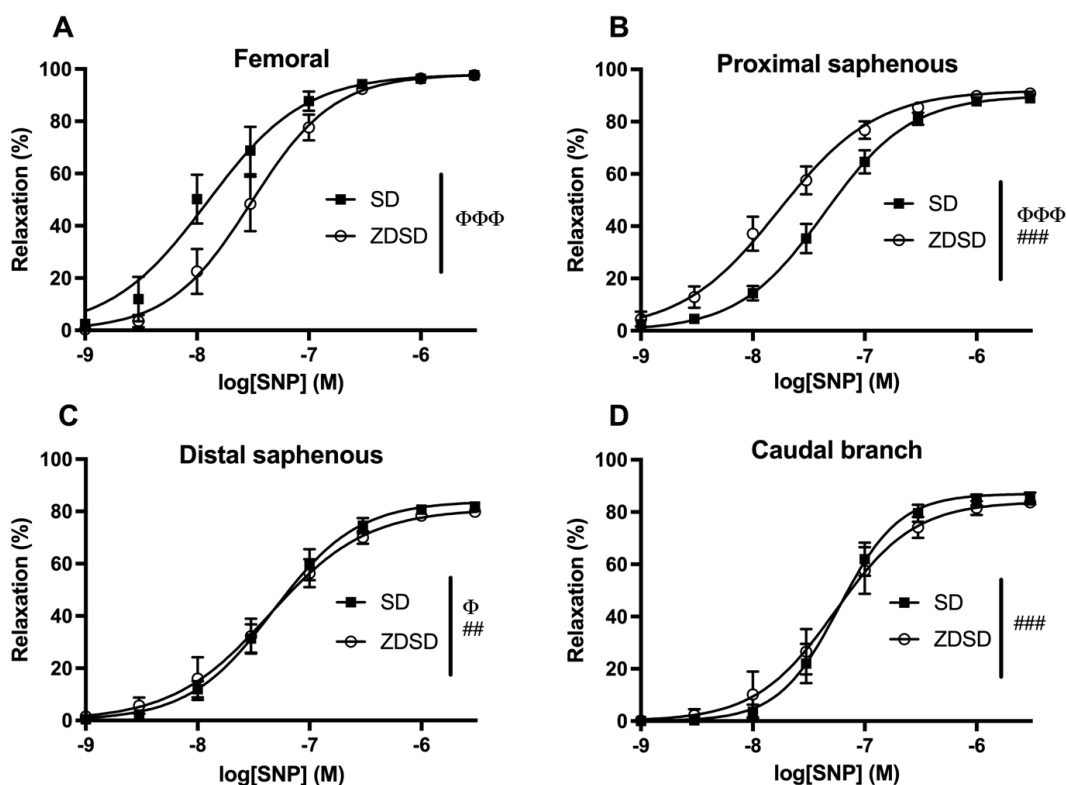


Figure 3.7 SNP concentration-response curves in hindlimb arteries of ZDSD and SD.

Arterial rings were contracted with U46619 and relative relaxation was measured in the femoral (A), proximal (B), distal (C), and caudal branch of the saphenous artery (D). Data points are mean \pm SEM and lines represent best-fit four parameter Sigmoidal dose response curves. For each vessel type $n=6$ for SD and $n=5$ for ZDSD. E_{max} , $-\log EC_{50}$, and Hill slope were compared between groups by Student's t -test. $\Phi p < 0.05$, $\Phi\Phi\Phi p < 0.001$ $-\log EC_{50}$; $### p < 0.01$, $#### p < 0.001$ Hill slope.

Table 3.6 Concentration-response curves of SNP with L-NAME in hindlimb arteries of SD and ZDSD rats.

Artery type	Strain	Treatment	E _{max} (%)	Hill slope	-logEC ₅₀ (M)
Femoral	SD	Control	98.1 ± 0.4	1.13 ± 0.10	7.91 ± 0.04
		L-NAME	99.9 ± 0.1	1.14 ± 0.07	8.39 ± 0.03
	ZDSD	Control	98.0 ± 0.4	1.18 ± 0.04	7.52 ± 0.01 ^c
		L-NAME	100	1.80 ± 0.14	8.09 ± 0.02
Proximal saphenous	SD	Control	90.1 ± 1.2	1.13 ± 0.02	7.36 ± 0.01
		L-NAME	94.9 ± 0.5	1.29 ± 0.10	7.99 ± 0.03
	ZDSD	Control	91.6 ± 0.6	0.95 ± 0.03 ^c	7.77 ± 0.02 ^c
		L-NAME	96.8 ± 0.9	1.30 ± 0.10	8.34 ± 0.03
Distal saphenous	SD	Control	83.9 ± 1.2	1.15 ± 0.03	7.33 ± 0.01
		L-NAME	90.8 ± 0.8	1.21 ± 0.04	7.60 ± 0.01
	ZDSD	Control	80.9 ± 1.0	0.98 ± 0.02 ^b	7.36 ± 0.01 ^a
		L-NAME	90.9 ± 1.6	1.33 ± 0.07	7.76 ± 0.02
Caudal branch of saphenous	SD	Control	87.4 ± 1.5	1.61 ± 0.06	7.23 ± 0.01
		L-NAME	91.2 ± 1.3	1.45 ± 0.04	7.36 ± 0.01
	ZDSD	Control	85.2 ± 1.6	1.22 ± 0.03 ^c	7.26 ± 0.01
		L-NAME	91.4 ± 0.8	1.19 ± 0.05	7.48 ± 0.02

Data are the mean ± SEM in SD (n=6) or ZDSD (n=5) at 20-21 weeks of age. E_{max}, maximum relaxation response by sodium nitroprusside (SNP); EC₅₀, molar concentration of drug producing 50% of E_{max}. EC₅₀ and Hill slope are determined by nonlinear regression analyses of group data using sigmoidal dose-curve equation. Data were analyzed with Student's *t*-test between SD and ZDSD with control treatment. ^a*p*<0.05; ^b*p*<0.01; ^c*p*<0.001

3.4.6 Contraction of ZDSD and SD hindlimb by the TP receptor agonist U46619

ZDSD and SD did not show increased maximal response to U46619-mediated contractions within vessel types (Figure 3.8). The distal saphenous artery and caudal branch of the saphenous artery of ZDSD showed increased sensitivity (1.4 to 1.7 times)

to U46619-mediated contractions compared to SD (Figure 3.8, Figure 3.9). The proximal saphenous artery instead showed a rightward shift in the CRC of ZDSD rats, indicating decreased sensitivity (1.4 times) to U46619 (Figure 3.8B). In SD, L-NAME treated vessels (femoral, proximal and distal saphenous) showed a decreased sensitivity (1.3 to 1.5 times) to U46619-mediated contractions. A similar effect (1.3 to 1.4 times decrease) was seen in L-NAME treated distal and caudal branches of ZDSD (Table 3.7).

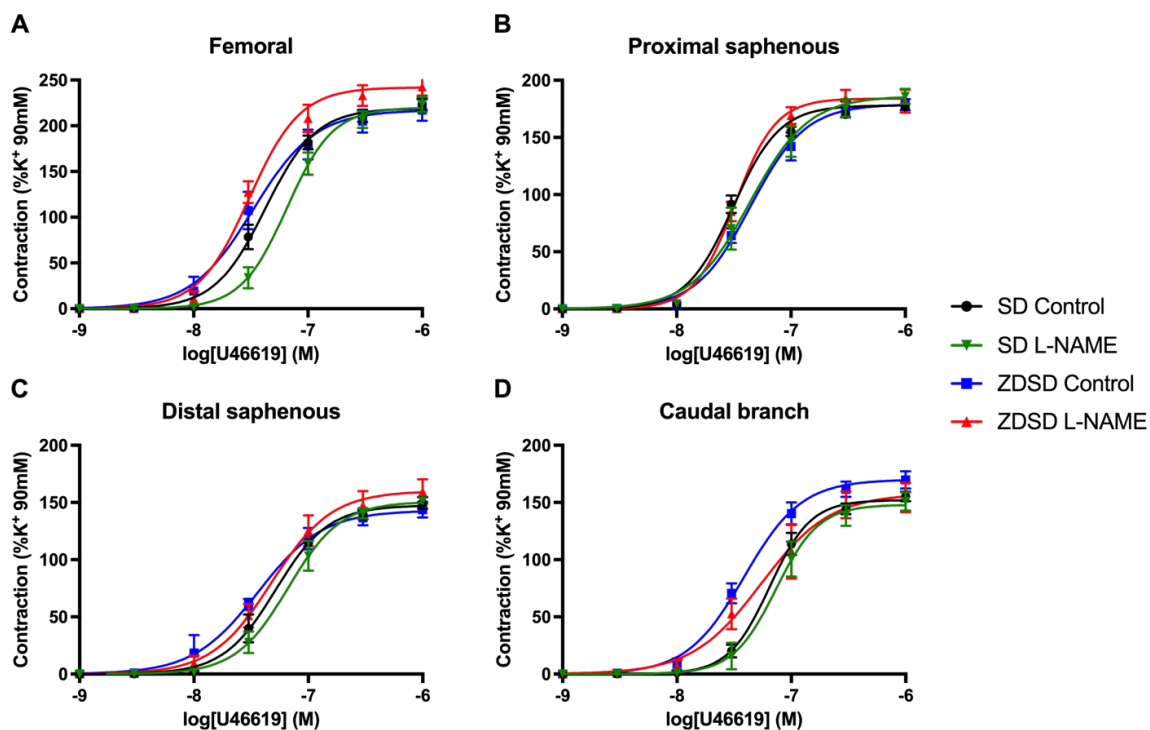


Figure 3.8 Normalized U46619 concentration-response curves in hindlimb arteries of ZDSD and SD.

The femoral (A), proximal (B), distal (C), and caudal branch of the saphenous artery (D) were contracted with U46619 and treated with L-NAME. Contractions were normalized to 90 mM of K^+ contractions in the same vessel. Data points are mean \pm SEM and lines represent best-fit four parameter Sigmoidal dose response curves. For each vessel type $n=6$ for SD and $n=5$ for ZDSD.

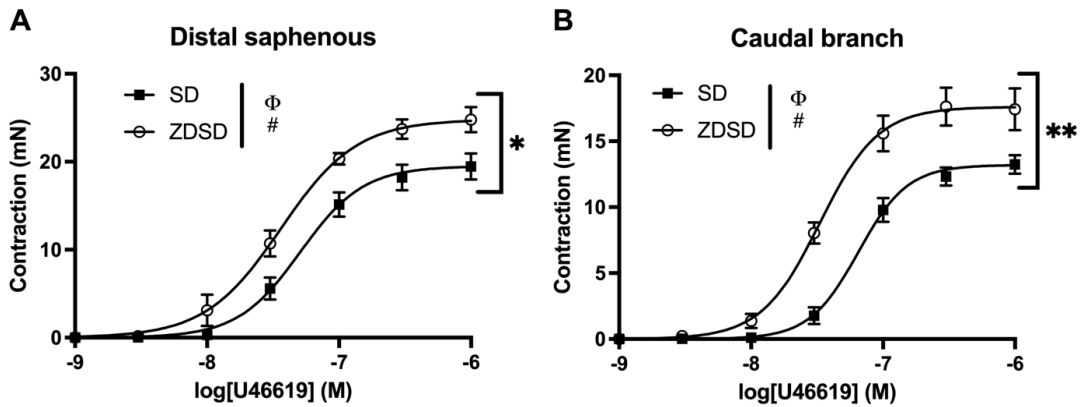


Figure 3.9 Non-normalized U46619 concentration-response curves in hindlimb arteries of ZDSD and SD.

The distal (A), and caudal branch of the saphenous artery (B) were contracted with U46619 in ZDSD and SD. Data points are mean \pm SEM and lines represent best-fit four parameter Sigmoidal dose response curves. For each vessel type $n=6$ for SD and $n=5$ for ZDSD. E_{max} , $-\log EC_{50}$, and Hill slope were compared between groups by Student's t -test. * $p < 0.05$, ** $p < 0.01$ E_{max} ; $\Phi p < 0.001$ $-\log EC_{50}$; # $p < 0.05$ Hill slope.

Table 3.7 Concentration-response curves of U46619 with L-NAME in hindlimb arteries of SD and ZDSD rats.

Artery type	Strain	Treatment	E _{max} (%K ⁺)	Hill slope	-logEC ₅₀ (M)
Femoral	SD	Control	223.9 ± 5.6	1.96 ± 0.23	7.37 ± 0.03
		L-NAME	223.5 ± 8.2	2.16 ± 0.12	7.19 ± 0.02*
	ZDSD	Control	217.0 ± 8.4	1.60 ± 0.15	7.48 ± 0.03
		L-NAME	242.5 ± 9.5	1.95 ± 0.26	7.51 ± 0.03*
Proximal saphenous	SD	Control	177.9 ± 6.8	2.54 ± 0.46	7.52 ± 0.02
		L-NAME	186.0 ± 6.6	1.75 ± 0.20	7.37 ± 0.04*
	ZDSD	Control	178.7 ± 5.1	1.80 ± 0.14	7.35 ± 0.02*
		L-NAME	184.3 ± 7.5	2.44 ± 0.18	7.49 ± 0.01#
Distal saphenous	SD	Control	149.6 ± 5.0	1.89 ± 0.13	7.29 ± 0.02
		L-NAME	151.2 ± 3.5	1.89 ± 0.07	7.18 ± 0.01*
	ZDSD	Control	143.7 ± 5.8	1.54 ± 0.04	7.44 ± 0.01*
		L-NAME	159.5 ± 10.6	1.66 ± 0.08	7.32 ± 0.01#
Caudal branch	SD	Control	155.3 ± 4.7	2.42 ± 0.15	7.19 ± 0.02
		L-NAME	150.1 ± 8.0	2.31 ± 0.16	7.14 ± 0.16
	ZDSD	Control	169.7 ± 7.5	1.73 ± 0.12*	7.41 ± 0.02*
		L-NAME	154.4 ± 12.9	1.43 ± 0.15*	7.27 ± 0.04#
Artery type	Strain	Treatment	E _{max} (mN)	Hill slope	-logEC ₅₀ (M)
Distal saphenous	SD	Control	19.5 ± 1.5	1.82 ± 0.11	7.29 ± 0.02
	ZDSD	Control	24.8 ± 1.4*	1.51 ± 0.04*	7.44 ± 0.01*
Caudal branch	SD	Control	13.2 ± 0.7	2.33 ± 0.14	7.19 ± 0.02
	ZDSD	Control	17.6 ± 1.4*	1.94 ± 0.07*	7.48 ± 0.01*

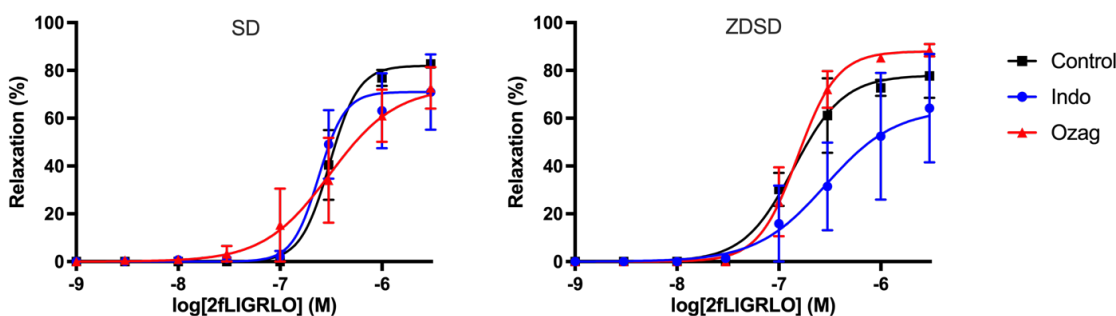
Data are the mean ± SEM in SD (n=6) or ZDSD (n=5) at 20-21 weeks of age. E_{max}, maximum contraction response by U46619 as a percentage of K⁺ 90 mM contraction or without normalization; EC₅₀, molar concentration of drug producing 50% of E_{max}. EC₅₀ and Hill slope are determined by nonlinear regression analyses of group data using sigmoidal dose-curve equation. Data were analyzed with 2-way ANOVA with Bonferroni post hoc test. **p*<0.05 to SD with control treatment; #*p*<0.05 between ZDSD with control and L-NAME treatment.

3.4.7 Effects of the nonselective cyclooxygenase inhibitor indomethacin and the thromboxane A₂ synthase inhibitor ozagrel on ZDSD and SD hindlimb arteries relaxations

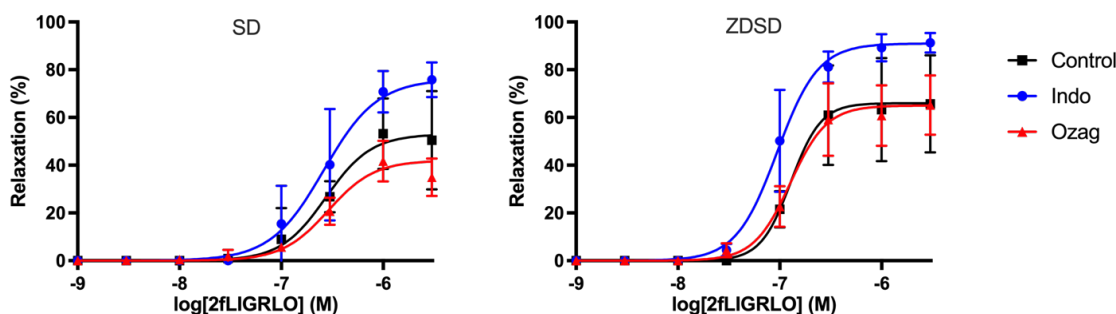
3.4.7.1 2fLIGRLO-induced relaxation mechanisms

Treatments of indomethacin and ozagrel did not change maximal relaxations to 2fLIGRLO compared to controls within animal strains (Figure 3.10). Indomethacin treated vessels showed an increased sensitivity (1.3 times) to 2fLIGRLO in the femoral artery of SD rats (Figure 3.10A, Table 3.8). In ZDSD rats, indomethacin treated femoral and distal saphenous arterial segments showed a decrease in sensitivity (1.5 to 2.1 times) to 2fLIGRLO, but proximal saphenous segments showed an increase in sensitivity (1.4 times) (Figure 3.10B, Table 3.8). Indomethacin treatment did not affect any of the 2fLIGRLO-mediated relaxations in the caudal branch of the saphenous artery of SD or ZDSD rats. In ZDSD rats, ozagrel treated vessels showed decreased sensitivity (1.6 to 1.7 times decrease) of the distal saphenous arterial segment and caudal branch. Ozagrel did not affect the 2fLIGRLO CRC of the femoral artery or proximal saphenous arterial segments.

A Femoral



B Proximal saphenous



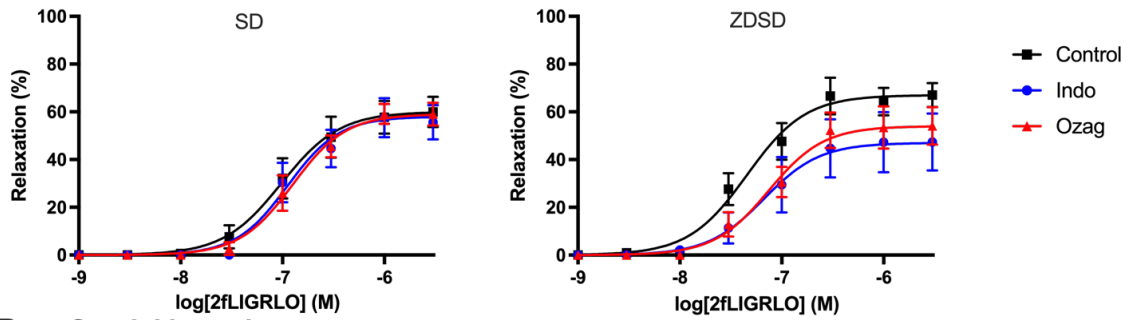
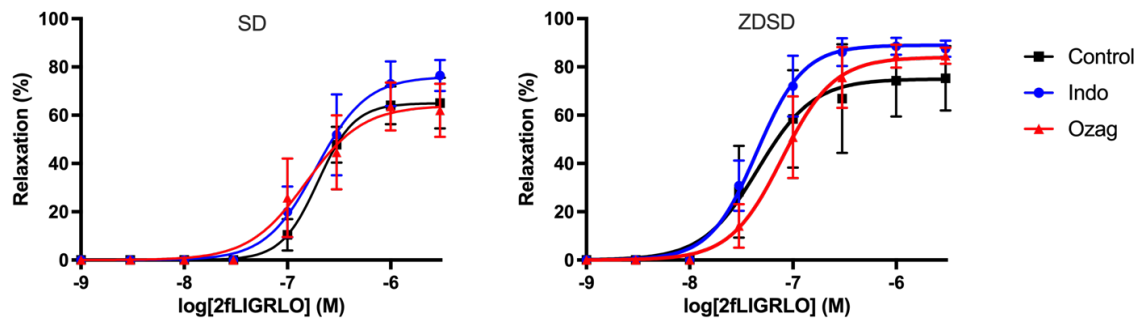
C Distal saphenous**D Caudal branch**

Figure 3.10 2fLIGRLO concentration-response curves with indomethacin and ozagrel treatment in ZDSD and SD.

The femoral (A), proximal (B), distal (C), and caudal branch of the saphenous artery (D) were treated with indomethacin or ozagrel 10 min prior to contraction with U46619. Data points are mean \pm SEM and lines represent best-fit four parameter Sigmoidal dose response curves. For each vessel type $n=5$ for SD and $n=4$ for ZDSD; values were excluded if U46619 contraction was $<1\text{mN}$.

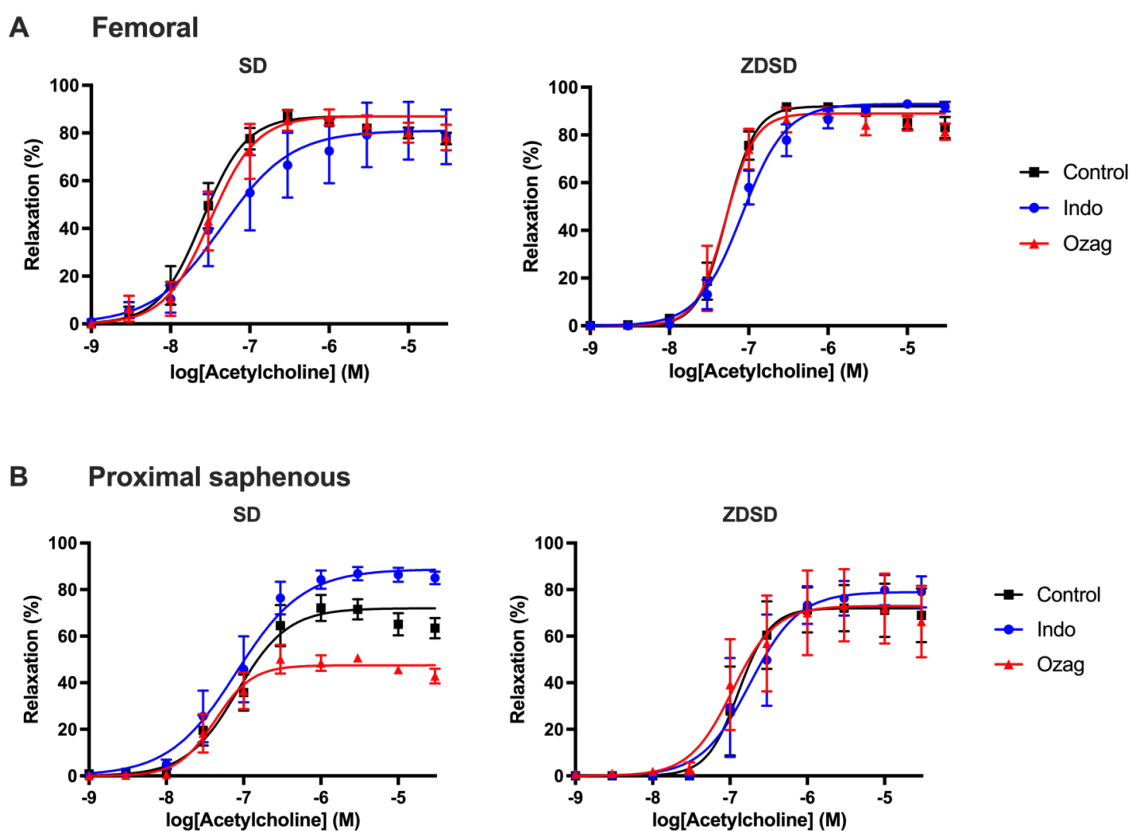
Table 3.8 Effects of indomethacin and ozagrel on 2fLIGRLO CRC in SD and ZDSD

Artery type	Strain	n	Treatment	E _{max} (%)	Hill slope	-logEC ₅₀ (M)	
Femoral	SD	4	Control	82.7 ± 1.3	3.04 ± 0.44	6.52 ± 0.01	
		4	Indomethacin	70.9 ± 15.7	3.37 ± 0.83	6.62 ± 0.03*	
		5	Ozagrel	72.7 ± 8.7	1.34 ± 0.08*	6.51 ± 0.02	
	ZDSD	4	Control	77.7 ± 9.2	1.77 ± 0.18	6.86 ± 0.03	
		4	Indomethacin	64.2 ± 22.6	1.28 ± 0.11	6.54 ± 0.03 [#]	
		4	Ozagrel	88.5 ± 2.6	2.24 ± 0.09	6.82 ± 0.01	
	Proximal saphenous	SD	5	Control	53.2 ± 6.6	1.95 ± 0.30	6.56 ± 0.03
			5	Indomethacin	75.6 ± 3.3	1.66 ± 0.13	6.58 ± 0.02
			5	Ozagrel	41.7 ± 3.8*	1.92 ± 0.49	6.54 ± 0.06
ZDSD		4	Control	65.7 ± 20.3	2.94 ± 0.22	6.89 ± 0.01	
		4	Indomethacin	91.3 ± 4.1	2.15 ± 0.17	7.03 ± 0.02 [#]	
		4	Ozagrel	65.2 ± 12.4	2.43 ± 0.28	6.90 ± 0.02	
Distal saphenous	SD	5	Control	60.0 ± 6.4	1.52 ± 0.08	7.01 ± 0.02	
		5	Indomethacin	57.5 ± 8.2	1.71 ± 0.32	6.95 ± 0.05	
		5	Ozagrel	59.2 ± 4.3	1.67 ± 0.15	6.90 ± 0.03	
	ZDSD	4	Control	67.0 ± 5.1	1.51 ± 0.22	7.34 ± 0.05	
		4	Indomethacin	47.4 ± 12.0	1.58 ± 0.10	7.18 ± 0.02 [#]	
		4	Ozagrel	54.1 ± 7.9	1.62 ± 0.20	7.13 ± 0.04 [#]	
Caudal branch	SD	5	Control	65.0 ± 10.5	2.45 ± 0.04	6.71 ± 0.01	
		5	Indomethacin	76.5 ± 6.4	1.78 ± 0.10*	6.72 ± 0.02	
		5	Ozagrel	63.6 ± 10.0	1.57 ± 0.22*	6.82 ± 0.04*	
	ZDSD	4	Control	75.3 ± 13.4	1.62 ± 0.21	7.34 ± 0.04	
		4	Indomethacin	88.5 ± 3.5	1.91 ± 0.16	7.35 ± 0.02	
		4	Ozagrel	84.7 ± 3.4	1.73 ± 0.08	7.11 ± 0.01 [#]	

Data are the mean ± SEM in SD (n=5) or ZDSD (n=4) at 20-21 weeks of age. E_{max}, maximum relaxation response by 2fLIGRLO; EC₅₀, molar concentration of drug producing 50% of E_{max}. EC₅₀ and Hill slope are determined by nonlinear regression analyses of group data using sigmoidal dose-curve equation. Samples were excluded based on U46619-contraction <1mN or control relaxation <10%. Data were analyzed with 2-way ANOVA with Bonferroni post hoc test. *p<0.05 to control treatment in SD; [#]p<0.05 to control treatment in ZDSD.

3.4.7.2 ACh-induced relaxation mechanisms

Indomethacin and ozagrel treatments did not reverse endothelial dysfunction in ZDSD. Indomethacin treatments decreased ACh-sensitivity in the femoral artery (1.6 to 1.8 times) and increased ACh-sensitivity in the caudal branch (1.4 to 1.6 times) in both ZDSD and SD (Figure 3.11, Table 3.9). Indomethacin treatment also decreased ACh-sensitivity (1.4 times) exclusively in the ZDSD proximal saphenous artery. Ozagrel treatments enhanced ACh sensitivity in the proximal saphenous artery of both SD and ZDSD rats (1.9 and 1.2 times respectively). Ozagrel treatments also decreased ACh sensitivity in the femoral (1.3 times) and caudal branch (1.5 times) of SD rat (Table 3.9). Ozagrel and indomethacin did not change the ACh CRC in distal saphenous arterial segment in either SD or ZDSD.



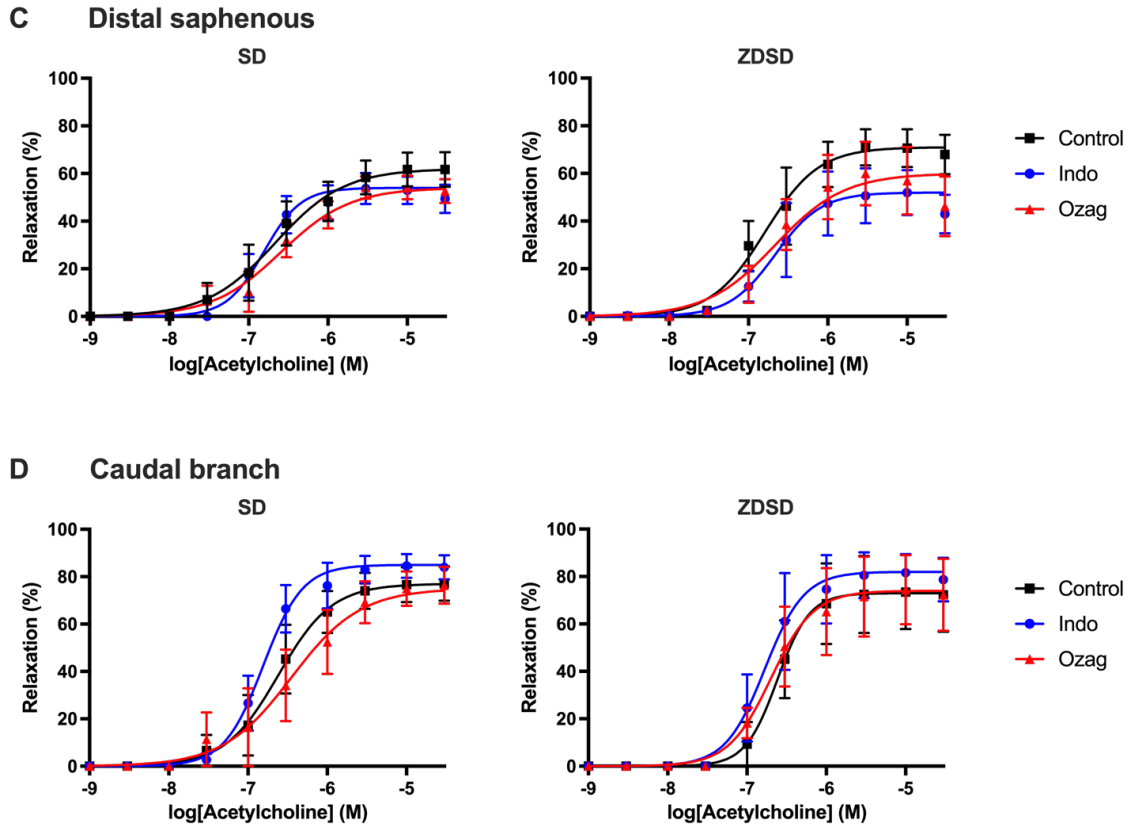


Figure 3.11 ACh concentration-response curves with indomethacin and ozagrel treatment in ZDSD and SD.

The femoral (A), proximal (B), distal (C), and caudal branch of the saphenous artery (D) were treated with indomethacin or ozagrel 10 min prior to contraction with U46619. Data points are mean \pm SEM and lines represent best-fit four parameter Sigmoidal dose response curves. For each vessel type $n=5$ for SD and $n=4$ for ZDSD; values were excluded if U46619 contraction was <1 mN.

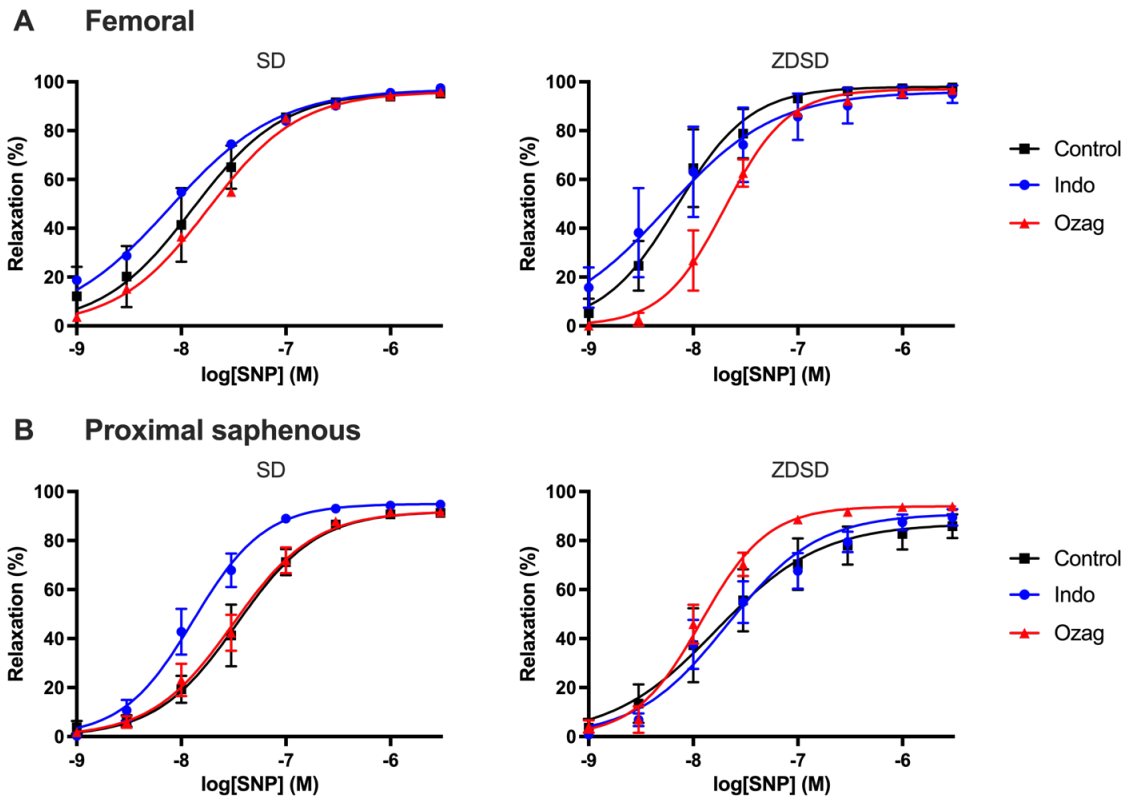
Table 3.9 Effects of indomethacin and ozagrel on ACh CRC in SD and ZDSD

Artery type	Strain	n	Treatment	E _{max} (%)	Hill slope	-logEC ₅₀ (M)
Femoral	SD	5	Control	87.3 ± 2.5	1.57 ± 0.08	7.60 ± 0.02
		4	Indomethacin	81.0 ± 12.1	0.91 ± 0.09*	7.35 ± 0.05*
		5	Ozagrel	86.5 ± 3.4	1.50 ± 0.12	7.50 ± 0.03*
	ZDSD	4	Control	91.7 ± 1.1	2.39 ± 0.06	7.28 ± 0.01
		4	Indomethacin	92.9 ± 1.8	1.56 ± 0.15*	7.09 ± 0.03 [#]
		4	Ozagrel	89.4 ± 2.2	2.35 ± 0.06	7.29 ± 0.01
Proximal saphenous	SD	5	Control	72.1 ± 5.6	1.32 ± 0.16	7.09 ± 0.05
		5	Indomethacin	86.9 ± 2.8	1.21 ± 0.12	7.11 ± 0.04
		5	Ozagrel	50.7 ± 1.9	1.81 ± 0.39	7.37 ± 0.06*
	ZDSD	4	Control	72.0 ± 9.9	2.12 ± 0.15	6.89 ± 0.02
		4	Indomethacin	79.0 ± 6.7	1.38 ± 0.15	6.74 ± 0.04 [#]
		4	Ozagrel	73.3 ± 15.6	1.57 ± 0.24	6.97 ± 0.05 [#]
Distal saphenous	SD	5	Control	61.7 ± 7.3	1.05 ± 0.07	6.66 ± 0.03
		5	Indomethacin	53.7 ± 6.5	1.85 ± 0.26*	6.81 ± 0.04
		5	Ozagrel	54.2 ± 4.7	1.23 ± 0.13	6.59 ± 0.04
	ZDSD	4	Control	71.0 ± 7.6	1.28 ± 0.14	6.79 ± 0.04
		4	Indomethacin	51.9 ± 9.4	1.50 ± 0.26	6.66 ± 0.06
		4	Ozagrel	60.0 ± 13.3	1.58 ± 0.39	6.67 ± 0.07
Caudal branch	SD	5	Control	77.1 ± 7.3	1.28 ± 0.05	6.62 ± 0.01
		5	Indomethacin	84.5 ± 5.0	1.75 ± 0.14*	6.81 ± 0.02*
		5	Ozagrel	76.3 ± 7.8	0.97 ± 0.08*	6.45 ± 0.04*
	ZDSD	4	Control	73.4 ± 15.7	2.14 ± 0.06	6.62 ± 0.01
		4	Indomethacin	81.7 ± 7.9	1.75 ± 0.15*	6.78 ± 0.02 [#]
		4	Ozagrel	74.4 ± 14.6	1.62 ± 0.13*	6.70 ± 0.02

Data are the mean ± SEM in SD (n=5) or ZDSD (n=4) at 20-21 weeks of age. E_{max}, maximum relaxation response by acetylcholine (ACh); EC₅₀, molar concentration of drug producing 50% of E_{max}. EC₅₀ and Hill slope are determined by nonlinear regression analyses of group data using sigmoidal dose-curve equation. Samples were excluded based on U46619-contraction <1mN. Data were analyzed with 2-way ANOVA with Bonferroni post hoc test. *p<0.05 to control treatment in SD; [#]p<0.05 to control treatment in ZDSD.

3.4.7.3 Nitroprusside-induced relaxations

Treatments of indomethacin and ozagrel did not change maximal relaxations to SNP within animal strains (Table 3.10, Figure 3.12). Indomethacin treatments decreased SNP sensitivity (1.3 to 2.1 times) in the saphenous artery of ZDSD (Figure 3.12B, 3.12C). Indomethacin treatments increased SNP sensitivity (2.1 times) in the caudal branch of ZDSD (Figure 3.12D). Ozagrel treatments decreased SNP sensitivity in the femoral artery of both SD (1.4 times) and ZDSD (2.9 times) (Figure 3.12A). However, ozagrel treatment increased SNP sensitivity (1.4 times) in the proximal saphenous artery of ZDSD (Figure 3.12B).



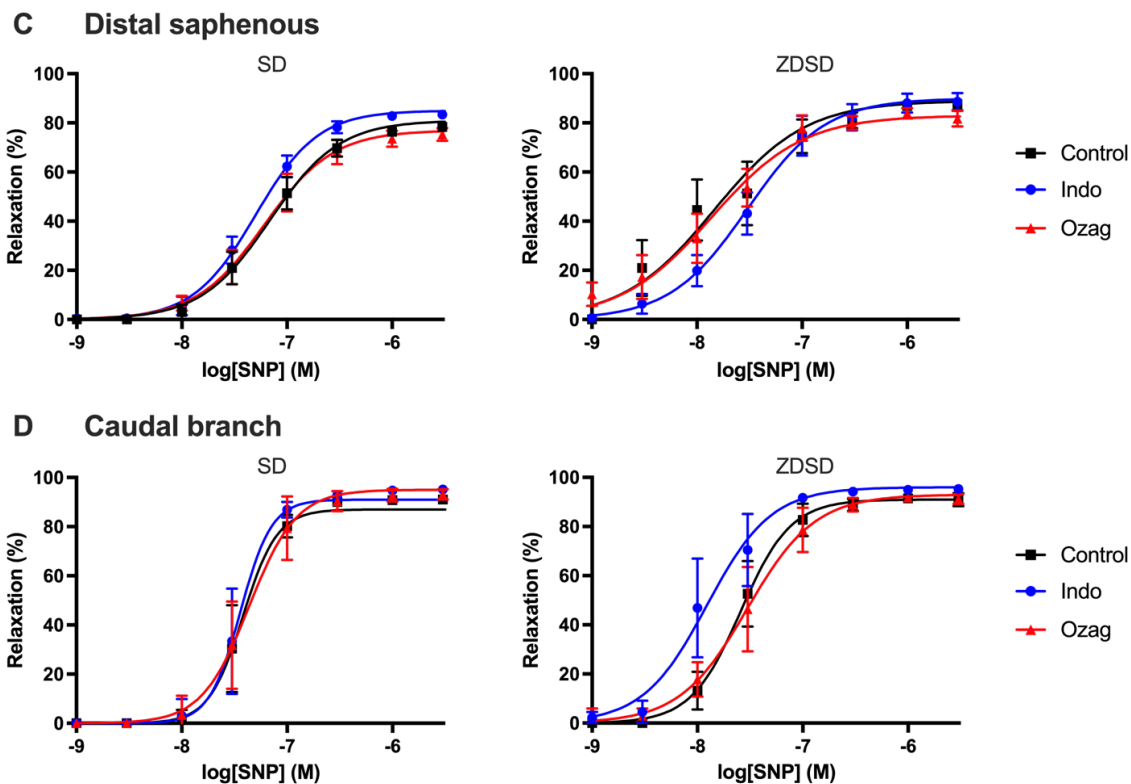


Figure 3.12 SNP concentration-response curves with indomethacin and ozagrel treatment in ZDSD and SD.

The femoral (A), proximal (B), distal (C), and caudal branch of the saphenous artery (D) were treated with indomethacin or ozagrel 10 min prior to contraction with U46619. Data points are mean \pm SEM and lines represent best-fit four parameter Sigmoidal dose response curves. For each vessel type $n=5$ for SD and $n=4$ for ZDSD; values were excluded if U46619 contraction was <1 mN.

Table 3.10 Effects of indomethacin and ozagrel on SNP CRC in SD and ZDSD

Artery type	Strain	n	Treatment	E _{max} (%)	Hill slope	-logEC ₅₀ (M)
Femoral	SD	4	Control	95.7 ± 1.6	0.92 ± 0.04	7.89 ± 0.02
		4	Indomethacin	97.4 ± 1.1	0.84 ± 0.05	8.11 ± 0.04*
		5	Ozagrel	95.8 ± 1.3	1.00 ± 0.06	7.74 ± 0.03*
	ZDSD	4	Control	98.0 ± 0.2	1.23 ± 0.09	8.16 ± 0.03
		4	Indomethacin	95.8 ± 2.4	0.84 ± 0.05 [#]	8.26 ± 0.03
		4	Ozagrel	97.1 ± 0.6	1.45 ± 0.08	7.70 ± 0.02 [#]
Proximal saphenous	SD	5	Control	91.6 ± 0.85	1.13 ± 0.03	7.47 ± 0.01
		5	Indomethacin	95.0 ± 0.1	1.28 ± 0.07	7.88 ± 0.02*
		5	Ozagrel	92.0 ± 1.1	1.12 ± 0.05	7.51 ± 0.02
	ZDSD	4	Control	87.2 ± 4.3	0.87 ± 0.05	7.78 ± 0.03
		4	Indomethacin	90.9 ± 3.6	0.87 ± 0.09	7.67 ± 0.06 [#]
		4	Ozagrel	94.4 ± 0.4	1.37 ± 0.10 [#]	7.92 ± 0.03 [#]
Distal saphenous	SD	5	Control	88.9 ± 1.0	0.84 ± 0.84	7.83 ± 0.06
		5	Indomethacin	85.2 ± 1.3	1.46 ± 0.05	7.30 ± 0.01*
		5	Ozagrel	77.5 ± 2.6	1.32 ± 0.04	7.22 ± 0.01
	ZDSD	4	Control	89.0 ± 1.0	0.84 ± 0.09	7.83 ± 0.06
		4	Indomethacin	90.1 ± 2.7	1.18 ± 0.04 [#]	7.51 ± 0.02 [#]
		4	Ozagrel	83.0 ± 3.3	0.98 ± 0.08	7.86 ± 0.04
Caudal branch	SD	5	Control	92.1 ± 0.7	2.67 ± 0.39	7.42 ± 0.02
		5	Indomethacin	96.0 ± 0.5	2.93 ± 0.48	7.44 ± 0.02
		5	Ozagrel	94.6 ± 0.9	1.93 ± 0.09	7.36 ± 0.01
	ZDSD	4	Control	92.5 ± 1.9	1.84 ± 0.07	7.59 ± 0.01
		4	Indomethacin	95.7 ± 1.5	1.43 ± 0.14	7.91 ± 0.03 [#]
		4	Ozagrel	93.1 ± 1.4	1.35 ± 0.05	7.53 ± 0.01

Data are the mean ± SEM in SD (n=5) or ZDSD (n=4) at 20-21 weeks of age. E_{max}, maximum relaxation response by SNP; EC₅₀, molar concentration of drug producing 50% of E_{max}. EC₅₀ and Hill slope are determined by nonlinear regression analyses of group data using sigmoidal dose-curve equation. Samples were excluded based on U46619-contraction <1mN or control relaxation <10%. Data were analyzed with 2-way ANOVA with Bonferroni post hoc test. *p<0.05 to control treatment in SD; [#]p<0.05 to control treatment in ZDSD.

3.4.7.4 NOS inhibition

Treatments of indomethacin and the NOS inhibitor, L-NAME decreased ACh relaxation in all arteries (40-80% of relaxation) of ZDSD and SD except for the femoral artery (Figure 3.13). Ozagrel and L-NAME treatments decreased ACh relaxation in all arterial segments (30-65% of relaxation) except for the saphenous artery in ZDSD (Figure 3.14).

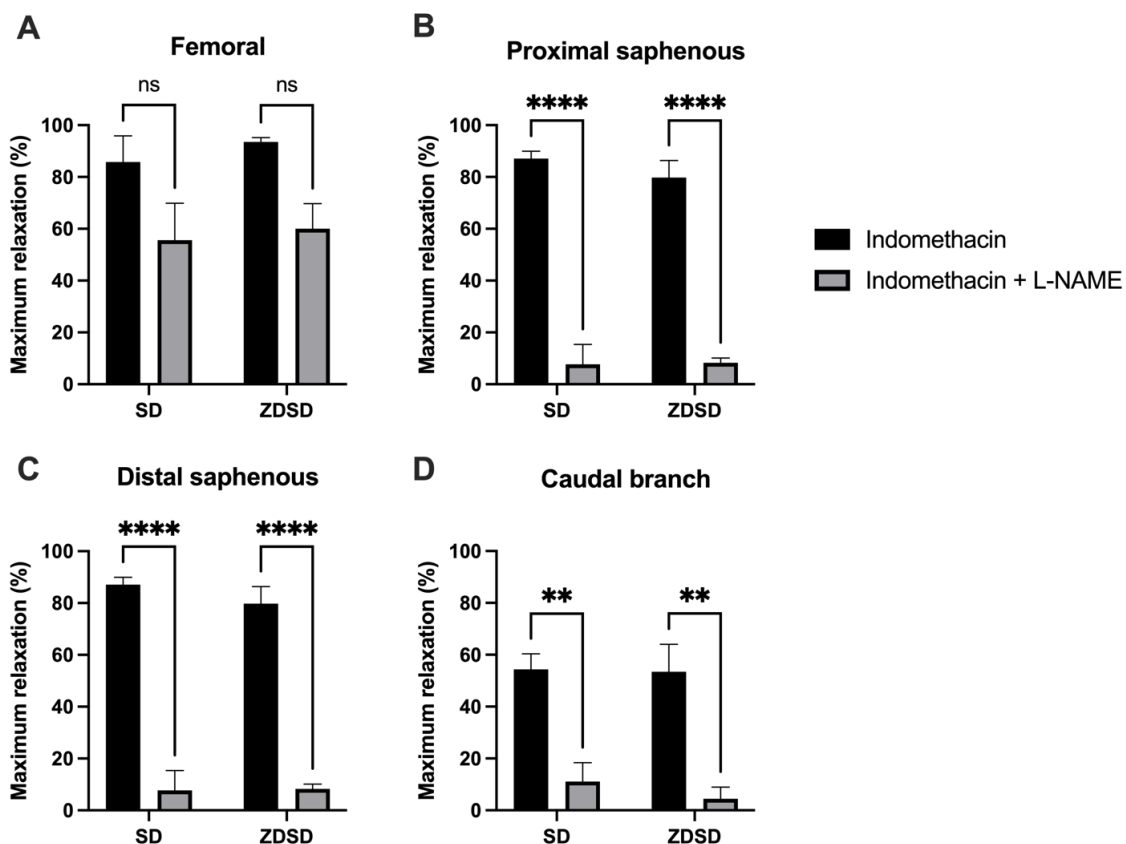


Figure 3.13 Maximum ACh relaxation with indomethacin and L-NAME treatment.

The femoral (A), proximal (B), distal (C), and caudal branch of the saphenous artery (D) were treated with indomethacin and L-NAME 10 min prior to contraction with U46619.

Data are mean \pm SEM. For each vessel type n=5 for SD and n=4 for ZDSD. * p <0.05,

** p <0.01, and **** p <0.0001 with 2-way ANOVA with Bonferroni post hoc test.

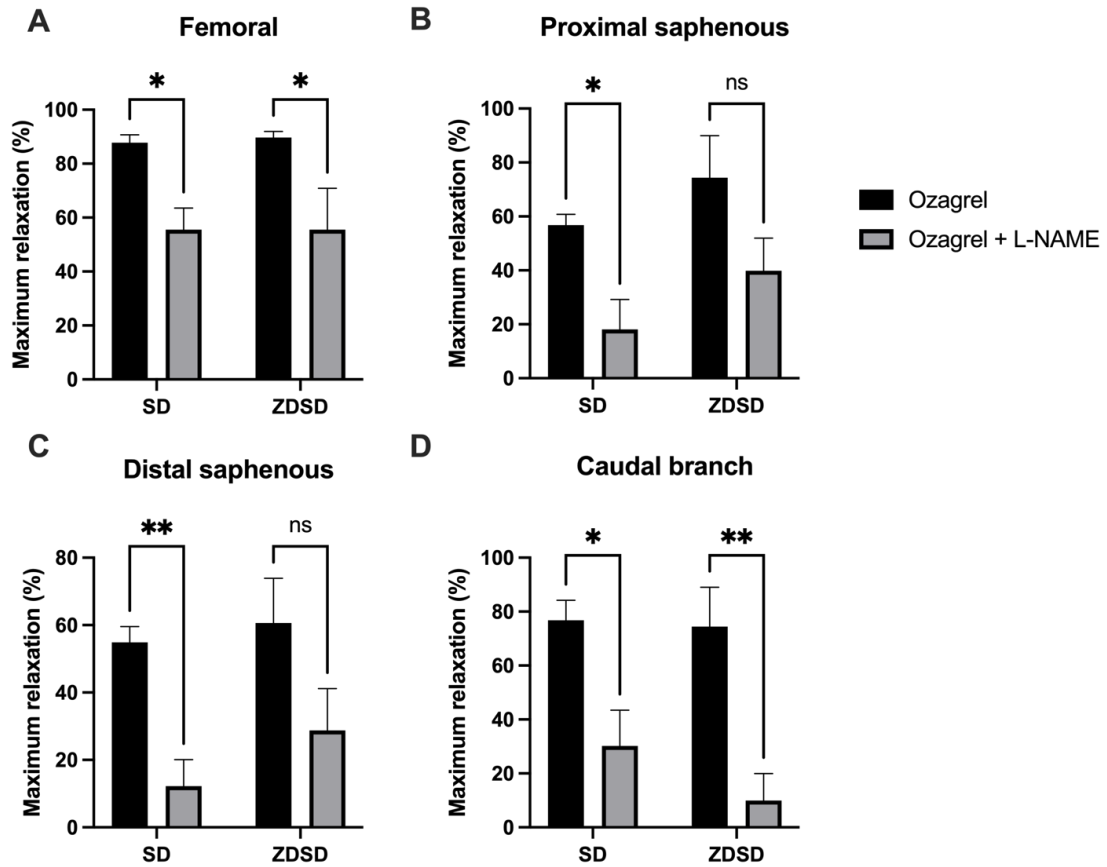


Figure 3.14 Maximum ACh relaxation with ozagrel and L-NAME treatment.

The femoral (A), proximal (B), distal (C), and caudal branch of the saphenous artery (D) were treated with ozagrel and L-NAME 10 min prior to contraction with U46619. Data are mean \pm SEM. For each vessel type $n=5$ for SD and $n=4$ for ZDSD. * $p < 0.05$ and ** $p < 0.01$ with 2-way ANOVA with Bonferroni post hoc test.

3.4.7.5 Denuded arteries

Denuded arteries demonstrated a significant decrease (50-70% of relaxation) in ACh-mediated vasodilation, with the exception of the femoral artery, indicating that relaxations observed are endothelium-dependent (Figure 3.15, Figure 3.16).

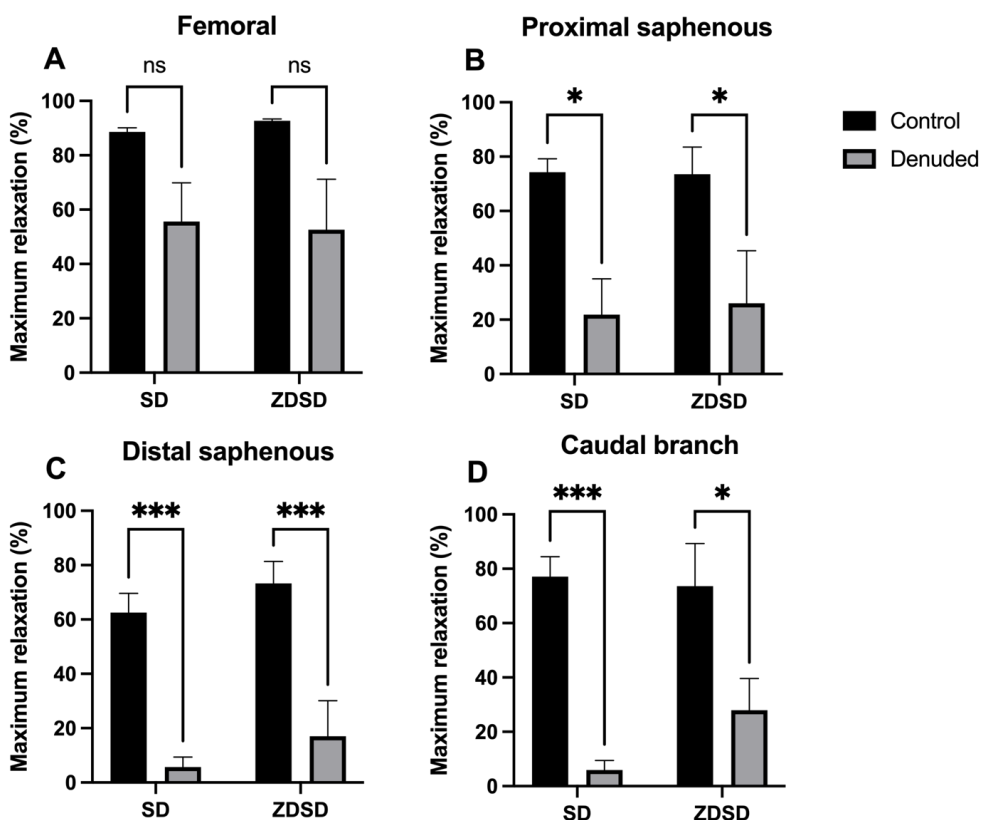
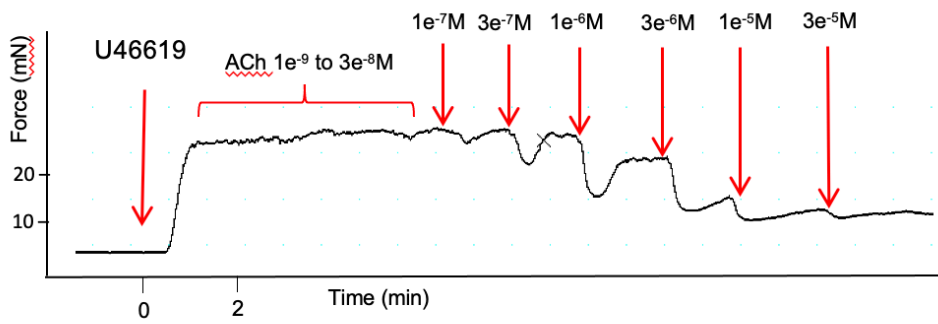
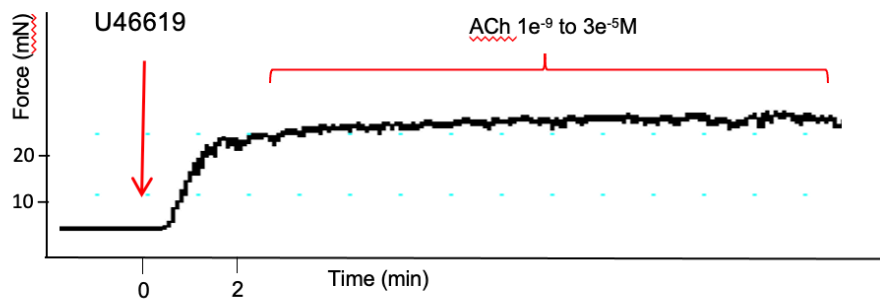


Figure 3.15 Maximum ACh relaxation in denuded arteries.

The endothelium of the femoral (A), proximal (B), distal (C), and caudal branch of the saphenous artery (D) were mechanically disrupted and the arteries were remounted and treated with ACh. Data are mean \pm SEM. For each vessel type $n=5$ for SD and $n=4$ for ZDSD. Samples were excluded if $<1\text{mN}$ U46619 contraction. $*p<0.05$ and $***p<0.001$ with 2-way ANOVA with Bonferroni post hoc test.



A. Intact endothelium
Dose response to acetylcholine (ACh) from 1nM–30 μ M



B. Endothelium denuded
Dose response to acetylcholine (ACh) from 1nM–30 μ M

Figure 3.16 Representative isometric tension recordings of ACh CRC in the saphenous artery with intact and denuded endothelium.

3.4.8 Endothelial cell gene expression in ZDSD and SD aortas

Thirteen endothelial cell genes were expressed differently between ZDSD and SD aorta according to microarray PCR (Table 3.12). In a second set of ZDSD and SD samples, we validated the gene expression for PGF, Col18a1, and PAR2 using product specific primers and qPCR (Figure 3.18).

Table 3.11 Endothelial cell gene expressions in ZDSD relative to SD thoracic aortas using PCR microarray

Gene symbol	Description	Upregulated or downregulated	Fold change	P-value
<i>Agtr1b</i>	angiotensin II receptor-1 subtype b	Up	6.98	0.04
<i>ApoE</i>	apolipoprotein E	Up	2.44	0.03
<i>Casp3</i>	caspase 3	Up	1.84	0.03
<i>Cdh5</i>	cadherin 5	Up	1.79	0.02
<i>Col18a1</i>	collagen type XVIII alpha 1 chain	Down	3.18	0.01
<i>Cxcr5</i>	C-X-C motif chemokine receptor 5	Up	3.02	0.03
<i>Kit</i>	KIT proto-oncogene receptor tyrosine kinase	Up	2.07	<0.01
<i>Pdgfra</i>	platelet derived growth factor receptor α	Up	1.76	0.01
<i>Pgf</i>	placental growth factor	Up	8.98	0.05
<i>Plau</i>	plasminogen activator, urokinase	Up	1.55	<0.01
<i>Tek</i>	TEK receptor tyrosine kinase	Up	1.56	0.02
<i>Tnfsf10</i>	TNF superfamily member 10	Up	1.64	<0.01
<i>Xdh</i>	xanthine dehydrogenase	Up	1.69	0.02

n=4 for SD and ZDSD. Data were analyzed with Student's *t*-test using CFX Maestro Software for CFX Real-Time PCR Instruments (Bio Rad Laboratories).

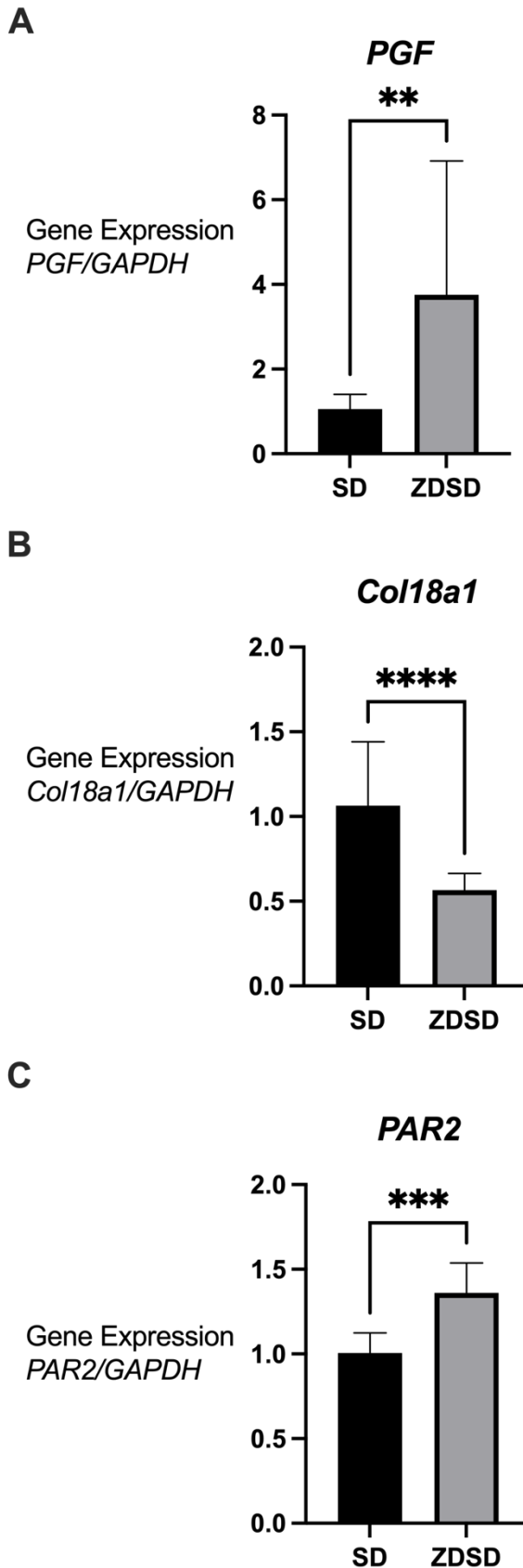


Figure 3.17 Aortic endothelial cell gene expression of ZDSD and SD.

Quantitative PCR data were analyzed by the delta-delta Cycle threshold (Ct) method ($2^{-\Delta\Delta Ct}$) with GAPDH as the housekeeping gene. Data were analyzed with unpaired Student's *t*-test between ZDSD and SD.

n=5 for both ZDSD and SD with PGF (A) and Col18a1 (B)

n=3 for ZDSD and SD with PAR2 (C)

** $p < 0.01$

*** $p < 0.001$

**** $p < 0.0001$

3.5 Discussion

The main findings are that ZDSD exhibit endothelial dysfunction and endothelial cell gene expression differences, including upregulated PAR2 expression when compared with nondiabetic controls. Endothelium-mediated relaxation mechanisms in ZDSD arteries differed by GPCR agonist and the selected segment of the hindlimb arteries studied in *ex vivo* assays. The endothelial cell gene expression patterns in ZDSD aorta suggest a broad impact and change to endothelium functions, including angiogenesis, GPCR function, production of cytokines, cell apoptosis, and differentiated endothelial cell phenotype.

3.5.1 Endothelium-dependent response to muscarinic agonist

This is the first study to focus on endothelium function in the ZDSD. We observed decreases in endothelial-dependent vasodilation with muscarinic receptor activation in the femoral artery and caudal branch of the saphenous artery. All arterial segments also demonstrated decreased sensitivity to ACh-mediated relaxation (Figure 3.5).

Additionally, ACh-mediated relaxation in the ZDSD is NOS-dependent as evidenced by the absence of relaxation following treatment with the NOS inhibitor L-NAME (Table 3.5). Endothelial dysfunction has only been previously examined in the ZDSD rat in one study where *in vitro* video microscopy technique was used to record internal diameters of pressurized blood vessels. Epineurial arterioles (small diameter blood vessels supplying nerves) showed reduced endothelium-dependent vasodilation responses with acetylcholine (approximately 50% reduction) and calcitonin gene-related peptide in 34-week-old ZDSD compared to SD (Davidson et al., 2014). While our study identified less impaired vasodilation in hindlimb arteries (20-25% in femoral and caudal branch) (Figure 3.5A, 3.5D), we may expect vasodilation to worsen at a later age, as we have displayed in Chapter 2. Nevertheless, decreases in ACh-mediated vasodilation have also been identified in the aorta, mesenteric, coronary, epineurial, renal, and cerebral arteries of other rat models of T2D such as the Goto-Kakizaki (Matsumoto, Ishida, et al., 2009; Pereira et al., 2017), Zucker Diabetic Fatty (Brøndum et al., 2010; Coppey et al., 2002; Oltman et al., 2008; Schwaninger et al., 2003), and the Otsuka Long-Evans Tokushima Fatty (Kagota et al., 2000; Matsumoto et al., 2007; Sakamoto et al., 1998). Thus, our

findings are consistent with endothelial dysfunction in the hindlimb arteries, which makes the ZDSD suitable as a model to explore mechanisms associated with endothelium dysfunction in T2D.

3.5.2 Nitric oxide pathways

To further examine the mechanisms underlying reduced responses to the endothelium-dependent vasodilator ACh, we studied the vascular smooth muscle response to the vasodilator SNP, which decomposes spontaneously to produce NO. ZDSD femoral arteries were less sensitive to SNP (Figure 3.7A). Hyperglycemic conditions are associated with an increase in production of superoxide which may decrease NO bioavailability (Beckman & Koppenol, 1996; A. Chatterjee & Catravas, 2008; Graier et al., 1999), however, a decrease in sensitivity to NO may be caused by changes to the sGC and cGMP second messenger signaling. Aorta and mesenteric arteries of type 2 diabetic Goto-Kakizaki rats also demonstrate decreased bioavailability of NO (Pereira et al., 2017). Additionally, db/db mice have previously demonstrated reduced sGC expression with attenuated ACh-mediated relaxation in mesenteric arteries (Kagota et al., 2011). Interestingly, ZDSD proximal saphenous arteries were more sensitive to SNP (Figure 3.7B). Our results are similar to previous studies which found increased sensitivity to SNP in aortas of eNOS knockout mice (Brandes et al., 2000) and endothelial denuded rabbit femoral arteries (Pohl & Busse, 1987). These results may infer a vascular smooth muscle compensation for reduced NO production or bioavailability in the ZDSD, or the change in sensitivity to SNP is a result of the reduction in baseline NO production in ZDSD (Bohlen & Lash, 1995). Consistent with our results, arteries treated with NOS inhibitors were also more sensitive to SNP-induced relaxation in controls (Brandes et al., 2000). Combined with the reduced ACh-mediated relaxation in all arterial segments with NOS inhibition, we can infer that although the degree may vary, eNOS is involved in relaxation mechanisms in all arteries of our study.

The most peripheral arteries of the SD in our study, distal and caudal branches of the saphenous artery, exhibited residual vasodilation with ACh in the presence of L-NAME (Table 3.5), which indicates a non-NO pathway. The present study also identified that the peripheral vasculature (distal saphenous and caudal branch) showed an increase in

sensitivity to thromboxane A₂ receptor induced vasoconstriction in the ZDSD (Figure 3.8) which has also been observed in streptozotocin-induced diabetic rat aortas (Hattori et al., 1999). These observations are consistent with mechanisms previously described in Chapter 2. These data indicate that aside from NO, other vasodilation mechanisms are impaired with T2D in peripheral vasculature. A decline of vasodilation in the ZDSD may also be due to an increased sensitivity to vasoconstrictors, which overrides the process of vasodilation. Together, our data indicate that the extremities are vulnerable in the early stages of hyperglycemia. Overall, we observed different pharmacological effects of vasculature dependent on the location of interest in the hindlimb in hyperglycemic animals. These data allude to differences in physiological roles of these vasculature and will provide more insight in disease progression as it pertains to vascular health.

3.5.3 PAR2 function in T2D

This is the first study to examine the effects of a PAR2-AP on arteries in ZDSD. The PAR2-AP 2fLIGRLO was more potent for relaxing arteries in the ZDSD than in the controls (Figure 3.6). Preserved or upregulated PAR2 function has also been found in coronary arteries of diabetic mice (Park et al., 2011) or mesenteric arteries of diabetic mice (Kagota et al., 2011) and rats (Matsumoto, Ishida, et al., 2009). One exception to this is db/db mice which showed reduced PAR2-mediated vasodilation (at 3 μ M SLIGRL) to controls in second or third-order mesenteric arteries (Lemmey et al., 2018). Our functional data were consistent with upregulation of PAR2 gene expression in aortas of ZDSD relative to controls (Figure 3.17). Our data are also corroborated by another study which found increased PAR2 protein and mRNA expression in aortas from nonobese diabetic mice, paralleled by increased PAR2 induced vasodilation with disease severity (glycosuria) (Roviezzo et al., 2005). Our PAR2-AP data show the effects of hyperglycemia and T2D on vascular function differed with endothelial GPCR as previously described (Chapter 2). This may be reconciled with heterogenous PAR2-mediated vascular function at differing ages which has been presented in a metabolic syndrome rat model (Maruyama et al., 2017). PAR2 may also be closely tied to ACh-induced relaxation as a study found that the inhibition of blood coagulation factor X,

which mediates vascular function through PAR2, improved ACh-mediated vasodilation in streptozotocin-induced diabetic mice (Pham et al., 2019).

The present study found increased PAR2 expression in aortas of ZDSD (Figure 3.17). PAR2 has several roles in cardiovascular disorders and has been investigated in models of genetic and induced hypertension, stroke, and atherosclerosis. In hypertension, PAR2 may be protective in cerebral vasculature as *in vivo* studies of spontaneously hypertensive rat basilar arteries found that PAR2 function was preserved (Sobey et al., 1999). In *ex vivo* studies, PAR2-mediated vasodilation in second order mesenteric arteries are also preserved or much less reduced than ACh in induced models of hypertension (chronic Angiotensin II treatment) (Chia et al., 2011), and genetic models of hypertension (McGuire et al., 2007) respectively. Chia et al. also found increased PAR2 expression in mesenteric arterial arcades. However, in another *ex vivo* study PAR2 function was impaired in aortas of hypertensive rats (Ando et al., 2018). Moreover, infusing mice with 2fLIGRLO (6nmol/kg/min for 7 days) has also decreased ACh-mediated vasodilation in aortas (Hughes et al., 2013). PAR2 also continued to induce vasodilation in a model of hemorrhagic stroke and was not affected with various treatments for hypertension (Smeda & McGuire, 2007). With regards to atherosclerosis, HFD induced increased expression of PAR2 in both mice aortas and human coronary smooth muscle cells (Indrakusuma et al., 2017). Subsequent activation of these cells induced inflammation (increased levels of COX2) and proliferation. PAR2 deficiency also attenuates the development of atherosclerosis in mice by reducing proatherogenic cytokines and macrophage content in lesions (Jones et al., 2018). This is corroborated by evidence of PAR2 being linked to the production of reactive oxygen species in human umbilical vein endothelial cells (Banfi et al., 2009) and coronary arterioles of mice (Park et al., 2011). PAR2 mechanisms and functions are dependent on the conditions of the local environment since the endogenous activators of PAR2 are local serine proteinases. Future studies may focus on understanding the endothelium PAR2 signaling pathways and responses in order to assess therapeutic usefulness in treatment of endothelial dysfunction in T2D.

3.5.4 COX and thromboxane synthase inhibition

Treatments with the cyclooxygenase inhibitor, indomethacin, provided information into the mechanisms by which hyperglycemia affects vasodilation. Exclusive changes in the ACh CRC of hyperglycemic animal were only observed in the proximal saphenous artery (Figure 3.11B). The COX-inhibition treatment decreased ACh sensitivity but increased sensitivity to 2fLIGRLO in the ZDSD rat. Additionally, the indomethacin treatment decreased ACh-mediated relaxations in the femoral artery (Figure 3.11A) but increased ACh-mediated relaxations in the caudal branch (Figure 3.11D) in both the ZDSD and SD rats. Increased ACh-mediated relaxation with indomethacin treatment has been shown in various models of T2D such as the Otsuka Long–Evans Tokushima Fatty rats (Kagota et al., 2000; Matsumoto et al., 2007), and insulin-resistance (ob/ob) mice (Okon et al., 2003). The disease state appears to affect how indomethacin interacts with ACh-mediated vasodilation, as rat models of metabolic syndrome (Vessières et al., 2010) and T2D (Lagaud et al., 2001) show improved vasodilation while their respective healthy counterparts showed decreased vasodilation. We may attribute improvements in vasodilation of the caudal branch with indomethacin primarily by decreasing levels of COX derived vasoconstrictive agents such as thromboxane A₂ (De Vriese et al., 2000b). The opposite may be true in the femoral artery which demonstrated decreased sensitivity ACh with COX inhibition; COX-produced vasodilation (eg. prostacyclin) outweighs that of vasoconstriction. For PAR2-mediated vasodilation, previous studies assessing 2fLIGRLO mediated relaxations with indomethacin have shown decreased vasodilation in coronary arteries of diabetic (db/db) mice (Park et al., 2011) or no changes present in mesenteric Goto-Kakizaki rats (Matsumoto, Ishida, et al., 2009). Our data demonstrate that under conditions of hyperglycemia certain sections (femoral and distal saphenous, Figure 3.10) of vasculature mediate PAR2 vasodilation through prostacyclin pathways; these data are corroborated with our data demonstrating the presence of non-NO pathways in the distal saphenous artery of ZDSD rats.

Ozagrel treated proximal saphenous arteries showed an increase in ACh-sensitivity (Figure 3.11B). Our data were similar to a previous study which administered ozagrel (100 mg/kg/day, p.o.) for 4 weeks in T2D rats (Otsuka Long-Evans Tokushima Fatty)

and found improved ACh-induced relaxation in mesenteric arteries through both EDHF and NO mechanisms in (Matsumoto, Takaoka, et al., 2009). However, our data differs from previous *ex vivo* studies with ozagrel which did not show differences in ACh-mediated vasodilation in the aorta of db/db mice at 10 μ M (Miike et al., 2008) or mesenteric arteries of Angiotensin II-infused mice at 1 μ M (Viridis et al., 2007). An *in vivo* administration of ozagrel (10 and 20mg/kg p.o.) in Wistar rats with bilateral common carotid artery occlusion, a condition T2D is positively associated with (Wagenknecht et al., 2003), also did not affect aortic ACh-mediated vasodilation (Bhatia et al., 2021). Our ozagrel data combined with indomethacin data supports that COX induces prostacyclin in the proximal saphenous artery, which, when inhibited by indomethacin, impairs ACh mediated relaxation in hyperglycemic animals. Another explanation may be the increase of spontaneous NO production, which has been previously found in porcine basilar arterial endothelial cells (Miyamoto et al., 2007). This is the first study to investigate endothelial PAR2 function with ozagrel treatment. 2fLIGRLO sensitivity was unaffected by ozagrel treatment in the proximal saphenous artery which supports differing agonist-induced mechanisms of relaxation. Interestingly, the distal saphenous and caudal branch from ZDSD rats showed decreased sensitivity to 2fLIGRLO with ozagrel treatment. These data suggest that thromboxane synthase inhibition may reduce PAR2 sensitivity in peripheral vasculature.

3.5.5 Aortic endothelial cell gene expression

We explored endothelial cell gene expression in the aortas of ZDSD in comparison to controls (Table 3.11). ZDSD aortas were associated with increased transcript levels of Pgf, Pdgf, Plau and Kit, and decreased transcript levels of Col18a1. Placental growth factor (PGF) is a member of the vascular endothelial growth factor (VEGF) family involved with endothelial cell growth, migration, and proliferation (De Falco, 2012; Fischer et al., 2008). PGF upregulation is associated with angiogenesis in pathological conditions such as in tumour development (Carmeliet et al., 2001). In macrophages, it induces the release of proinflammatory cytokines (e.g. tumor necrosis factor α) and chemokines (e.g. monocyte chemoattractant protein-1) (Carmeliet et al., 2001; Selvaraj et al., 2003). Interestingly, PGF has demonstrated endothelial dependent vasodilation in

aorta of Wistar rats which was changed to vasoconstriction under ischemic conditions (Parenti et al., 2002). PGF expression is also increased in retinal microvascular endothelial cells during conditions of hyperglycemia (B. Zhao et al., 2004). Platelet-derived growth factor (PDGF) shares homologies with VEGF and there has also been evidence of cross-family ligand-receptor binding (Mamer et al., 2017; Tischer et al., 1989). Unlike VEGF, PDGF may only contribute to angiogenesis in certain organs (Heldin & Westermark, 1999); PDGF communication in cardiac endothelial cells indicated increased levels of angiogenic signalling (Edelberg et al., 1998). PDGF has been found to both induce endothelial-mediated vasodilation via NO pathways (Cunningham et al., 1992) or induce vasoconstriction (Berk et al., 1986; Sachinidis et al., 1990) in rat aortas. KIT proto-oncogene receptor tyrosine kinase (KIT) is a receptor for a stem cell factor which has been found in several tumours (Matsui et al., 2004; Miettinen et al., 2000). The role of KIT in mature endothelial cells is unclear however it may play a role in angiogenesis with some similarities to VEGF signalling (Matsui et al., 2004). Plasminogen activator, urokinase (Plau) contributes to the regulation of angiogenesis (Langer et al., 1993) and up-regulates its own expression (Li et al., 2001). However, in human endothelial cells Plau has also been shown to play a role in apoptosis when activated by cleaved high molecular weight kininogen (Cao et al., 2004). Collagen type XVIII alpha 1 chain (Col18a1) is the only gene transcript that we detected as being significantly downregulated in ZDSD rats. The C-terminal domain of Col18a1 contains a 20 kDa sequence of endostatin, which is an inhibitor of endothelial cell proliferation and angiogenesis (O'Reilly et al., 1997; Ständker et al., 1997). The endostatin domain may additionally negatively regulate the non-collagenous domain of Col18a1 which regulates extracellular matrix motility and morphogenesis (Kuo et al., 2001). Overall, these data indicate an increase in angiogenic factors in ZDSD endothelial cells. Angiogenesis in T2D is viewed paradoxically as diabetic retinopathy is the result of excessive angiogenesis and subsequent hemorrhaging, while delayed wound healing, another attribute of T2D, is due to reduced angiogenesis (Cheng & Ma, 2015; Crawford et al., 2009). We may speculate that the increased gene angiogenic factors may be pathological and contribute to diabetic retinopathy. This mechanism may also be compensatory and found in the early stages of T2D due to reduced vascular perfusion to the peripheries.

Additional upregulated endothelial cell genes included Xdh, Agtr1b, and ApoE in the ZDSD. Xanthine dehydrogenase (Xdh) is the substrate reducing form of xanthine oxidoreductase, which is an enzyme that can be converted through proteolysis or sulfhydryl oxidation to the substrate oxidizing form xanthine oxidase (XO) (Nishino, 1994). XO is a source of reactive oxygen species, specifically superoxide, and is proposed to promote atherosclerosis (Landmesser et al., 2007). Endothelial bound XO activity negatively correlated to endothelial-mediated vasodilation in patients with coronary artery disease (Spiekermann et al., 2003) and inhibition of XO improves ACh-mediated vasodilation in hypercholesterolemic rabbit aortas (White et al., 1996). Angiotensin II, the endogenous agonist of angiotensin II receptor type 1b (Agtr1b), another gene which we found that was upregulated, may produce oxidative stress through xanthine oxidase (Landmesser et al., 2007). Angiotensin II receptor 1 (AT1) produces vasoconstriction and is classified into two different subtypes a and b, the latter being found in the endothelium (Pueyo et al., 1996). Inhibition of angiotensin II receptor 1 (AT1) reduces insulin resistance in obese Zucker rats (Henriksen et al., 2001). AT1 has been suggested to mediate apoptosis and may inhibit eNOS activity (Marrero et al., 1999; Watanabe et al., 2005). Apolipoprotein E (ApoE) is a plasma protein that is a ligand for low density lipoprotein (LDL) receptors and in the cardiovascular system, it can increase the risk of atherosclerosis (Bennet et al., 2007; Mahley, 1988, 2016). Increases in ApoE can lead to hyperlipidemia, which corroborates previous studies in the ZDSD that showed increased free fatty acids, cholesterol, and triglycerides (L. Han et al., 2020; Peterson et al., 2015; Reinwald et al., 2009). Specific to the endothelium, ApoE can increase eNOS production to increase NO-dependent vasodilation by reducing inhibitory caveolin-eNOS interactions (Yue et al., 2012). However, aged ApoE deficient mice with established atherosclerosis have also shown decline in ACh-mediated vasodilation (Crauwels et al., 2003; Meyrelles et al., 2011). Mechanisms of endothelial dysfunction in ApoE deficient mice have been attributed to decreased bioavailability of NO (D'Uscio et al., 2001).

3.5.6 Development of T2D and obesity

Based on our study, a significant difference in endothelium function was detected in the ZDSD within 2 weeks of the end of HFD feeding at 20-21 weeks of age. The specific diet

used in our study (Research Diet D12079B) has not been used before with the ZDSD. Its composition differs in total fat calories and the sources of fat is milk fat versus lard. However, the Research Diet D12079B has been used as a Western diet for mice (Furuhashi et al., 2007; Heinonen et al., 2014). Our endothelial dysfunction data is consistent with Davidson et al.'s study which found reduced ACh relaxation in epineurial arteries of 34-week-old ZDSD after a 6 week HFD feeding period (between 16-22 weeks of age). The introduction of a HFD for a short period between 16-19 weeks of age has been used to accelerate diabetes development in order to reduce the time-frame for study and reduce variability within cohorts of ZDSD (Bhamb et al., 2019; Glaeser et al., 2020; Hammond et al., 2014; Suckow et al., 2017). We found that diabetic blood glucose criterion were satisfied in 90% of the ZDSD by 20 weeks of age. The blood glucose levels of SD controls with the same protocol remained unchanged over the time-course of this study. Therefore, the ZDSD with the HFD protocol described in this study is suitable for use as a model system for further investigation of T2D and endothelium dysfunction, especially for treatments and therapeutics.

ZDSD are obese and reported to develop additional characteristics of metabolic syndrome in older animals (S. Chatterjee et al., 2017; Peterson et al., 2015). In the present study, ZDSD rats demonstrated lower body weight at the time of the experiment (20-21 weeks of age) compared to SD rats (Table 3.3). However, total body weight may not be reflective of obesity in rat models and further information on the body composition is necessary in rat models (Gerbaix et al., 2010); both diabetic and non-diabetic ZDSD rats demonstrated elevated body weights at 17 weeks (Suckow et al., 2017). Waist circumference and more generally, obesity correlates with dual-energy X-ray absorptiometry measurements of several depots of fat in rats (Gerbaix et al., 2010) and is associated with increases in cardiovascular disease in humans (T. S. Han et al., 1995; Perticone et al., 2001). While ZDSD did not demonstrate greater abdominal circumference, previous studies found an greater epididymal fat depots in ZDSD compared to control as the model aged (between 26-33 weeks of age) (L. Han et al., 2020; Reinwald et al., 2009). We would expect that elevated abdominal circumference are more apparent at later ages of the ZDSD from our study. Additionally, ZDSD demonstrated elevated abdominal circumference/body length ratio, which is an index of

abdominal obesity (Kagota et al., 2019). Visceral fat and organ weights have also been previously compared in studies examining the obesity phenotype in ZDSD. While we did not observe differences in the total heart mass, we observed a greater left ventricle/total heart mass ratio, which is indicative of hypertrophy and potentially the presence of hypertension (Doggrell & Brown, 1998). We may expect an increased heart mass at later ages of the ZDSD since another study found 26-week-old ZDSD and ZDF demonstrated greater heart mass compared to controls (nondiabetic or lean control groups) using dual-energy X-ray absorptiometry (L. Han et al., 2020). Additionally, the kidney, liver, heart, peritoneal, and retroperitoneal fat depot weights (normalized to body mass) were larger in ZDSD and ZDF compared to the controls (nondiabetic or lean control groups) (L. Han et al., 2020; Reinwald et al., 2009).

3.5.7 Significance of study

Cardiovascular diseases (coronary heart disease, ischemic stroke) associated with T2D are a major causes of morbidity and mortality and is associated with reduced vasodilation (De Vriese et al., 2000b). Furthering the understanding of endothelial regulation of blood flow to peripheral vasculature under hyperglycemic conditions is essential especially in the early developing stages of diabetes/prediabetes and is relevant for the development of preventative therapies. Preservation of peripheral arterial blood flow to limbs could have profound effects for diabetic care, particularly avoiding limb amputations in critical limb ischemia (Brem & Tomic-Canic, 2007; Game, 2012). This study looked at the arteries that feed the blood supply to the microvasculature of skeletal muscle. Endothelial dysfunction may have profound effects gas-exchange, capillary network blood flow, and glucose uptake at the interface of capillaries and skeletal muscle. Further investigations of the arterioles and capillary networks in ZDSD are warranted.

3.6 Conclusion

Endothelial dysfunction is present throughout the arteries supplying the hindlimb of ZDSD. Vascular function is dependent on the GPCR agonist and PAR2 sensitivity and expression were upregulated in ZDSD. Various potential mechanisms or balance of mechanisms exist for the regulation of vascular tone in the saphenous artery and its

branches. The endothelial cell gene expression patterns in ZDSD aorta suggest large scale change to endothelium functions with T2D including those involving angiogenesis, cytokine production, and cell differentiation.

Chapter 4

4 Summary of thesis

Overall, the results of our studies reveal evidence of impaired endothelium-mediated smooth muscle relaxation in hindlimb vasculature of ageing (Chapter 2) and T2D rats (Chapter 3). However, the effects of age and T2D on endothelial function are dependent on the GPCR. While we identified reduced ACh to muscarinic receptor mediated vasodilation in hindlimb vasculature, we found increased sensitivity to PAR2-mediated vasodilation. Our results demonstrate the presence of non-NO mediated pathways of vasodilation in the vasculature studied. The distal saphenous artery and caudal branch of the saphenous artery showed residual ACh-mediated relaxation when NOS was inhibited in control animals. Additionally, the basal NO modulation of vasoconstrictor tone was decreased with age in the saphenous artery, but was not affected in its caudal branches. Our results appear to confirm that non-NO mediated vasodilation are more predominant in distal and peripheral vasculature of the hindlimb (Hill et al., 2001). Both NO and non-NO mechanisms appear to be impaired in peripheral vasculature in T2D. ZDSD proximal saphenous arteries and NOS inhibitor treated vessels were more sensitive to endothelial-independent induced vasodilation indicating potential compensatory mechanisms with reduced NO. Indomethacin and ozagrel treatments did not repair endothelial dysfunction in ZDSD but provided insight on mechanisms of vasodilation in hindlimb arteries (e.g. prostacyclin in distal saphenous arteries). Aortic gene expression of PAR2 were consistent with our wire myography studies. Other genes that differed provide further insight on endothelial function with T2D, including with broad roles in angiogenesis, apoptosis, vasoreactivity, among others.

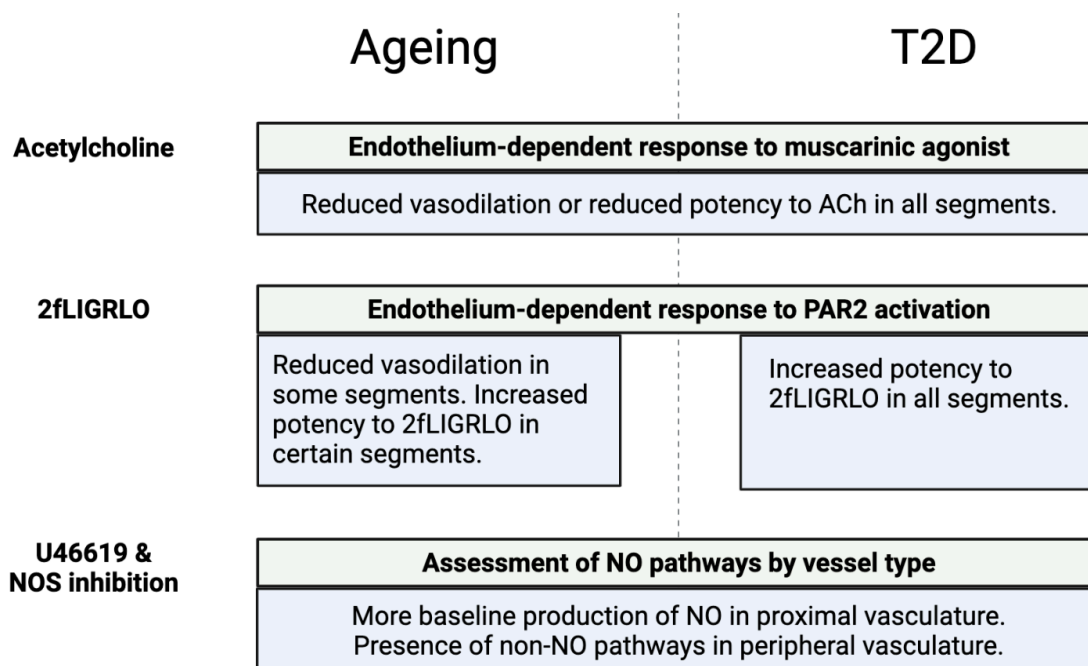


Figure 4.1 Summary of thesis

4.1 Significance

Cardiovascular diseases are the leading cause of death globally and the risk of cardiovascular disease increases with age. Type 2 diabetes is a major risk factor of cardiovascular disease. Given that skeletal muscle glucose uptake represents a great majority of glucose metabolism in the body (Thiebaud et al., 1982), understanding the pharmacological pathways of vascular regulation in this area may lead to synthesis of new therapeutics. Furthering our knowledge of vasculature supplying the extremities is also essential in context of advancing therapies of peripheral arterial disease, which are associated with stroke and myocardial infarction. This is the first study to demonstrate decreased vasodilation and differences in vasoreactivity within the saphenous artery and branches in Sprague Dawley rat. This is also the first study to focus on endothelial function in the Zucker Diabetic Sprague Dawley rat. Our data presents evidence that ZSDS demonstrate endothelial dysfunction in the femoral, saphenous, and caudal branch of the saphenous artery. Finally, we have advanced the knowledge on mechanisms of PAR2-mediated vasodilation. ZSDS demonstrated increased PAR2 sensitivity and

increased PAR2 gene expression in aortas. This is also the first study to employ the ozagrel treatment with PAR2-AP to examine endothelial function. PAR2 may be a therapeutic target for vascular health in the future.

The ZDSD is a relatively novel model of T2D which develops hyperglycemia that is accelerated through the introduction of a high fat diet. We identified that 90% of the ZDSD rats developed hyperglycemia by 20 weeks of age, while controls that received the same diet (SD rats) maintained a lower blood glucose level. Male ZDSD rats develop hyperglycemia markedly later than ZDF rats which develop hyperglycemia between 8-10 weeks of age (King, 2012). The development of hyperglycemia in the ZDSD model qualitatively resembles prediabetic changes of blood glucose concentration and insulin sensitivity that occur in humans (Choy et al., 2016; L. Han et al., 2020; Peterson et al., 2015). Additionally, the extended period of development of T2D in ZDSD rats as opposed to shorter periods in other models, has led to uncovering the merit of using the ZDSD to study longer term developmental changes such as bone turnover and skeletal development (Reinwald et al., 2009). One consideration in using the ZDSD is the sex-related differences in the development of hyperglycemia. Like ZDF rats, female ZDSD are more resistant in developing T2D and require the implementation of a HFD (Gallant et al., 2014). Only two studies have currently studied the development of T2D in female ZDSD and found hyperglycemia at 32 weeks of age with a 12-week HFD feeding period (Gallant et al., 2014; Gonzalez et al., 2014). Overall, the age-dependent development of hyperglycemia in the ZDSD rat requires further refinement, but the information currently available are indicative of the ZDSD presenting as an advantageous novel model of T2D.

4.2 Future work

The results from this study indicate that hindlimb vasculature of aged SD and T2D ZDSD demonstrate evidence of endothelial dysfunction. We have shown that the saphenous artery and caudal branches are targets that may be used to examine endothelial dysfunction in the future. However, considerations should be taken as separate segments of the saphenous artery and its branches demonstrate different vasoreactivity responses to GPCRs agonists. In particular, we found that larger and more proximal arteries such as the femoral artery predominantly use NO pathways to modulate vascular tone, which

differ from distal vasculature demonstrate different mechanisms of than those of the caudal branch of the saphenous artery which may use prostacyclin and EDHF pathways. These data will be of greatest significance for studies to further pharmacological understanding on EDHF which increases as a gradient from proximal to distal vasculature (Hill, Phillips, and Sandow 2001). Furthermore, arteries and microvasculature (arterioles, capillaries) branching away from the saphenous artery to feed the medial thigh muscles (e.g. gracilis) (Kochi et al., 2013) and caudal branches may be investigated, as non-NO mechanisms are likely to be even more pronounced in peripheral vasculature. Broadly, these data will contribute to the physiological understanding of skeletal muscle perfusion, which has already shown increased level with oxygen demand (Bockman, 1983; Mohrman & Regal, 1988). These data will also provide insight on mechanisms impaired in cardiovascular disorders such as peripheral arterial disease (Chapter 1.1.2) and may be investigated in T2D models to better understand glucose regulation and insulin sensitivity (Chapter 1.1.3).

Since we have identified endothelial dysfunction in hindlimb arteries of aged and T2D models, future studies may focus on targetting pharmacological pathways to restore endothelial function. While we found that inhibition of COX (indomethacin) and thromboxane synthase (ozagrel) did not restore endothelial function in ZDSD, these pathways may still be assessed with *in vivo* treatments. For one, omega-3 polyunsaturated fatty acids such as eicosapentaenoic acid are metabolized by COX to produce protective prostanoids; the oral intake of these compounds improved endothelial function in the femoral artery of aged rats (Gaertner et al., 2020). The oral administration of glycine, a compound to reduce oxidative stress, has also improved endothelial function in aged rats (Gómez-Zamudio et al., 2015). Given that we found that distal vasculature demonstrate impairments in both NO and non-NO pathways, EDHF may also be targeted in peripheral vasculature. Notably, a previous study has identified improved EDHF-type relaxation of mesenteric arteries in ZDF rats when vessels were treated with NS309, an activator of small-conductance, calcium-activated potassium channel (Brøndum et al., 2010). Other more rudimentary methods such as exercise or diet-restriction have also improved endothelial-mediated vasodilation (Durrant et al., 2009; Sakamoto et al., 1998) and would be relevant to study in hindlimb arteries given that they supply the skeletal muscle.

We identified that PAR2 function was upregulated in the hindlimb vasculature and gene expression was increased in the aorta of ZDSD. These data add to existing literature that have found upregulated PAR2 in various models of cardiovascular (Chia et al., 2011; Sobey et al., 1999) and metabolic (Maruyama et al., 2017) disorders, including T2D (Kagota et al., 2011; Matsumoto, Ishida, et al., 2009; Park et al., 2011). While our data indicates that PAR2 is vasoprotective and vasodilation is preserved in spite of endothelial dysfunction with T2D, PAR2 mechanisms and functions are dependent on the conditions of the local environment (Chapter 3). There is also heterogeneity in the expression of PAR2 at different ages (Maruyama et al., 2017), as we have roughly demonstrated between Chapter 2 and Chapter 3 results. Future studies on the mechanisms of PAR2 are necessary to assess its potential of as a therapeutic target for vascular health. This may involve using *in vivo* treatments of PAR2-AP to determine whether there are changes to vasoreactivity as previously described (Smeda & McGuire, 2007).

Finally, in a T2D model, we have identified upregulation and downregulation of endothelial cell genes in the aorta. These genes have roles in cardiovascular health including angiogenesis, atherosclerosis, and GPCR function. Future studies may confirm gene upregulation with immunohistochemistry for levels of protein. Specifically, genes that were upregulated and related to angiogenesis (Pgf, Pdgf, Plau, Kit) may be related to diabetic retinopathy (Crawford et al., 2009) and should be investigated in retinal vasculature in the future.

Overall, the results of our study address our research question on endothelial dysfunction with ageing and T2D in hindlimb arteries with different GPCRs. Our conclusions offer a wide field of future directions to further knowledge on endothelial function, skeletal muscle perfusion and peripheral vascular disease, ageing and T2D, and GPCRs.

References

- Adelnia, F., Cameron, D., Bergeron, C. M., Fishbein, K. W., Spencer, R. G., Reiter, D. A., & Ferrucci, L. (2019). The role of muscle perfusion in the age-associated decline of mitochondrial function in healthy individuals. *Frontiers in Physiology, 10*(APR), 1–9. <https://doi.org/10.3389/fphys.2019.00427>
- Al-Ani, B., Saifeddine, M., & Hollenberg, M. D. (1995). Detection of functional receptors for the proteinase-activated-receptor-2-activating polypeptide, SLIGRL-NH₂, in rat vascular and gastric smooth muscle. *Canadian Journal of Physiology and Pharmacology, 73*(8), 1203–1207. <https://doi.org/10.1139/y95-172>
- Aljada, A., & Dandona, P. (2000). Effect of insulin on human aortic endothelial nitric oxide synthase. *Metabolism, 49*(2), 147–150. [https://doi.org/10.1016/S0026-0495\(00\)91039-4](https://doi.org/10.1016/S0026-0495(00)91039-4)
- American Diabetes Association. (2021). *Hyperglycemia (High Blood Glucose)*. <https://www.diabetes.org/healthy-living/medication-treatments/blood-glucose-testing-and-control/hyperglycemia>
- Ando, M., Matsumoto, T., Kobayashi, S., Iguchi, M., Taguchi, K., & Kobayashi, T. (2018). Impairment of protease-activated receptor 2-induced relaxation of aortas of aged spontaneously hypertensive rat. *Biological and Pharmaceutical Bulletin, 41*(5), 815–819. <https://doi.org/10.1248/bpb.b17-00987>
- Aronow, W. S. (2007). Peripheral arterial disease in the elderly. In *Clinical interventions in aging* (Vol. 2, Issue 4, pp. 645–654). <https://doi.org/10.1161/01.atv.18.2.185>
- Aronow, W. S. (2012). Peripheral arterial disease of the lower extremities. *Archives of Medical Science, 8*(2), 375–388. <https://doi.org/10.5114/aoms.2012.28568>
- Arribas, S. M., Vila, E., & McGrath, J. C. (1997). Impairment of vasodilator function in basilar arteries from aged rats. *Stroke, 28*(9), 1812–1820. <https://doi.org/10.1161/01.STR.28.9.1812>
- Banerjee, A., Fowkes, F. G., & Rothwell, P. M. (2010). Associations between peripheral artery disease and ischemic stroke: Implications for primary and secondary prevention. *Stroke, 41*(9), 2102–2107. <https://doi.org/10.1161/STROKEAHA.110.582627>
- Banfi, C., Brioschi, M., Barbieri, S. S., Eligini, S., Barcella, S., Tremoli, E., Colli, S., & Mussoni, L. (2009). Mitochondrial reactive oxygen species: A common pathway for PAR1- and PAR2-mediated tissue factor induction in human endothelial cells. *Journal of Thrombosis and Haemostasis, 7*(1), 206–216. <https://doi.org/10.1111/j.1538-7836.2008.03204.x>
- Baron, A. D., & Brechtel, G. (1993). Insulin differentially regulates systemic and skeletal

- muscle vascular resistance. *American Journal of Physiology-Endocrinology and Metabolism*, 265(1), E61–E67. <https://doi.org/10.1152/ajpendo.1993.265.1.E61>
- Barton, M., Cosentino, F., Brandes, R. P., Moreau, P., Shaw, S., & Lüscher, T. F. (1997). Anatomic Heterogeneity of Vascular Aging. *Hypertension*, 30(4), 817–824. <https://doi.org/10.1161/01.hyp.30.4.817>
- Beckman, J. S., & Koppenol, W. H. (1996). Nitric oxide, superoxide, and peroxynitrite: the good, the bad, and ugly. *American Journal of Physiology-Cell Physiology*, 271(5), C1424–C1437. <https://doi.org/10.1152/ajpcell.1996.271.5.C1424>
- Bennet, A. M., Di Angelantonio, E., Ye, Z., Wensley, F., Dahlin, A., Ahlbom, A., Keavney, B., Collins, R., Wiman, B., de Faire, U., & Danesh, J. (2007). Association of Apolipoprotein E Genotypes With Lipid Levels and Coronary Risk. *JAMA*, 298(11), 1300. <https://doi.org/10.1001/jama.298.11.1300>
- Berk, B. C., Wayne Alexander, R., Brock, T. A., Gimbrone, M. A., & Clinton Webb, R. (1986). Vasoconstriction: A new activity for platelet-derived growth factor. *Science*, 232(4746), 87–90. <https://doi.org/10.1126/science.3485309>
- Berridge, M. J. (2016). The inositol trisphosphate/calcium signaling pathway in health and disease. *Physiological Reviews*, 96(4), 1261–1296. <https://doi.org/10.1152/physrev.00006.2016>
- Bhamb, N., Kanim, L. E. A., Maldonado, R. C., Nelson, T. J., Salehi, K., Glaeser, J. D., & Metzger, M. F. (2019). The impact of type 2 diabetes on bone metabolism and growth after spinal fusion. *Spine Journal*, 19(6), 1085–1093. <https://doi.org/10.1016/j.spinee.2018.12.003>
- Bhatia, P., Kaur, G., & Singh, N. (2021). Ozagrel a thromboxane A2 synthase inhibitor extenuates endothelial dysfunction, oxidative stress and neuroinflammation in rat model of bilateral common carotid artery occlusion induced vascular dementia. *Vascular Pharmacology*, 137(June 2020), 106827. <https://doi.org/10.1016/j.vph.2020.106827>
- Bierhaus, A., Humpert, P. M., Morcos, M., Wendt, T., Chavakis, T., Arnold, B., Stern, D. M., & Nawroth, P. P. (2005). Understanding RAGE, the receptor for advanced glycation end products. *Journal of Molecular Medicine*, 83(11), 876–886. <https://doi.org/10.1007/s00109-005-0688-7>
- Blackwell, K. A., Sorenson, J. P., Richardson, D. M., Smith, L. A., Suda, O., Nath, K., & Katusic, Z. S. (2004). Mechanisms of aging-induced impairment of endothelium-dependent relaxation: Role of tetrahydrobiopterin. *American Journal of Physiology - Heart and Circulatory Physiology*, 287(6 56-6), 2448–2453. <https://doi.org/10.1152/ajpheart.00248.2004>
- Blaslov, K., Naranda, F. S., Kruljac, I., & Renar, I. P. (2018). Treatment approach to type 2 diabetes: Past, present and future. *World Journal of Diabetes*, 9(12), 209–219.

<https://doi.org/10.4239/wjd.v9.i12.209>

- Bliss, M. R. (1998). Hyperaemia. *Journal of Tissue Viability*, 8(4), 4–13.
[https://doi.org/10.1016/S0965-206X\(98\)80028-4](https://doi.org/10.1016/S0965-206X(98)80028-4)
- Bockman, E. L. (1983). Blood flow and oxygen consumption in active soleus and gracilis muscles in cats. *American Journal of Physiology - Heart and Circulatory Physiology*, 13(4). <https://doi.org/10.1152/ajpheart.1983.244.4.h546>
- Bohlen, H. G., & Lash, J. M. (1995). Endothelial-dependent vasodilation is preserved in non-insulin-dependent Zucker fatty diabetic rats. *American Journal of Physiology - Heart and Circulatory Physiology*, 268(6 37-6).
<https://doi.org/10.1152/ajpheart.1995.268.6.h2366>
- Bonetti, P. O., Lerman, L. O., & Lerman, A. (2003). Endothelial dysfunction: A marker of atherosclerotic risk. *Arteriosclerosis, Thrombosis, and Vascular Biology*, 23(2), 168–175. <https://doi.org/10.1161/01.ATV.0000051384.43104.FC>
- Brandes, R. P. (2014). Endothelial dysfunction and hypertension. *Hypertension*, 64(5), 924–928. <https://doi.org/10.1161/HYPERTENSIONAHA.114.03575>
- Brandes, R. P., Fleming, I., & Busse, R. (2005). Endothelial aging. *Cardiovascular Research*, 66(2), 286–294. <https://doi.org/10.1016/j.cardiores.2004.12.027>
- Brandes, R. P., Kim, D. Y., Schmitz-Winnenthal, F. H., Amidi, M., Gödecke, A., Mülsch, A., & Busse, R. (2000). Increased nitrovasodilator sensitivity in endothelial nitric oxide synthase knockout mice: Role of soluble guanylyl cyclase. *Hypertension*, 35(1 II), 231–236. <https://doi.org/10.1161/01.hyp.35.1.231>
- Brøndum, E., Kold-Petersen, H., Simonsen, U., & Aalkjaer, C. (2010). NS309 restores EDHF-type relaxation in mesenteric small arteries from type 2 diabetic ZDF rats. *British Journal of Pharmacology*, 159(1), 154–165. <https://doi.org/10.1111/j.1476-5381.2009.00525.x>
- Bucci, M., Gratton, J. P., Rudic, R. D., Acevedo, L., Roviezzo, F., Cirino, G., & Sessa, W. C. (2000). In vivo delivery of the caveolin-1 scaffolding domain inhibits nitric oxide synthesis and reduces inflammation. *Nature Medicine*, 6(12), 1362–1367.
<https://doi.org/10.1038/82176>
- Burnham, M. P., Johnson, I. T., & Weston, A. H. (2006). Impaired small-conductance Ca²⁺-activated K⁺ channel-dependent EDHF responses in Type II diabetic ZDF rats. *British Journal of Pharmacology*, 148(4), 434–441.
<https://doi.org/10.1038/sj.bjp.0706748>
- Calles-Escandon, J., & Cipolla, M. (2001). Diabetes and endothelial dysfunction: A clinical perspective. *Endocrine Reviews*, 22(1), 36–52.
<https://doi.org/10.1210/edrv.22.1.0417>

- Cao, D. J., Guo, Y. L., & Colman, R. W. (2004). Urokinase-type plasminogen activator receptor is involved in mediating the apoptotic effect of cleaved high molecular weight kininogen in human endothelial cells. *Circulation Research*, *94*(9), 1227–1234. <https://doi.org/10.1161/01.RES.0000126567.75232.46>
- Carmeliet, P., Moons, L., Luttun, A., Vincenti, V., Compernelle, V., De Mol, M., Wu, Y., Bono, F., Devy, L., Beck, H., Scholz, D., Acker, T., Dipalma, T., Dewerchin, M., Noel, A., Stalmans, I., Barra, A., Blacher, S., Vandendriessche, T., ... Persico, M. G. (2001). Synergism between vascular endothelial growth factor and placental growth factor contributes to angiogenesis and plasma extravasation in pathological conditions. *Nature Medicine*, *7*(5), 575–583. <https://doi.org/10.1038/87904>
- Centers for Disease Control and Prevention. (2020). *National Diabetes Statistics Report, 2020*. <https://www.cdc.gov/diabetes/data/statistics-report/index.html>
- Chatterjee, A., & Catravas, J. D. (2008). Endothelial nitric oxide (NO) and its pathophysiologic regulation. In *Vascular Pharmacology* (Vol. 49, Issues 4–6, pp. 134–140). <https://doi.org/10.1016/j.vph.2008.06.008>
- Chatterjee, S., Khunti, K., & Davies, M. J. (2017). Type 2 diabetes. *The Lancet*, *389*(10085), 2239–2251. [https://doi.org/10.1016/S0140-6736\(17\)30058-2](https://doi.org/10.1016/S0140-6736(17)30058-2)
- Chen, G., Suzuki, H., & Weston, A. H. (1988). Acetylcholine releases endothelium-derived hyperpolarizing factor and EDRF from rat blood vessels. *British Journal of Pharmacology*, *95*(4), 1165–1174. <https://doi.org/10.1111/j.1476-5381.1988.tb11752.x>
- Cheng, R., & Ma, J. (2015). Angiogenesis in diabetes and obesity. *Reviews in Endocrine and Metabolic Disorders*, *16*(1), 67–75. <https://doi.org/10.1007/s11154-015-9310-7>
- Chennupati, R., Lamers, W. H., Koehler, S. E., & De Mey, J. G. R. (2013). Endothelium-dependent hyperpolarization-related relaxations diminish with age in murine saphenous arteries of both sexes. *British Journal of Pharmacology*, *169*(7), 1486–1499. <https://doi.org/10.1111/bph.12175>
- Chia, E., Kagota, S., Wijekoon, E. P., & McGuire, J. J. (2011). Protection of protease-activated receptor 2 mediated vasodilatation against angiotensin II-induced vascular dysfunction in mice. *BMC Pharmacology*, *11*(1), 10. <https://doi.org/10.1186/1471-2210-11-10>
- Chinellato, A., Pandolfo, L., Ragazzi, E., Zambonin, M. R., Frolidi, G., De Biasi, M., Caparrotta, L., & Fassina, G. (1991). Effect of Age on Rabbit Aortic Responses to Relaxant Endothelium-Dependent and Endothelium-Independent Agents. *Journal of Vascular Research*, *28*(5), 358–365. <https://doi.org/10.1159/000158882>
- Choy, S., de Winter, W., Karlsson, M. O., & Kjellsson, M. C. (2016). Modeling the Disease Progression from Healthy to Overt Diabetes in ZDSD Rats. *AAPS Journal*, *18*(5), 1203–1212. <https://doi.org/10.1208/s12248-016-9931-0>

- Cicala, C. (2002). Protease activated receptor 2 and the cardiovascular system. *British Journal of Pharmacology*, *135*(1), 14–20. <https://doi.org/10.1038/sj.bjp.0704438>
- Collins, P., Griffith, T. M., Henderson, A. H., & Lewis, M. J. (1986). Endothelium-derived relaxing factor alters calcium fluxes in rabbit aorta: a cyclic guanosine monophosphate-mediated effect. *The Journal of Physiology*, *381*(1), 427–437. <https://doi.org/10.1113/jphysiol.1986.sp016336>
- Coppey, L. J., Gellett, J. S., Davidson, E. P., Dunlap, J. A., & Yorek, M. A. (2002). Changes in endoneurial blood flow, motor nerve conduction velocity and vascular relaxation of epineurial arterioles of the sciatic nerve in ZDF-obese diabetic rats. *Diabetes/Metabolism Research and Reviews*, *18*(1), 49–56. <https://doi.org/10.1002/dmrr.257>
- Cottrell, G. S., Amadesi, S., Schmidlin, F., & Bunnett, N. (2003). Protease-activated receptor 2: activation, signalling and function. *Biochemical Society Transactions*, *31*(6), 1191–1197. <https://doi.org/10.1042/bst0311191>
- Crauwels, H. M., Van Hove, C. E., Holvoet, P., Herman, A. G., & Bult, H. (2003). Plaque-associated endothelial dysfunction in apolipoprotein E-deficient mice on a regular diet. Effect of human apolipoprotein AI. *Cardiovascular Research*, *59*(1), 189–199. [https://doi.org/10.1016/S0008-6363\(03\)00353-5](https://doi.org/10.1016/S0008-6363(03)00353-5)
- Crawford, T., Alfaro III, D., Kerrison, J., & Jablon, E. (2009). Diabetic Retinopathy and Angiogenesis. *Current Diabetes Reviews*, *5*(1), 8–13. <https://doi.org/10.2174/157339909787314149>
- Creecy, A., Uppuganti, S., Merkel, A. R., O’Neal, D., Makowski, A. J., Granke, M., Voziyan, P., & Nyman, J. S. (2016). Changes in the Fracture Resistance of Bone with the Progression of Type 2 Diabetes in the ZDSD Rat. *Calcified Tissue International*, *99*(3), 289–301. <https://doi.org/10.1007/s00223-016-0149-z>
- Csiszar, A., Ungvari, Z., Edwards, J. G., Kaminski, P., Wolin, M. S., Koller, A., & Kaley, G. (2002). Aging-induced phenotypic changes and oxidative stress impair coronary arteriolar function. *Circulation Research*, *90*(11), 1159–1166. <https://doi.org/10.1161/01.RES.0000020401.61826.EA>
- Cunningham, L. D., Brecher, P., & Cohen, R. A. (1992). Platelet-derived growth factor receptors on macrovascular endothelial cells mediate relaxation via nitric oxide in rat aorta. *Journal of Clinical Investigation*, *89*(3), 878–882. <https://doi.org/10.1172/JCI115667>
- D’Uscio, L. V., Baker, T. A., Mantilla, C. B., Smith, L., Weiler, D., Sieck, G. C., & Katusic, Z. S. (2001). Mechanism of endothelial dysfunction in apolipoprotein E-deficient mice. *Arteriosclerosis, Thrombosis, and Vascular Biology*, *21*(6), 1017–1022. <https://doi.org/10.1161/01.ATV.21.6.1017>
- Davidson, E. P., Coppey, L. J., Holmes, A., Lupachyk, S., Dake, B. L., Oltman, C. L.,

- Peterson, R. G., & Yorek, M. A. (2014). Characterization of diabetic neuropathy in the Zucker diabetic Sprague-Dawley rat: A new animal model for type 2 diabetes. *Journal of Diabetes Research*, 2014. <https://doi.org/10.1155/2014/714273>
- Davignon, J., & Ganz, P. (2004). Role of endothelial dysfunction in atherosclerosis. *Circulation*, 109(23 SUPPL.). <https://doi.org/10.1161/01.cir.0000131515.03336.f8>
- Davis, J. E., Cain, J., Banz, W. J., & Peterson, R. G. (2013). Age-Related Differences in Response to High-Fat Feeding on Adipose Tissue and Metabolic Profile in ZSD Rats. *ISRN Obesity*, 2013, 1–8. <https://doi.org/10.1155/2013/584547>
- De Falco, S. (2012). The discovery of placenta growth factor and its biological activity. *Experimental and Molecular Medicine*, 44(1), 1–9. <https://doi.org/10.3858/emm.2012.44.1.025>
- De Vriese, A. S., Verbeuren, T. J., Van de Voorde, J., Lameire, N. H., & Vanhoutte, P. M. (2000a). Endothelial dysfunction in diabetes. *British Journal of Pharmacology*, 130(5), 963–974. <https://doi.org/10.1038/sj.bjp.0703393>
- De Vriese, A. S., Verbeuren, T. J., Van de Voorde, J., Lameire, N. H., & Vanhoutte, P. M. (2000b). Endothelial dysfunction in diabetes. *British Journal of Pharmacology*, 130(5), 963–974. <https://doi.org/10.1038/sj.bjp.0703393>
- DeFronzo, R. A., & Tripathy, D. (2009). Skeletal muscle insulin resistance is the primary defect in type 2 diabetes. *Diabetes Care*, 32 Suppl 2. <https://doi.org/10.2337/dc09-s302>
- DeSouza, C. A., Clevenger, C. M., Greiner, J. J., Smith, D. T., Hoetzer, G. L., Shapiro, L. F., & Stauffer, B. L. (2002). Evidence for agonist-specific endothelial vasodilator dysfunction with ageing in healthy humans. *Journal of Physiology*, 542(1), 255–262. <https://doi.org/10.1113/jphysiol.2002.019166>
- Ding, H., & Triggle, C. R. (2005). Endothelial cell dysfunction and the vascular complications associated with type 2 diabetes: assessing the health of the endothelium. *Vascular Health and Risk Management*, 1(1), 55–71. <https://doi.org/10.2147/vhrm.1.1.55.58939>
- Doggrell, S. A., & Brown, L. (1998). Rat models of hypertension, cardiac hypertrophy and failure. *Cardiovascular Research*, 39(1), 89–105. [https://doi.org/10.1016/S0008-6363\(98\)00076-5](https://doi.org/10.1016/S0008-6363(98)00076-5)
- Donato, A. J., Magerko, K. A., Lawson, B. R., Durrant, J. R., Lesniewski, L. A., & Seals, D. R. (2011). SIRT-1 and vascular endothelial dysfunction with ageing in mice and humans. *Journal of Physiology*, 589(18), 4545–4554. <https://doi.org/10.1113/jphysiol.2011.211219>
- Duprez, D. A. (2010). Arterial stiffness and endothelial function: Key players in vascular health. *Hypertension*, 55(3), 612–613.

<https://doi.org/10.1161/HYPERTENSIONAHA.109.144725>

- Durrant, J. R., Seals, D. R., Connell, M. L., Russell, M. J., Lawson, B. R., Folian, B. J., Donato, A. J., & Lesniewski, L. A. (2009). Voluntary wheel running restores endothelial function in conduit arteries of old mice: Direct evidence for reduced oxidative stress, increased superoxide dismutase activity and down-regulation of NADPH oxidase. *Journal of Physiology*, *587*(13), 3271–3285. <https://doi.org/10.1113/jphysiol.2009.169771>
- Edelberg, J. M., Aird, W. C., Wu, W., Rayburn, H., Mamuya, W. S., Mercola, M., & Rosenberg, R. D. (1998). PDGF mediates cardiac microvascular communication. *Journal of Clinical Investigation*, *102*(4), 837–843. <https://doi.org/10.1172/JCI3058>
- Edwards, G., Félétou, M., & Weston, A. H. (2010). Endothelium-derived hyperpolarising factors and associated pathways: A synopsis. *Pflugers Archiv European Journal of Physiology*, *459*(6), 863–879. <https://doi.org/10.1007/s00424-010-0817-1>
- Egashira, K., Inou, T., Hirooka, Y., Kai, H., Sugimachi, M., Suzuki, S., Kuga, T., Urabe, Y., & Takeshita, A. (1993). Effects of age on endothelium-dependent vasodilation of resistance coronary artery by acetylcholine in humans. *Circulation*, *88*(1), 77–81. <https://doi.org/10.1161/01.CIR.88.1.77>
- El-Daly, M., Pulakazhi Venu, V. K., Saifeddine, M., Mihara, K., Kang, S., Fedak, P. W. M., Alston, L. A., Hirota, S. A., Ding, H., Triggle, C. R., & Hollenberg, M. D. (2018). Hyperglycaemic impairment of PAR2-mediated vasodilation: Prevention by inhibition of aortic endothelial sodium-glucose-co-Transporter-2 and minimizing oxidative stress. *Vascular Pharmacology*, *109*(February), 56–71. <https://doi.org/10.1016/j.vph.2018.06.006>
- Enderle, M.-D., Benda, N., Schmuelling, R.-M., Haering, H. U., & Pfohl, M. (1998). Preserved Endothelial Function in IDDM Patients, but Not in NIDDM Patients, Compared With Healthy Subjects. *Diabetes Care*, *21*(2), 271–277. <https://doi.org/10.2337/diacare.21.2.271>
- Félétou, M., & Vanhoutte, P. M. (2007). Endothelium-dependent hyperpolarizations: Past beliefs and present facts. *Annals of Medicine*, *39*(7), 495–516. <https://doi.org/10.1080/07853890701491000>
- Félétou, M., Verbeuren, T. J., & Vanhoutte, P. M. (2009). Endothelium-dependent contractions in SHR: A tale of prostanoid TP and IP receptors. *British Journal of Pharmacology*, *156*(4), 563–574. <https://doi.org/10.1111/j.1476-5381.2008.00060.x>
- Ferrucci, L., Cooper, R., Shardell, M., Simonsick, E. M., Schrack, J. A., & Kuh, D. (2016). Age-related change in mobility: Perspectives from life course epidemiology and geroscience. *Journals of Gerontology - Series A Biological Sciences and Medical Sciences*, *71*(9), 1184–1194. <https://doi.org/10.1093/gerona/glw043>
- Finkel, T., & Holbrook, N. J. (2000). Oxidants, oxidative stress and the biology of

- ageing. *Nature*, 408(6809), 239–247. <https://doi.org/10.1038/35041687>
- Fischer, C., Mazzone, M., Jonckx, B., & Carmeliet, P. (2008). FLT1 and its ligands VEGFB and PlGF: Drug targets for anti-angiogenic therapy? *Nature Reviews Cancer*, 8(12), 942–956. <https://doi.org/10.1038/nrc2524>
- Fujii, K., Ohmori, S., Tominaga, M., Abe, I., Takata, Y., Ohya, Y., Kobayashi, K., & Fujishima, M. (1993). Age-related changes in endothelium-dependent hyperpolarization in the rat mesenteric artery. *American Journal of Physiology-Heart and Circulatory Physiology*, 265(2), H509–H516. <https://doi.org/10.1152/ajpheart.1993.265.2.H509>
- Fujimoto, Y., Donahue, E. P., & Shiota, M. (2004). Defect in glucokinase translocation in Zucker diabetic fatty rats. *American Journal of Physiology-Endocrinology and Metabolism*, 287(3), E414–E423. <https://doi.org/10.1152/ajpendo.00575.2003>
- Furchgott, R., & Zawadzki, J. V. (1980). The obligatory role of endothelial cells in the relaxation of atrial smooth muscle. *Nature*, 288(November), 373–376.
- Furuhashi, M., Tuncman, G., Görgün, C. Z., Makowski, L., Atsumi, G., Vaillancourt, E., Kono, K., Babaev, V. R., Fazio, S., Linton, M. F., Sulsky, R., Robl, J. A., Parker, R. A., & Hotamisligil, G. S. (2007). Treatment of diabetes and atherosclerosis by inhibiting fatty-acid-binding protein aP2. *Nature*, 447(7147), 959–965. <https://doi.org/10.1038/nature05844>
- Gaertner, S., Auger, C., Farooq, M. A., Pollet, B., Khemais-Benkhiat, S., Niazi, Z. R., Schrevens, S., Park, S. H., Toti, F., Stephan, D., & Schini-Kerth, V. B. (2020). Oral intake of EPA:DHA 6:1 by middle-aged rats for one week improves age-related endothelial dysfunction in both the femoral artery and vein: Role of cyclooxygenases. *International Journal of Molecular Sciences*, 21(3), 1–13. <https://doi.org/10.3390/ijms21030920>
- Gallant, K. M. H., Gallant, M. A., Brown, D. M., Sato, A. Y., Williams, J. N., & Burr, D. B. (2014). Raloxifene prevents skeletal fragility in adult female zucker diabetic sprague-dawley rats. *PLoS ONE*, 9(9), 1–7. <https://doi.org/10.1371/journal.pone.0108262>
- Galley, H. F., & Webster, N. R. (2004). Physiology of the endothelium. *British Journal of Anaesthesia*, 93(1), 105–113. <https://doi.org/10.1093/bja/ae163>
- Geraldes, P., & King, G. L. (2010). Activation of protein kinase C isoforms and its impact on diabetic complications. *Circulation Research*, 106(8), 1319–1331. <https://doi.org/10.1161/CIRCRESAHA.110.217117>
- Gerbaix, M., Metz, L., Ringot, E., & Courteix, D. (2010). Visceral fat mass determination in rodent: Validation of dual-energy x-ray absorptiometry and anthropometric techniques in fat and lean rats. *Lipids in Health and Disease*, 9(1), 140. <https://doi.org/10.1186/1476-511X-9-140>

- Gerhard, M., Roddy, M. A., Creager, S. J., & Creager, M. A. (1996). Aging progressively impairs endothelium-dependent vasodilation in forearm resistance vessels of humans. *Hypertension*, 27(4), 849–853. <https://doi.org/10.1161/01.HYP.27.4.849>
- Gimbrone, M. A., & García-Cardeña, G. (2016). Endothelial Cell Dysfunction and the Pathobiology of Atherosclerosis. *Circulation Research*, 118(4), 620–636. <https://doi.org/10.1161/CIRCRESAHA.115.306301>
- Glaeser, J. D., Ju, D., Tawackoli, W., Yang, J. H., Salehi, K., Stefanovic, T., Kanim, L. E. A., Avalos, P., Kaneda, G., Stephan, S., Metzger, M. F., Bae, H. W., & Sheyn, D. (2020). Advanced glycation end product inhibitor pyridoxamine attenuates IVD degeneration in type 2 diabetic rats. *International Journal of Molecular Sciences*, 21(24), 1–15. <https://doi.org/10.3390/ijms21249709>
- Gómez-Zamudio, J. H., García-Macedo, R., Lázaro-Suárez, M., Ibarra-Barajas, M., Kumate, J., & Cruz, M. (2015). Vascular endothelial function is improved by oral glycine treatment in aged rats. *Canadian Journal of Physiology and Pharmacology*, 93(6), 465–473. <https://doi.org/10.1139/cjpp-2014-0393>
- Gonzalez, A. D., Gallant, M. A., Burr, D. B., & Wallace, J. M. (2014). Multiscale analysis of morphology and mechanics in tail tendon from the ZSD rat model of type 2 diabetes. *Journal of Biomechanics*, 47(3), 681–686. <https://doi.org/10.1016/j.jbiomech.2013.11.045>
- Gragasin, F. S., & Davidge, S. T. (2009). The effects of propofol on vascular function in mesenteric arteries of the aging rat. *American Journal of Physiology - Heart and Circulatory Physiology*, 297(1), 466–474. <https://doi.org/10.1152/ajpheart.01317.2008>
- Graier, W. F., Posch, K., Fleischhacker, E., Wascher, T. C., & Kostner, G. M. (1999). Increased superoxide anion formation in endothelial cells during hyperglycemia: An adaptive response or initial step of vascular dysfunction? *Diabetes Research and Clinical Practice*, 45(2–3), 153–160. [https://doi.org/10.1016/S0168-8227\(99\)00045-5](https://doi.org/10.1016/S0168-8227(99)00045-5)
- Guo, F., Moellering, D. R., & Garvey, W. T. (2014). Use of HbA1c for diagnoses of diabetes and prediabetes: comparison with diagnoses based on fasting and 2-hr glucose values and effects of gender, race, and age. *Metabolic Syndrome and Related Disorders*, 12(5), 258–268. <https://doi.org/10.1089/met.2013.0128>
- Hadi, H. A. R., & Al Suwaidi, J. A. (2007). Endothelial dysfunction in diabetes mellitus. *Vascular Health and Risk Management*, 3(6), 853–876. <https://doi.org/10.1055/s-2000-13206>
- Haidet, G. C., Wennberg, P. W., & Rector, T. S. (1995). Aging and vasoreactivity: in vivo responses in the beagle hindlimb. *American Journal of Physiology-Heart and Circulatory Physiology*, 268(1), H92–H99. <https://doi.org/10.1152/ajpheart.1995.268.1.H92>

- Hammond, M. A., Gallant, M. A., Burr, D. B., & Wallace, J. M. (2014). Nanoscale changes in collagen are reflected in physical and mechanical properties of bone at the microscale in diabetic rats. *Bone*, *60*(1), 26–32. <https://doi.org/10.1016/j.bone.2013.11.015>
- Han, L., Bittner, S., Dong, D., Cortez, Y., Bittner, A., Chan, J., Umar, M., Shen, W.-J., Peterson, R. G., Kraemer, F. B., & Azhar, S. (2020). Molecular changes in hepatic metabolism in ZDSD rats—A new polygenic rodent model of obesity, metabolic syndrome, and diabetes. *Biochimica et Biophysica Acta (BBA) - Molecular Basis of Disease*, *1866*(5), 165688. <https://doi.org/10.1016/j.bbadis.2020.165688>
- Han, T. S., Van Leer, E. M., Seidell, J. C., & Lean, M. E. J. (1995). Waist circumference action levels in the identification of cardiovascular risk factors: Prevalence study in a random sample. *Bmj*, *311*(7017), 1401. <https://doi.org/10.1136/bmj.311.7017.1401>
- Harris, M. B., Slack, K. N., Prestosa, D. T., & Hryvniak, D. J. (2010). Resistance training improves femoral artery endothelial dysfunction in aged rats. *European Journal of Applied Physiology*, *108*(3), 533–540. <https://doi.org/10.1007/s00421-009-1250-z>
- Harris, M. I., Klein, R., Welborn, T. A., & Knudman, M. W. (1992). Onset of NIDDM occurs at Least 4-7 yr Before Clinical Diagnosis. *Diabetes Care*, *15*(7), 815–819. <https://doi.org/10.2337/diacare.15.7.815>
- Hatake, K., Kakishita, E., Wakabayashi, I., Sakiyama, N., & Hishida, S. (1990). Effect of aging on endothelium-dependent vascular relaxation of isolated human basilar artery to thrombin and bradykinin. *Stroke*, *21*(7), 1039–1043. <https://doi.org/10.1161/01.STR.21.7.1039>
- Hattori, Y., Kawasaki, H., & Kanno, M. (1999). Increased contractile responses to endothelin-1 and U46619 via a protein kinase C-mediated nifedipine-sensitive pathway in diabetic rat aorta. *Research Communications in Molecular Pathology and Pharmacology*, *104*(1), 73–80. <http://www.ncbi.nlm.nih.gov/pubmed/10604280>
- Heinonen, I., Rinne, P., Ruohonen, S. T., Ruohonen, S., Ahotupa, M., & Savontaus, E. (2014). The effects of equal caloric high fat and western diet on metabolic syndrome, oxidative stress and vascular endothelial function in mice. *Acta Physiologica*, *211*(3), 515–527. <https://doi.org/10.1111/apha.12253>
- Heldin, C. H., & Westermark, B. (1999). Mechanism of action and in vivo role of platelet-derived growth factor. *Physiological Reviews*, *79*(4), 1283–1316. <https://doi.org/10.1152/physrev.1999.79.4.1283>
- Hellingman, A. A., Bastiaansen, A. J. N. M., De Vries, M. R., Seghers, L., Lijkwan, M. A., Löwik, C. W., Hamming, J. F., & Quax, P. H. A. (2010). Variations in surgical procedures for hind limb ischaemia mouse models result in differences in collateral formation. *European Journal of Vascular and Endovascular Surgery*, *40*(6), 796–803. <https://doi.org/10.1016/j.ejvs.2010.07.009>

- Hellsten, Y., Nyberg, M., Jensen, L. G., & Mortensen, S. P. (2012). Vasodilator interactions in skeletal muscle blood flow regulation. *Journal of Physiology*, *590*(24), 6297–6305. <https://doi.org/10.1113/jphysiol.2012.240762>
- Helmersson, J., Vessby, B., Larsson, A., & Basu, S. (2004). Association of Type 2 Diabetes with Cyclooxygenase-Mediated Inflammation and Oxidative Stress in an Elderly Population. *Circulation*, *109*(14), 1729–1734. <https://doi.org/10.1161/01.CIR.0000124718.99562.91>
- Henriksen, E. J., Jacob, S., Kinnick, T. R., Teachey, M. K., & Krekler, M. (2001). Selective angiotensin II receptor antagonism reduces insulin resistance in obese Zucker rats. *Hypertension*, *38*(4), 884–890. <https://doi.org/10.1161/hy1101.092970>
- Heuberger, D. M., & Schuepbach, R. A. (2019). Correction to: Protease-activated receptors (PARs): Mechanisms of action and potential therapeutic modulators in PAR-driven inflammatory diseases (*Thrombosis Journal* (2019) 17: 4 DOI: 10.1186/s12959-019-0194-8). *Thrombosis Journal*, *17*(1), 1–24. <https://doi.org/10.1186/s12959-019-0212-x>
- Hill, C. E., Phillips, J. K., & Sandow, S. L. (2001). Heterogeneous control of blood flow amongst different vascular beds. *Medicinal Research Reviews*, *21*(1), 1–60. [https://doi.org/10.1002/1098-1128\(200101\)21:1<1::AID-MED1>3.0.CO;2-6](https://doi.org/10.1002/1098-1128(200101)21:1<1::AID-MED1>3.0.CO;2-6)
- Howitt, L., Morris, M. J., Sandow, S. L., & Murphy, T. V. (2014). Effect of diet-induced obesity on BKCa function in contraction and dilation of rat isolated middle cerebral artery. *Vascular Pharmacology*, *61*(1), 10–15. <https://doi.org/10.1016/j.vph.2014.02.002>
- Huang, A., Sun, D., Smith, C. J., Connetta, J. A., Shesely, E. G., Koller, A., & Kaley, G. (2000). In eNOS knockout mice skeletal muscle arteriolar dilation to acetylcholine is mediated by EDHF. *American Journal of Physiology - Heart and Circulatory Physiology*, *278*(3 47-3), 762–768. <https://doi.org/10.1152/ajpheart.2000.278.3.h762>
- Hudspeth, B. (2018). The burden of cardiovascular disease in patients with diabetes. *The American Journal of Managed Care*, *24*(13 Suppl), S268–S272. <http://www.ncbi.nlm.nih.gov/pubmed/30160393>
- Hughes, K. H., Wijekoon, E. P., Valcour, J. E., Chia, E. W., & McGuire, J. J. (2013). Effects of chronic in-vivo treatments with protease-activated receptor 2 agonist on endothelium function and blood pressures in mice. *Canadian Journal of Physiology and Pharmacology*, *91*(4), 295–305. <https://doi.org/10.1139/cjpp-2012-0266>
- Hutter, M. (2019). *Effect of intensive medical management and weight loss on urinary biomarkers of diabetic kidney disease in the Zucker Diabetic Sprague Dawley (ZDSD) rat* [University of Zurich]. <https://doi.org/10.5167/uzh-172302>
- Ignarro, L. J., Byrns, R. E., Buga, G. M., & Wood, K. S. (1987). Endothelium-derived relaxing factor from pulmonary artery and vein possesses pharmacologic and

- chemical properties identical to those of nitric oxide radical. *Circulation Research*, 61(6), 866–879. <https://doi.org/10.1161/01.RES.61.6.866>
- Ignarro, L. J., Harbison, R. G., Wood, K. S., & Kadowitz, P. J. (1986). Activation of purified soluble guanylate cyclase by endothelium-derived relaxing factor from intrapulmonary artery and vein: stimulation by acetylcholine, bradykinin and arachidonic acid. *The Journal of Pharmacology and Experimental Therapeutics*, 237(3), 893–900. <http://www.ncbi.nlm.nih.gov/pubmed/2872327>
- Incalza, M. A., D’Oria, R., Natalicchio, A., Perrini, S., Laviola, L., & Giorgino, F. (2018). Oxidative stress and reactive oxygen species in endothelial dysfunction associated with cardiovascular and metabolic diseases. *Vascular Pharmacology*, 100(May 2017), 1–19. <https://doi.org/10.1016/j.vph.2017.05.005>
- Indrakusuma, I., Romacho, T., & Eckel, J. (2017). Protease-Activated Receptor 2 Promotes Pro-Atherogenic Effects through Transactivation of the VEGF Receptor 2 in Human Vascular Smooth Muscle Cells. *Frontiers in Pharmacology*, 7(JAN), 1–12. <https://doi.org/10.3389/fphar.2016.00497>
- International Diabetes Federation. (2019). *IDF Diabetes Atlas* (9th ed.). International Diabetes Federation. <http://www.diabetesatlas.org/>
- Jiang, R. S., Zhang, L., Yang, H., Zhou, M. Y., Deng, C. Y., & Wu, W. (2021). Signalling pathway of U46619-induced vascular smooth muscle contraction in mouse coronary artery. *Clinical and Experimental Pharmacology and Physiology*, 48(7), 996–1006. <https://doi.org/10.1111/1440-1681.13502>
- Johnstone, M. T., Creager, S. J., Scales, K. M., Cusco, J. A., Lee, B. K., & Creager, M. A. (1993). Impaired endothelium-dependent vasodilation in patients with insulin-dependent diabetes mellitus. *Circulation*, 88(6), 2510–2516. <https://doi.org/10.1161/01.CIR.88.6.2510>
- Jones, S. M., Mann, A., Conrad, K., Saum, K., Hall, D. E., McKinney, L. M., Robbins, N., Thompson, J., Peairs, A. D., Camerer, E., Rayner, K. J., Tranter, M., Mackman, N., & Owens, A. P. (2018). PAR2 (Protease-Activated Receptor 2) Deficiency Attenuates Atherosclerosis in Mice. *Arteriosclerosis, Thrombosis, and Vascular Biology*, 38(6), 1271–1282. <https://doi.org/10.1161/ATVBAHA.117.310082>
- Kagota, S., Chia, E., & McGuire, J. J. (2011). Preserved arterial vasodilatation via endothelial protease-activated receptor-2 in obese type 2 diabetic mice. *British Journal of Pharmacology*, 164(2), 358–371. <https://doi.org/10.1111/j.1476-5381.2011.01356.x>
- Kagota, S., Maruyama-Fumoto, K., Iwata, S., Shimari, M., Koyanagi, S., Shiokawa, Y., McGuire, J. J., & Shinozuka, K. (2019). Perivascular adipose tissue-enhanced vasodilation in metabolic syndrome rats by apelin and N-acetyl-L-cysteine-sensitive factor(s). *International Journal of Molecular Sciences*, 20(1). <https://doi.org/10.3390/ijms20010106>

- Kagota, S., Maruyama, K., & McGuire, J. J. (2016). Characterization and Functions of Protease-Activated Receptor 2 in Obesity, Diabetes, and Metabolic Syndrome: A Systematic Review. *BioMed Research International*, 2016. <https://doi.org/10.1155/2016/3130496>
- Kagota, S., Maruyama, K., Wakuda, H., McGuire, J. J., Yoshikawa, N., Nakamura, K., & Shinozuka, K. (2014). Disturbance of vasodilation via protease-activated receptor 2 in SHRSP.Z-Leprfa/IzmDmcr rats with metabolic syndrome. *Vascular Pharmacology*, 63(1), 46–54. <https://doi.org/10.1016/j.vph.2014.06.005>
- Kagota, S., Yamaguchi, Y., Nakamura, K., & Kunitomo, M. (2000). Altered endothelium-dependent responsiveness in the aortas and renal arteries of Otsuka Long-Evans Tokushima Fatty (OLETF) rats, a model of non-insulin-dependent diabetes mellitus. *General Pharmacology: The Vascular System*, 34(3), 201–209. [https://doi.org/10.1016/S0306-3623\(00\)00061-6](https://doi.org/10.1016/S0306-3623(00)00061-6)
- Kaiser, L., & Ptui, S. (1992). Effects of Increasing Age on Vascular Responses of the in vivo Femoral Artery of Adult Beagles. *Gerontology*, 38(3), 121–126. <https://doi.org/10.1159/000213318>
- Kent, K. C., Collins, L. J., Schwerin, F. T., Raychowdhury, M. K., & Ware, J. A. (1993). Identification of functional PGH2/TxA2 receptors on human endothelial cells. *Circulation Research*, 72(5), 958–965. <https://doi.org/10.1161/01.res.72.5.958>
- King, A. J. F. (2012). The use of animal models in diabetes research. *British Journal of Pharmacology*, 166(3), 877–894. <https://doi.org/10.1111/j.1476-5381.2012.01911.x>
- Kingwell, B. A., Formosa, M., Muhlmann, M., Bradley, S. J., & McConell, G. K. (2003). Type 2 diabetic individuals have impaired leg blood flow responses to exercise: Role of endothelium-dependent vasodilation. *Diabetes Care*, 26(3), 899–904. <https://doi.org/10.2337/diacare.26.3.899>
- Kochi, T., Imai, Y., Takeda, A., Watanabe, Y., Mori, S., Tachi, M., & Kodama, T. (2013). Characterization of the arterial anatomy of the murine hindlimb: Functional role in the design and understanding of ischemia models. *PLoS ONE*, 8(12). <https://doi.org/10.1371/journal.pone.0084047>
- Kubota, T., Kubota, N., Moroi, M., Terauchi, Y., Kobayashi, T., Kamata, K., Suzuki, R., Tobe, K., Namiki, A., Aizawa, S., Nagai, R., Kadowaki, T., & Yamaguchi, T. (2003). Lack of insulin receptor substrate-2 causes progressive neointima formation in response to vessel injury. *Circulation*, 107(24), 3073–3080. <https://doi.org/10.1161/01.CIR.0000070937.52035.25>
- Kuo, C. J., LaMontagne, K. R., Garcia-Cardena, G., Ackley, B. D., Kalman, D., Park, S., Christofferson, R., Kamihara, J., Ding, Y. H., Lo, K. M., Gillies, S., Folkman, J., Mulligan, R. C., & Javaherian, K. (2001). Oligomerization-dependent regulation of motility and morphogenesis by the collagen XVIII NC1/endostatin domain. *Journal of Cell Biology*, 152(6), 1233–1246. <https://doi.org/10.1083/jcb.152.6.1233>

- Lagaud, G. J. L., Masih-Khan, E., Kai, S., Van Breemen, C., & Dubé, G. P. (2001). Influence of type II diabetes on arterial tone and endothelial function in murine mesenteric resistance arteries. *Journal of Vascular Research*, *38*(6), 578–589. <https://doi.org/10.1159/000051094>
- Lakatta, E. G., & Levy, D. (2003). Arterial and cardiac aging: Major shareholders in cardiovascular disease enterprises: Part I: Aging arteries: A “set up” for vascular disease. *Circulation*, *107*(1), 139–146. <https://doi.org/10.1161/01.CIR.0000048892.83521.58>
- Lalande, S., Gusso, S., Hofman, P. L., & Baldi, J. C. (2008). Reduced leg blood flow during submaximal exercise in type 2 diabetes. *Medicine and Science in Sports and Exercise*, *40*(4), 612–617. <https://doi.org/10.1249/MSS.0b013e318161aa99>
- Landmesser, U., Spiekermann, S., Preuss, C., Sorrentino, S., Fischer, D., Manes, C., Mueller, M., & Drexler, H. (2007). Angiotensin II induces endothelial xanthine oxidase activation: Role for endothelial dysfunction in patients with coronary disease. *Arteriosclerosis, Thrombosis, and Vascular Biology*, *27*(4), 943–948. <https://doi.org/10.1161/01.ATV.0000258415.32883.bf>
- Langer, D. J., Kuo, A., Kariko, K., Ahuja, M., Klugherz, B. D., Ivanics, K. M., Hoxie, J. A., Williams, W. V., Liang, B. T., Cines, D. B., & Barnathan, E. S. (1993). Regulation of the endothelial cell urokinase-type plasminogen activator receptor: Evidence for cyclic AMP-dependent and protein kinase C-dependent pathways. *Circulation Research*, *72*(2), 330–340. <https://doi.org/10.1161/01.RES.72.2.330>
- Lee, S., & Harris, N. R. (2008). Losartan and ozagrel reverse retinal arteriolar constriction in non-obese diabetic mice. *Microcirculation*, *15*(5), 379–387. <https://doi.org/10.1080/10739680701829802>
- Lemmey, H. A. L., Ye, X., Ding, H. C., Triggle, C. R., Garland, C. J., & Dora, K. A. (2018). Hyperglycaemia disrupts conducted vasodilation in the resistance vasculature of db/db mice. *Vascular Pharmacology*, *103–105*(November 2017), 29–35. <https://doi.org/10.1016/j.vph.2018.01.002>
- Lesniewski, L. A., Connell, M. L., Durrant, J. R., Folian, B. J., Anderson, M. C., Donato, A. J., & Seals, D. R. (2009). B6D2F1 mice are a suitable model of oxidative stress-mediated impaired endothelium-dependent dilation with aging. *Journals of Gerontology - Series A Biological Sciences and Medical Sciences*, *64*(1), 9–20. <https://doi.org/10.1093/gerona/gln049>
- Li, C., Zhang, J., Jiang, Y., Gurewich, V., Chen, Y., & Liu, J.-N. (2001). Urokinase-Type Plasminogen Activator Up-Regulates Its Own Expression by Endothelial Cells and Monocytes via the u-PAR Pathway. *Thrombosis Research*, *103*(3), 221–232. [https://doi.org/10.1016/S0049-3848\(01\)00322-X](https://doi.org/10.1016/S0049-3848(01)00322-X)
- Lillioja, S., Mott, D. M., Howard, B. V., Bennett, P. H., Yki-Järvinen, H., Freymond, D., Nyomba, B. L., Zurlo, F., Swinburn, B., & Bogardus, C. (1988). Impaired Glucose

- Tolerance as a Disorder of Insulin Action. *New England Journal of Medicine*, 318(19), 1217–1225. <https://doi.org/10.1056/NEJM198805123181901>
- Liu, C. Q., Leung, F. P., Wong, S. L., Wong, W. T., Lau, C. W., Lu, L., Yao, X., Yao, T., & Huang, Y. (2009). Thromboxane prostanoid receptor activation impairs endothelial nitric oxide-dependent vasorelaxations: The role of Rho kinase. *Biochemical Pharmacology*, 78(4), 374–381. <https://doi.org/10.1016/j.bcp.2009.04.022>
- Livak, K. J., & Schmittgen, T. D. (2001). Analysis of relative gene expression data using real-time quantitative PCR and the 2- $\Delta\Delta$ CT method. *Methods*, 25(4), 402–408. <https://doi.org/10.1006/meth.2001.1262>
- Luksha, L., Agewall, S., & Kublickiene, K. (2009). Endothelium-derived hyperpolarizing factor in vascular physiology and cardiovascular disease. *Atherosclerosis*, 202(2), 330–344. <https://doi.org/10.1016/j.atherosclerosis.2008.06.008>
- Luttrell, M., Kim, H., Shin, S. Y., Holly, D., Massett, M. P., & Woodman, C. R. (2020). Heterogeneous effect of aging on vasorelaxation responses in large and small arteries. *Physiological Reports*, 8(1), 1–11. <https://doi.org/10.14814/phy2.14341>
- Lyons, T. J., & Basu, A. (2012). Biomarkers in diabetes: hemoglobin A1c, vascular and tissue markers. *Translational Research*, 159(4), 303–312. <https://doi.org/10.1016/j.trsl.2012.01.009>
- Mackie, B. G., & Terjung, R. L. (1983). Blood flow to different skeletal muscle fiber types during contraction. *American Journal of Physiology - Heart and Circulatory Physiology*, 14(2). <https://doi.org/10.1152/ajpheart.1983.245.2.h265>
- Mahley, R. W. (1988). Apolipoprotein E: Cholesterol transport protein with expanding role in cell biology. *Science*, 240(4852), 622–630. <https://doi.org/10.1126/science.3283935>
- Mahley, R. W. (2016). Apolipoprotein E: from cardiovascular disease to neurodegenerative disorders. *Journal of Molecular Medicine*, 94(7), 739–746. <https://doi.org/10.1007/s00109-016-1427-y>
- Majed, B. H., & Khalil, R. A. (2012). Molecular mechanisms regulating the vascular prostacyclin pathways and their adaptation during pregnancy and in the newborn. *Pharmacological Reviews*, 64(3), 540–582. <https://doi.org/10.1124/pr.111.004770>
- Majesky, M. W., Dong, X. R., Høglund, V., Mahoney, W. M., & Daum, G. (2011). The adventitia: A dynamic interface containing resident progenitor cells. *Arteriosclerosis, Thrombosis, and Vascular Biology*, 31(7), 1530–1539. <https://doi.org/10.1161/ATVBAHA.110.221549>
- Mamer, S. B., Chen, S., Weddell, J. C., Palasz, A., Wittenkeller, A., Kumar, M., & Imoukhuede, P. I. (2017). Discovery of High-Affinity PDGF-VEGFR Interactions:

- Redefining RTK Dynamics. *Scientific Reports*, 7(1), 1–14.
<https://doi.org/10.1038/s41598-017-16610-z>
- Marrero, M. B., Venema, V. J., Ju, H., He, H., Liang, H., Caldwell, R. B., & Venema, R. C. (1999). Endothelial nitric oxide synthase interactions with G-protein-coupled receptors. *The Biochemical Journal*, 343 Pt 2, 335–340.
<http://www.ncbi.nlm.nih.gov/pubmed/10510297>
- Maruyama-Fumoto, K., McGuire, J. J., Fairlie, D. P., Shinozuka, K., & Kagota, S. (2021). Activation of protease-activated receptor 2 is associated with blood pressure regulation and proteinuria reduction in metabolic syndrome. *Clinical and Experimental Pharmacology and Physiology*, 48(2), 211–220.
<https://doi.org/10.1111/1440-1681.13431>
- Maruyama, K., Kagota, S., McGuire, J. J., Wakuda, H., Yoshikawa, N., Nakamura, K., & Shinozuka, K. (2016). Enhanced nitric oxide synthase activation via protease-activated receptor 2 is involved in the preserved vasodilation in aortas from metabolic syndrome rats. *Journal of Vascular Research*, 52(4), 232–243.
<https://doi.org/10.1159/000442415>
- Maruyama, K., Kagota, S., McGuire, J. J., Wakuda, H., Yoshikawa, N., Nakamura, K., & Shinozuka, K. (2017). Age-related changes to vascular protease-activated receptor 2 in metabolic syndrome: A relationship between oxidative stress, receptor expression, and endothelium-dependent vasodilation. *Canadian Journal of Physiology and Pharmacology*, 95(4), 356–364. <https://doi.org/10.1139/cjpp-2016-0298>
- Matsui, J., Wakabayashi, T., Asada, M., Yoshimatsu, K., & Okada, M. (2004). Stem Cell Factor/c-kit Signaling Promotes the Survival, Migration, and Capillary Tube Formation of Human Umbilical Vein Endothelial Cells. *Journal of Biological Chemistry*, 279(18), 18600–18607. <https://doi.org/10.1074/jbc.M311643200>
- Matsumoto, T., Ishida, K., Taguchi, K., Kobayashi, T., & Kamata, K. (2009). Mechanisms underlying enhanced vasorelaxant response to protease-activated receptor 2-activating peptide in type 2 diabetic Goto-Kakizaki rat mesenteric artery. *Peptides*, 30(9), 1729–1734. <https://doi.org/10.1016/j.peptides.2009.06.014>
- Matsumoto, T., Kakami, M., Noguchi, E., Kobayashi, T., & Kamata, K. (2007). Imbalance between endothelium-derived relaxing and contracting factors in mesenteric arteries from aged OLETF rats, a model of Type 2 diabetes. *American Journal of Physiology - Heart and Circulatory Physiology*, 293(3), 1480–1490.
<https://doi.org/10.1152/ajpheart.00229.2007>
- Matsumoto, T., Takaoka, E., Ishida, K., Nakayama, N., Noguchi, E., Kobayashi, T., & Kamata, K. (2009). Abnormalities of endothelium-dependent responses in mesenteric arteries from Otsuka Long-Evans Tokushima Fatty (OLETF) rats are improved by chronic treatment with thromboxane A2 synthase inhibitor. *Atherosclerosis*, 205(1), 87–95.
<https://doi.org/10.1016/j.atherosclerosis.2008.11.015>

- Matz, R. L., Schott, C., Stoclet, J. C., & Andriantsitohaina, R. (2000). Age-related endothelial dysfunction with respect to nitric oxide, endothelium-derived hyperpolarizing factor and cyclooxygenase products. *Physiological Research*, *49*(1), 11–18. <http://www.ncbi.nlm.nih.gov/pubmed/10805400>
- Matz, Rachel L., & Andriantsitohaina, R. (2003). Age-related endothelial dysfunction: Potential implications for pharmacotherapy. *Drugs and Aging*, *20*(7), 527–550. <https://doi.org/10.2165/00002512-200320070-00005>
- McGuire, J. J., Ding, H., & Triggle, C. R. (2001). Endothelium-derived relaxing factors: A focus on endothelium-derived hyperpolarizing factor(s). *Canadian Journal of Physiology and Pharmacology*, *79*(6), 443–470. <https://doi.org/10.1139/cjpp-79-6-443>
- McGuire, J. J., Hollenberg, M. D., Andrade-Gordon, P., & Triggle, C. R. (2002a). Multiple mechanisms of vascular smooth muscle relaxation by the activation of proteinase-activated receptor 2 in mouse mesenteric arterioles. *British Journal of Pharmacology*, *135*(1), 155–169. <https://doi.org/10.1038/sj.bjp.0704469>
- McGuire, J. J., Hollenberg, M. D., Andrade-Gordon, P., & Triggle, C. R. (2002b). Multiple mechanisms of vascular smooth muscle relaxation by the activation of proteinase-activated receptor 2 in mouse mesenteric arterioles. *British Journal of Pharmacology*, *135*(1), 155–169. <https://doi.org/10.1038/sj.bjp.0704469>
- McGuire, J. J., Saifeddine, M., Triggle, C. R., Sun, K., & Hollenberg, M. D. (2004). 2-Furoyl-LIGRLO-amide: A potent and selective proteinase-activated receptor 2 agonist. *Journal of Pharmacology and Experimental Therapeutics*, *309*(3), 1124–1131. <https://doi.org/10.1124/jpet.103.064584>
- McGuire, J. J., Van Vliet, B. N., Giménez, J., King, J. C., & Halfyard, S. J. (2007). Persistence of PAR-2 vasodilation despite endothelial dysfunction in BPH/2 hypertensive mice. *Pflugers Archiv European Journal of Physiology*, *454*(4), 535–543. <https://doi.org/10.1007/s00424-007-0226-2>
- McKenzie, C., MacDonald, A., & Shaw, A. M. (2009). Mechanisms of U46619-induced contraction of rat pulmonary arteries in the presence and absence of the endothelium. *British Journal of Pharmacology*, *157*(4), 581–596. <https://doi.org/10.1111/j.1476-5381.2008.00084.x>
- Meyrelles, S. S., Peotta, V. A., Pereira, T. M. C., & Vasquez, E. C. (2011). Endothelial Dysfunction in the Apolipoprotein E-deficient Mouse: Insights into the influence of diet, gender and aging. *Lipids in Health and Disease*, *10*, 1–18. <https://doi.org/10.1186/1476-511X-10-211>
- Miettinen, M., Sarlomo-Rikala, M., & Lasota, J. (2000). KIT expression in angiosarcomas and fetal endothelial cells: Lack of mutations of Exon 11 and Exon 17 of C-kit. *Modern Pathology*, *13*(5), 536–541. <https://doi.org/10.1038/modpathol.3880093>

- Miike, T., Kunishiro, K., Kanda, M., Azukizawa, S., Kurahashi, K., & Shirahase, H. (2008). Impairment of endothelium-dependent ACh-induced relaxation in aorta of diabetic db/db mice-possible dysfunction of receptor and/or receptor-G protein coupling. *Naunyn-Schmiedeberg's Archives of Pharmacology*, 377(4–6), 401–410. <https://doi.org/10.1007/s00210-008-0261-3>
- Miyamoto, A., Hashiguchi, Y., Obi, T., Ishiguro, S., & Nishio, A. (2007). Ibuprofen or ozagrel increases NO release and l-nitro arginine induces TXA2 release from cultured porcine basilar arterial endothelial cells. *Vascular Pharmacology*, 46(2), 85–90. <https://doi.org/10.1016/j.vph.2006.06.018>
- Mohrman, D. E., & Regal, R. R. (1988). Relation of blood flow to VO₂, PO₂, and PCO₂ in dog gastrocnemius muscle. *American Journal of Physiology-Heart and Circulatory Physiology*, 255(5), H1004–H1010. <https://doi.org/10.1152/ajpheart.1988.255.5.H1004>
- Mokhtar, S. S., Vanhoutte, P. M., Leung, S. W. S., Yusof, M. I., Wan Sulaiman, W. A., Mat Saad, A. Z., Suppian, R., & Rasool, A. H. G. (2016). Endothelium dependent hyperpolarization-type relaxation compensates for attenuated nitric oxide-mediated responses in subcutaneous arteries of diabetic patients. *Nitric Oxide - Biology and Chemistry*, 53, 35–44. <https://doi.org/10.1016/j.niox.2015.12.007>
- Moncada, S., & Higgs, E. A. (2006). The discovery of nitric oxide and its role in vascular biology. *British Journal of Pharmacology*, 147(SUPPL. 1), 193–201. <https://doi.org/10.1038/sj.bjp.0706458>
- Morinelli, T. A., Mais, D. E., Oatis, J. E., Crumbley, A. J., & Halushka, P. V. (1990). Characterization of thromboxane A₂/prostaglandin H₂ receptors in human vascular smooth muscle cells. *Life Sciences*, 46(24), 1765–1772. [https://doi.org/10.1016/0024-3205\(90\)90140-M](https://doi.org/10.1016/0024-3205(90)90140-M)
- Muller-Delp, J. M., Spier, S. A., Ramsey, M. W., & Delp, M. D. (2002). Aging impairs endothelium-dependent vasodilation in rat skeletal muscle arterioles. *American Journal of Physiology - Heart and Circulatory Physiology*, 283(4 52-4), 1662–1672. <https://doi.org/10.1152/ajpheart.00004.2002>
- Mulvany, M. J., & Halpern, W. (1977). Contractile properties of small arterial resistance vessels in spontaneously hypertensive and normotensive rats. *Circulation Research*, 41(1), 19–26. <https://doi.org/10.1161/01.RES.41.1.19>
- Muniyappa, R., & Sowers, J. R. (2013). Role of insulin resistance in endothelial dysfunction. *Reviews in Endocrine and Metabolic Disorders*, 14(1), 5–12. <https://doi.org/10.1007/s11154-012-9229-1>
- Murohara, T., Yasue, H., Ohgushi, M., Sakaino, N., & Jougasaki, M. (1991). Age related attenuation of the endothelium dependent relaxation to noradrenaline in isolated pig coronary arteries. *Cardiovascular Research*, 25(12), 1002–1009. <https://doi.org/10.1093/cvr/25.12.1002>

- Naser, N., Januszewski, A. S., Brown, B. E., Jenkins, A. J., Hill, M. A., & Murphy, T. V. (2013). Advanced Glycation End Products Acutely Impair Ca²⁺ Signaling in Bovine Aortic Endothelial Cells. *Frontiers in Physiology*, 4(March), 1–14. <https://doi.org/10.3389/fphys.2013.00038>
- Negre-Salvayre, A., Salvayre, R., Augé, N., Pamplona, R., & Portero-Otín, M. (2009). Hyperglycemia and glycation in diabetic complications. *Antioxidants and Redox Signaling*, 11(12), 3071–3109. <https://doi.org/10.1089/ars.2009.2484>
- Newcomer, S. C., Leuenberger, U. A., Hogeman, C. S., & Proctor, D. N. (2005). Heterogeneous vasodilator responses of human limbs: Influence of age and habitual endurance training. *American Journal of Physiology - Heart and Circulatory Physiology*, 289(1 58-1), 308–315. <https://doi.org/10.1152/ajpheart.01151.2004>
- Nishino, T. (1994). The conversion of xanthine dehydrogenase to xanthine oxidase and the role of the enzyme in reperfusion injury. *Journal of Biochemistry*, 116(1), 1–6. <https://doi.org/10.1093/oxfordjournals.jbchem.a124480>
- North, B. J., & Sinclair, D. A. (2012). The intersection between aging and cardiovascular disease. *Circulation Research*, 110(8), 1097–1108. <https://doi.org/10.1161/CIRCRESAHA.111.246876>
- Novella, S., Dantas, A. P., Segarra, G., Novensa, L., Heras, M., Hermenegildo, C., & Medina, P. (2013). Aging enhances contraction to thromboxane A₂ in aorta from female senescence-accelerated mice. *Age*, 35(1), 117–128. <https://doi.org/10.1007/s11357-011-9337-y>
- O'Driscoll, G., Green, D., Maiorana, A., Stanton, K., Colreavy, F., & Taylor, R. (1999). Improvement in endothelial function by angiotensin-converting enzyme inhibition in non-insulin-dependent diabetes mellitus. *Journal of the American College of Cardiology*, 33(6), 1506–1511. [https://doi.org/10.1016/S0735-1097\(99\)00065-0](https://doi.org/10.1016/S0735-1097(99)00065-0)
- O'Reilly, M. S., Boehm, T., Shing, Y., Fukai, N., Vasios, G., Lane, W. S., Flynn, E., Birkhead, J. R., Olsen, B. R., & Folkman, J. (1997). Endostatin: An Endogenous Inhibitor of Angiogenesis and Tumor Growth. *Cell*, 88(2), 277–285. [https://doi.org/10.1016/S0092-8674\(00\)81848-6](https://doi.org/10.1016/S0092-8674(00)81848-6)
- Okon, E. B., Szado, T., Laher, I., McManus, B., & Van Breemena, C. (2003). Augmented Contractile Response of Vascular Smooth Muscle in a Diabetic Mouse Model. *Journal of Vascular Research*, 40(6), 520–530. <https://doi.org/10.1159/000075238>
- Oltman, C. L., Kleinschmidt, T. L., Davidson, E. P., Coppey, L. J., Lund, D. D., & Yorek, M. A. (2008). Treatment of cardiovascular dysfunction associated with the metabolic syndrome and type 2 diabetes. *Vascular Pharmacology*, 48(1), 47–53. <https://doi.org/10.1016/j.vph.2007.11.005>
- Ozen, G., Aljesri, K., Celik, Z., Turkyılmaz, G., Turkyılmaz, S., Teskin, O., Norel, X., & Topal, G. (2020). Mechanism of thromboxane receptor-induced vasoconstriction in

- human saphenous vein. *Prostaglandins and Other Lipid Mediators*, 151(April), 106476. <https://doi.org/10.1016/j.prostaglandins.2020.106476>
- Palmer, R. M. J., Ashton, D. S., & Moncada, S. (1988). Vascular endothelial cells synthesize nitric oxide from L-arginine. *Nature*, 333(6174), 664–666. <https://doi.org/10.1038/333664a0>
- Pannirselvam, M., Ding, H., Anderson, T. J., & Triggle, C. R. (2006). Pharmacological characteristics of endothelium-derived hyperpolarizing factor-mediated relaxation of small mesenteric arteries from db/db mice. *European Journal of Pharmacology*, 551(1–3), 98–107. <https://doi.org/10.1016/j.ejphar.2006.08.086>
- Parenti, A., Brogelli, L., Filippi, S., Donnini, S., & Ledda, F. (2002). Effect of hypoxia and endothelial loss on vascular smooth muscle cell responsiveness to VEGF-A: Role of flt-1/VEGF-receptor-1. *Cardiovascular Research*, 55(1), 201–212. [https://doi.org/10.1016/S0008-6363\(02\)00326-7](https://doi.org/10.1016/S0008-6363(02)00326-7)
- Park, Y., Capobianco, S., Gao, X., Falck, J. R., Dellsperger, K. C., & Zhang, C. (2008). Role of EDHF in type 2 diabetes-induced endothelial dysfunction. *American Journal of Physiology-Heart and Circulatory Physiology*, 295(5), H1982–H1988. <https://doi.org/10.1152/ajpheart.01261.2007>
- Park, Y., Yang, J., Zhang, H., Chen, X., & Zhang, C. (2011). Effect of PAR2 in regulating TNF- α and NAD(P)H oxidase in coronary arterioles in type 2 diabetic mice. *Basic Research in Cardiology*, 106(1), 111–123. <https://doi.org/10.1007/s00395-010-0129-9>
- Pereira, A., Fernandes, R., Crisóstomo, J., Seiça, R. M., & Sena, C. M. (2017). The Sulforaphane and pyridoxamine supplementation normalize endothelial dysfunction associated with type 2 diabetes. *Scientific Reports*, 7(1), 13–15. <https://doi.org/10.1038/s41598-017-14733-x>
- Perticone, F., Ceravolo, R., Candigliota, M., Ventura, G., Iacopino, S., Sinopoli, F., & Mattioli, P. L. (2001). Obesity and body fat distribution induce endothelial dysfunction by oxidative stress: Protective effect of vitamin C. *Diabetes*, 50(1), 159–165. <https://doi.org/10.2337/diabetes.50.1.159>
- Peterson, R. G., Jackson, C. V., Zimmerman, K., De Winter, W., Huebert, N., & Hansen, M. K. (2015). Characterization of the ZDSD rat: A translational model for the study of metabolic syndrome and type 2 diabetes. *Journal of Diabetes Research*, 2015. <https://doi.org/10.1155/2015/487816>
- Peterson, R. G., Jackson, C. Van, & Zimmerman, K. M. (2017). The ZDSD rat: a novel model of diabetic nephropathy. *American Journal of Translational Research*, 9(9), 4236–4249. <http://www.ncbi.nlm.nih.gov/pubmed/28979697>
- Pham, P. T., Fukuda, D., Yagi, S., Kusunose, K., Yamada, H., Soeki, T., Shimabukuro, M., & Sata, M. (2019). Rivaroxaban, a specific FXa inhibitor, improved

- endothelium-dependent relaxation of aortic segments in diabetic mice. *Scientific Reports*, 9(1), 1–11. <https://doi.org/10.1038/s41598-019-47474-0>
- Pick, A., Clark, J., Kubstrup, C., Levisetti, M., Pugh, W., Bonner-Weir, S., & Polonsky, K. S. (1998). Role of apoptosis in failure of beta-cell mass compensation for insulin resistance and beta-cell defects in the male Zucker diabetic fatty rat. *Diabetes*, 47(3), 358–364. <https://doi.org/10.2337/diabetes.47.3.358>
- Pires, A. F., Madeira, S. V. F., Soares, P. M. G., Montenegro, C. M., Souza, E. P., Resende, A. C., Soares de Moura, R., Assreuy, A. M. S., & Criddle, D. N. (2012). The role of endothelium in the vasorelaxant effects of the essential oil of *ocimum gratissimum* in aorta and mesenteric vascular bed of rats. *Canadian Journal of Physiology and Pharmacology*, 90(10), 1380–1385. <https://doi.org/10.1139/Y2012-095>
- Pohl, U., & Busse, R. (1987). Endothelium-derived relaxant factor inhibits effects of nitrocompounds in isolated arteries. *American Journal of Physiology-Heart and Circulatory Physiology*, 252(2), H307–H313. <https://doi.org/10.1152/ajpheart.1987.252.2.H307>
- Prisby, R. D., Ramsey, M. W., Behnke, B. J., Dominguez, J. M., Donato, A. J., Allen, M. R., & Delp, M. D. (2007). Aging reduces skeletal blood flow, endothelium-dependent vasodilation, and bioavailability in rats. *Journal of Bone and Mineral Research*, 22(8), 1280–1288. <https://doi.org/10.1359/jbmr.070415>
- Pueyo, M. E., N'Diaye, N., & Michel, J. B. (1996). Angiotensin II-elicited signal transduction via AT1 receptors in endothelial cells. *British Journal of Pharmacology*, 118(1), 79–84. <https://doi.org/10.1111/j.1476-5381.1996.tb15369.x>
- Púzserová, A., Kopincová, J., Slezák, P., Bališ, P., & Bernátová, I. (2013). Endothelial dysfunction in femoral artery of the hypertensive rats is nitric oxide independent. *Physiological Research*, 62(6), 615–629.
- Rajendran, P., Rengarajan, T., Thangavel, J., Nishigaki, Y., Sakthisekaran, D., Sethi, G., & Nishigaki, I. (2013). The vascular endothelium and human diseases. *International Journal of Biological Sciences*, 9(10), 1057–1069. <https://doi.org/10.7150/ijbs.7502>
- Reinwald, S., Peterson, R. G., Allen, M. R., & Burr, D. B. (2009). Skeletal changes associated with the onset of type 2 diabetes in the ZDF and ZDSD rodent models. *American Journal of Physiology-Endocrinology and Metabolism*, 296(4), E765–E774. <https://doi.org/10.1152/ajpendo.90937.2008>
- Robin, J., Kharbanda, R., Mclean, P., Campbell, R., & Vallance, P. (2003). Protease-activated receptor 2-mediated vasodilatation in humans in vivo: Role of nitric oxide and prostanoids. *Circulation*, 107(7), 954–959. <https://doi.org/10.1161/01.CIR.0000050620.37260.75>
- Rossi, E., Biasucci, L. M., Citterio, F., Pelliccioni, S., Monaco, C., Ginnetti, F.,

- Angiolillo, D. J., Grieco, G., Liuzzo, G., & Maseri, A. (2002). Risk of myocardial infarction and angina in patients with severe peripheral vascular disease predictive role of C-reactive protein. *Circulation*, *105*(7), 800–803. <https://doi.org/10.1161/hc0702.104126>
- Roviezzo, F., Bucci, M., Brancaleone, V., Di Lorenzo, A., Geppetti, P., Farneti, S., Parente, L., Lungarella, G., Fiorucci, S., & Cirino, G. (2005). Proteinase-activated receptor-2 mediates arterial vasodilation in diabetes. *Arteriosclerosis, Thrombosis, and Vascular Biology*, *25*(11), 2349–2354. <https://doi.org/10.1161/01.ATV.0000184770.01494.2e>
- Rubanyi, G. M., Romero, J. C., & Vanhoutte, P. M. (1986). Flow-induced release of endothelium-derived relaxing factor. *American Journal of Physiology-Heart and Circulatory Physiology*, *250*(6), H1145–H1149. <https://doi.org/10.1152/ajpheart.1986.250.6.H1145>
- Sachinidis, A., Locher, R., Hoppe, J., & Vetter, W. (1990). The platelet-derived growth factor isomers, PDGF-AA, PDGF-AB and PDGF-BB, induce contraction of vascular smooth muscle cells by different intracellular mechanisms. *FEBS Letters*, *275*(1–2), 95–98. [https://doi.org/10.1016/0014-5793\(90\)81447-V](https://doi.org/10.1016/0014-5793(90)81447-V)
- Saifeddine, M., Al-ani, B., Cheng, C. H., Wang, L., & Hollenberg, M. D. (1996). Rat proteinase-activated receptor-2 (PAR-2): cDNA sequence and activity of receptor-derived peptides in gastric and vascular tissue. *British Journal of Pharmacology*, *118*(3), 521–530. <https://doi.org/10.1111/j.1476-5381.1996.tb15433.x>
- Sakamoto, S., Minami, K., Niwa, Y., Ohnaka, M., Nakaya, Y., Mizuno, A., Kuwajima, M., & Shima, K. (1998). Effect of exercise training and food restriction endothelium-dependent relaxation in the Otsuka Long-Evans Tokushima fatty rat, a model of spontaneous NIDDM. *Diabetes*, *47*(1), 82–86. <https://doi.org/10.2337/diab.47.1.82>
- Saltin, B., Rådegran, G., Koskolou, M. D., & Roach, R. C. (1998). Skeletal muscle blood flow in humans and its regulation during exercise. *Acta Physiologica Scandinavica*, *162*(3), 421–436. <https://doi.org/10.1046/j.1365-201X.1998.0293e.x>
- Sandoo, A., Veldhuijzen van Zanten, J. J. C. ., Metsios, G. S., Carroll, D., & Kitas, G. D. (2015). The Endothelium and Its Role in Regulating Vascular Tone. *The Open Cardiovascular Medicine Journal*, *4*(1), 302–312. <https://doi.org/10.2174/1874192401004010302>
- Sarelius, I., & Pohl, U. (2010). Control of muscle blood flow during exercise: Local factors and integrative mechanisms. *Acta Physiologica*, *199*(4), 349–365. <https://doi.org/10.1111/j.1748-1716.2010.02129.x>
- Scherrer, U., Randin, D., Vollenweider, P., Vollenweider, L., & Nicod, P. (1994). Nitric oxide release accounts for insulin's vascular effects in humans. *Journal of Clinical Investigation*, *94*(6), 2511–2515. <https://doi.org/10.1172/JCI117621>

- Schulz, E., Gori, T., & Münzel, T. (2011). Oxidative stress and endothelial dysfunction in hypertension. *Hypertension Research*, *34*(6), 665–673. <https://doi.org/10.1038/hr.2011.39>
- Schwaninger, R. A. M., Sun, H., & Mayhan, W. G. (2003). Impaired nitric oxide synthase-dependent dilatation of cerebral arterioles in type II diabetic rats. *Life Sciences*, *73*(26), 3415–3425. <https://doi.org/10.1016/j.lfs.2003.06.029>
- Seals, D. R., Jablonski, K. L., & Donato, A. J. (2011). Aging and vascular endothelial function in humans. *Clinical Science*, *120*(9), 357–375. <https://doi.org/10.1042/CS20100476>
- Selvaraj, S. K., Giri, R. K., Perelman, N., Johnson, C., Malik, P., & Kalra, V. K. (2003). Mechanism of monocyte activation and expression of proinflammatory cytochemokines by placenta growth factor. *Blood*, *102*(4), 1515–1524. <https://doi.org/10.1182/blood-2002-11-3423>
- Sengupta, P. (2013). The laboratory rat: Relating its age with human's. *International Journal of Preventive Medicine*, *4*(6), 624–630.
- Shi, Y., Man, R. Y. K., & Vanhoutte, P. M. (2008). Two isoforms of cyclooxygenase contribute to augmented endothelium- dependent contractions in femoral arteries of 1-year-old rats. *Acta Pharmacologica Sinica*, *29*(2), 185–192. <https://doi.org/10.1111/j.1745-7254.2008.00749.x>
- Shimokawa, H., Yasutake, H., Fujii, K., Owada, M. K., Nakaike, R., Fukumoto, Y., Takayanagi, T., Nagao, T., Egashira, K., Fujishima, M., & Takeshita, A. (1996). The Importance of the Hyperpolarizing Mechanism Increases as the Vessel Size Decreases in Endothelium-Dependent Relaxations in Rat Mesenteric Circulation. *Journal of Cardiovascular Pharmacology*, *28*(5), 703–711. <https://doi.org/10.1097/00005344-199611000-00014>
- Shiota, M., & Printz, R. L. (2012). Diabetes in Zucker Diabetic Fatty Rat. In H.-G. Joost, H. Al-Hasani, & A. Schürmann (Eds.), *Animal Models in Diabetes Research* (Vol. 25, Issue 4, pp. 103–123). Humana Press. https://doi.org/10.1007/978-1-62703-068-7_8
- Siehler, S. (2009). Regulation of RhoGEF proteins by G 12/13-coupled receptors. *British Journal of Pharmacology*, *158*(1), 41–49. <https://doi.org/10.1111/j.1476-5381.2009.00121.x>
- Smeda, J. S., & McGuire, J. J. (2007). Effects of poststroke losartan versus captopril treatment on myogenic and endothelial function in the cerebrovasculature of SHRsp. *Stroke*, *38*(5), 1590–1596. <https://doi.org/10.1161/STROKEAHA.106.475087>
- Sobey, C. G., Moffatt, J. D., & Cocks, T. M. (1999). Evidence for selective effects of chronic hypertension on cerebral artery vasodilatation to protease-activated receptor-2 activation. *Stroke*, *30*(9), 1933–1941. <https://doi.org/10.1161/01.STR.30.9.1933>

- Soltis, E. E. (1987). Effect of age on blood pressure and membrane-dependent vascular responses in the rat. *Circulation Research*, *61*(6), 889–897. <https://doi.org/10.1161/01.RES.61.6.889>
- Sontheimer, D. L. (2006). Peripheral vascular disease: Diagnosis and treatment. *American Family Physician*, *73*(11), 1971–1976. <https://doi.org/10.1097/00000441-194001000-00027>
- Sowers, J. R. (2013). Diabetes mellitus and vascular disease. *Hypertension*, *61*(5), 943–947. <https://doi.org/10.1161/HYPERTENSIONAHA.111.00612>
- Spiekermann, S., Landmesser, U., Dikalov, S., Brecht, M., Gamez, G., Tatge, H., Reepschläger, N., Hornig, B., Drexler, H., & Harrison, D. G. (2003). Electron spin resonance characterization of vascular xanthine and NAD(P)H oxidase activity in patients with coronary artery disease: Relation to endothelium-dependent vasodilation. *Circulation*, *107*(10), 1383–1389. <https://doi.org/10.1161/01.CIR.0000056762.69302.46>
- Ständker, L., Schrader, M., Kanse, S. M., Jürgens, M., Forssmann, W.-G., & Preissner, K. T. (1997). Isolation and characterization of the circulating form of human endostatin. *FEBS Letters*, *420*(2–3), 129–133. [https://doi.org/10.1016/S0014-5793\(97\)01503-2](https://doi.org/10.1016/S0014-5793(97)01503-2)
- Stirban, A., Gawlowski, T., & Roden, M. (2014). Vascular effects of advanced glycation endproducts: Clinical effects and molecular mechanisms. *Molecular Metabolism*, *3*(2), 94–108. <https://doi.org/10.1016/j.molmet.2013.11.006>
- Suckow, M. A., Gobbett, T. A., & Peterson, R. G. (2017). Wound Healing Delay in the ZDSD Rat. *In Vivo*, *31*(1), 55–60. <https://doi.org/10.21873/invivo.11025>
- Sun, G., Zhang, G., V. Jackson, C., & Wang, Y.-X. (Jim). (2018). Zucker Diabetic Sprague Dawley (ZDSD) Rat, A Spontaneously Diabetic Rat Model Develops Cardiac Dysfunction and Compromised Cardiac Reserve. *Cardiology Research and Cardiovascular Medicine*, *3*(1). <https://doi.org/10.29011/2575-7083.000033>
- Swaminathan, A., Vemulapalli, S., Patel, M. R., & Jones, W. S. (2014). Lower extremity amputation in peripheral artery disease: Improving patient outcomes. *Vascular Health and Risk Management*, *10*, 417–424. <https://doi.org/10.2147/VHRM.S50588>
- Szerafin, T., Erdei, N., Fülöp, T., Pasztor, E. T., Édes, I., Koller, A., & Bagi, Z. (2006). Increased Cyclooxygenase-2 Expression and Prostaglandin-Mediated Dilation in Coronary Arterioles of Patients With Diabetes Mellitus. *Circulation Research*, *99*(5), 2510–2516. <https://doi.org/10.1161/01.RES.0000241051.83067.62>
- Tang, E. H. C., & Vanhoutte, P. M. (2010). Endothelial dysfunction: A strategic target in the treatment of hypertension? *Pflugers Archiv European Journal of Physiology*, *459*(6), 995–1004. <https://doi.org/10.1007/s00424-010-0786-4>

- Thiebaud, D., Jacot, E., Defronzo, R. A., Maeder, E., Jequier, E., & Felber, J.-P. (1982). The Effect of Graded Doses of Insulin on Total Glucose Uptake, Glucose Oxidation, and Glucose Storage in Man. *Diabetes*, *31*(11), 957–963. <https://doi.org/10.2337/diacare.31.11.957>
- Tischer, E., Gospodarowicz, D., Mitchell, R., Silva, M., Schilling, J., Lau, K., Crisp, T., Fiddes, J. C., & Abraham, J. A. (1989). Vascular endothelial growth factor: A new member of the platelet-derived growth factor gene family. *Biochemical and Biophysical Research Communications*, *165*(3), 1198–1206. [https://doi.org/10.1016/0006-291X\(89\)92729-0](https://doi.org/10.1016/0006-291X(89)92729-0)
- Torres, T. P., Fujimoto, Y., Donahue, E. P., Printz, R. L., Houseknecht, K. L., Treadway, J. L., & Shiota, M. (2011). Defective glycogenesis contributes toward the inability to suppress hepatic glucose production in response to hyperglycemia and hyperinsulinemia in Zucker diabetic fatty rats. *Diabetes*, *60*(9), 2225–2233. <https://doi.org/10.2337/db09-1156>
- Tosun, M., Paul, R. J., & Rapoport, R. M. (1998). Role of extracellular Ca⁺⁺ influx via L-type and non-L-type Ca⁺⁺ channels in thromboxane A₂ receptor-mediated contraction in rat aorta. *The Journal of Pharmacology and Experimental Therapeutics*, *284*(3), 921–928. <http://www.ncbi.nlm.nih.gov/pubmed/9495850>
- Tousoulis, D., Kampoli, A.-M., Tentolouris Nikolaos Papageorgiou, C., & Stefanadis, C. (2011). The Role of Nitric Oxide on Endothelial Function. *Current Vascular Pharmacology*, *10*(1), 4–18. <https://doi.org/10.2174/157016112798829760>
- Triggle, C. R., Samuel, S. M., Ravishankar, S., Marei, I., Arunachalam, G., & Ding, H. (2012). The endothelium: influencing vascular smooth muscle in many ways. *Canadian Journal of Physiology and Pharmacology*, *90*(6), 713–738. <https://doi.org/10.1139/y2012-073>
- Trottier, G., Hollenberg, M., Wang, X., Gui, Y., Loutzenhiser, K., & Loutzenhiser, R. (2002). PAR-2 elicits afferent arteriolar vasodilation by NO-dependent and NO-independent actions. *American Journal of Physiology - Renal Physiology*, *282*(5), F891–F897. <https://doi.org/10.1152/ajprenal.00233.2001>
- Tschudi, M. R., Barton, M., Bersinger, N. A., Moreau, P., Cosentino, F., Noll, G., Malinski, T., & Lüscher, T. F. (1996). Effect of age on kinetics of nitric oxide release in rat aorta and pulmonary artery. *Journal of Clinical Investigation*, *98*(4), 899–905. <https://doi.org/10.1172/JCI118872>
- Van Der Loo, B., Labugger, R., Skepper, J. N., Bachschmid, M., Kilo, J., Powell, J. M., Palacios-Callender, M., Erusalimsky, J. D., Quaschnig, T., Malinski, T., Gygi, D., Ullrich, V., & Lüscher, T. F. (2000). Enhanced peroxynitrite formation is associated with vascular aging. *Journal of Experimental Medicine*, *192*(12), 1731–1743. <https://doi.org/10.1084/jem.192.12.1731>
- Vanhoutte, P. M., Feletou, M., & Taddei, S. (2005). Endothelium-dependent contractions

- in hypertension. *British Journal of Pharmacology*, *144*(4), 449–458.
<https://doi.org/10.1038/sj.bjp.0706042>
- Versari, D., Daghini, E., Viridis, A., Ghiadoni, L., & Taddei, S. (2009). Endothelial Dysfunction as a Target for Prevention of Cardiovascular Disease. *Diabetes Care*, *32*(suppl_2), S314–S321. <https://doi.org/10.2337/dc09-S330>
- Vessières, E., Belin de Chantemèle, E. J., Toutain, B., Guihot, A.-L., Jardel, A., Loufrani, L., & Henrion, D. (2010). Cyclooxygenase-2 Inhibition Restored Endothelium-Mediated Relaxation in Old Obese Zucker Rat Mesenteric Arteries. *Frontiers in Physiology*, *1*(November), 1–10. <https://doi.org/10.3389/fphys.2010.00145>
- Viridis, A., Colucci, R., Fornai, M., Duranti, E., Giannarelli, C., Bernardini, N., Segnani, C., Ippolito, C., Antonioli, L., Blandizzi, C., Taddei, S., Salvetti, A., & Del Tacca, M. (2007). Cyclooxygenase-1 Is Involved in Endothelial Dysfunction of Mesenteric Small Arteries From Angiotensin II-Infused Mice. *Hypertension*, *49*(3), 679–686. <https://doi.org/10.1161/01.HYP.0000253085.56217.11>
- Vlassara, H. (1997). Recent Progress in Advanced Glycation End Products and Diabetic Complications. *Diabetes*, *46*(Supplement_2), S19–S25. <https://doi.org/10.2337/diab.46.2.S19>
- Wagenknecht, L. E., Zaccaro, D., Espeland, M. A., Karter, A. J., O’Leary, D. H., & Haffner, S. M. (2003). Diabetes and Progression of Carotid Atherosclerosis. *Arteriosclerosis, Thrombosis, and Vascular Biology*, *23*(6), 1035–1041. <https://doi.org/10.1161/01.ATV.0000072273.67342.6D>
- Warram, J. H. (1990). Slow Glucose Removal Rate and Hyperinsulinemia Precede the Development of Type II Diabetes in the Offspring of Diabetic Parents. *Annals of Internal Medicine*, *113*(12), 909. <https://doi.org/10.7326/0003-4819-113-12-909>
- Watanabe, T., Barker, T. A., & Berk, B. C. (2005). Angiotensin II and the endothelium: Diverse signals and effects. *Hypertension*, *45*(2), 163–169. <https://doi.org/10.1161/01.HYP.0000153321.13792.b9>
- White, C. R., Darley-Usmar, V., Berrington, W. R., McAdams, M., Gore, J. Z., Thompson, J. A., Parks, D. A., Tarpey, M. M., & Freeman, B. A. (1996). Circulating plasma xanthine oxidase contributes to vascular dysfunction in hypercholesterolemic rabbits. *Proceedings of the National Academy of Sciences of the United States of America*, *93*(16), 8745–8749. <https://doi.org/10.1073/pnas.93.16.8745>
- Wilson, D. P., Susnjar, M., Kiss, E., Sutherland, C., & Walsh, M. P. (2005). Thromboxane A₂-induced contraction of rat caudal arterial smooth muscle involves activation of Ca²⁺ entry and Ca²⁺ sensitization: Rho-associated kinase-mediated phosphorylation of MYPT1 at Thr-855, but not Thr-697. *Biochemical Journal*, *389*(3), 763–774. <https://doi.org/10.1042/BJ20050237>
- Wong, C. M., Yao, X., Au, C. L., Tsang, S. Y., Fung, K. P., Laher, I., Vanhoutte, P. M.,

- & Huang, Y. (2006). Raloxifene prevents endothelial dysfunction in aging ovariectomized female rats. *Vascular Pharmacology*, *44*(5), 290–298. <https://doi.org/10.1016/j.vph.2005.12.005>
- Woodman, C. R., Price, E. M., & Laughlin, M. H. (2002). Aging induces muscle-specific impairment of endothelium-dependent dilation in skeletal muscle feed arteries. *Journal of Applied Physiology*, *93*(5), 1685–1690. <https://doi.org/10.1152/jappphysiol.00461.2002>
- World Health Organization. (2021). *Cardiovascular diseases*. [https://www.who.int/en/news-room/fact-sheets/detail/cardiovascular-diseases-\(cvds\)](https://www.who.int/en/news-room/fact-sheets/detail/cardiovascular-diseases-(cvds))
- Wright, W. S., & Harris, N. R. (2008). Ozagrel attenuates early streptozotocin-induced constriction of arterioles in the mouse retina. *Experimental Eye Research*, *86*(3), 528–536. <https://doi.org/10.1016/j.exer.2007.12.012>
- Xu, B., Ji, Y., Yao, K., Cao, Y.-X., & Ferro, A. (2005). Inhibition of human endothelial cell nitric oxide synthesis by advanced glycation end-products but not glucose: relevance to diabetes. *Clinical Science*, *109*(5), 439–446. <https://doi.org/10.1042/CS20050183>
- Yang, Y. M., Huang, A., Kaley, G., & Sun, D. (2009). eNOS uncoupling and endothelial dysfunction in aged vessels. *American Journal of Physiology - Heart and Circulatory Physiology*, *297*(5), 1829–1836. <https://doi.org/10.1152/ajpheart.00230.2009>
- Yue, L., Bian, J.-T., Grizelj, I., Cavka, A., Phillips, S. A., Makino, A., & Mazzone, T. (2012). Apolipoprotein E Enhances Endothelial-NO Production by Modulating Caveolin 1 Interaction With Endothelial NO Synthase. *Hypertension*, *60*(4), 1040–1046. <https://doi.org/10.1161/HYPERTENSIONAHA.112.196667>
- Zhao, B., Cai, J., & Boulton, M. (2004). Expression of placenta growth factor is regulated by both VEGF and hyperglycaemia via VEGFR-2. *Microvascular Research*, *68*(3), 239–246. <https://doi.org/10.1016/j.mvr.2004.07.004>
- Zhao, P., Metcalf, M., & Bunnett, N. W. (2014). Biased Signaling of Protease-Activated Receptors. *Frontiers in Endocrinology*, *5*(MAY), 1–16. <https://doi.org/10.3389/fendo.2014.00067>
- Zhou, E., Qing, D., & Li, J. (2010). Age-associated endothelial dysfunction in rat mesenteric arteries: Roles of calcium-activated K⁺ channels (Kca). *Physiological Research*, *59*(4), 499–508. <https://doi.org/10.33549/physiolres.931761>

Appendices

Appendix A Targets from Endothelial Cell Biology (SAB Target List) R384

Actb	Hif1a	Tnf
Bax	Il7	Gapdh
Ccl5	Mmp2	Il11
Edn2	Pf4	Itgb3
Fgf2	Sele	Npr1
Il1b	Thbd	Plg
Kdr	Vwf	Sod1
Ocln	RQ2	Tnfsf10
Ptgis	Angpt1	Hprt1
Tek	Casp1	
Tymp	Cxcl1	
gDNA	F3	
Adam17	Hmox1	
Bcl2	Itga5	
Cdh5	Mmp9	
Ednra	Pgf	
Fn1	Sell	
Il3	Thbs1	
Kit	Xdh	
Pdgfra	RT	
Ptgs2	Anxa5	
Tfpi	Casp3	
Vcam1	Cxcl2	
PCR	Fas	
Agt	Hsp90ab1	
Bcl2l1	Itgav	
Col18a1	Nos3	
Eng	Plat	
Gusb	Selp	
Il6	Timp1	
Mmp1a	Tbp	
Pecam1	Apoe	
Ptk2	Cav1	
Tgfb1	Cxcr5	
Vegfa	Faslg	
RQ1	Icam1	
Agtr1b	Itgb1	
Calca	Nppb	
Cx3cl1	Plau	
F2r	Serpine1	

Appendix B Animal use protocol



PI :	McGuire, John
Protocol #	2019-071
Status :	Approved (w/o Stipulation)
Approved :	10/01/2019
Expires :	10/01/2023
Title :	Microvascular function in diabetic rats

Table of Contents

- [Animal Use Protocol Overview](#)
- [Funding Source List](#)
- [Purpose of Animal Use](#)
- [Hazardous Materials](#)
- [Animal Movement Outside of Animal Facilities](#)
- [Animal Groups and Experimental Timelines Overview](#)
- [Rat](#)
 - [Tissue Collection](#)
 - [Justification for Choice of Species](#)
 - [the 3Rs: Replace, Reduce, Refine](#)
 - [Species Strains](#)
 - [Animal Transfers](#)
 - [Environmental Enrichment](#)
 - [Animal Holding/Housing and Use Location Information](#)
 - [Animal Holding within Extra Vivarium Spaces \(EVSs\)](#)
 - [Acclimatization Period & Quarantine](#)
 - [Veterinary Drugs](#)
 - [SOP List](#)
 - [Procedures Checklist for Reporting and Training](#)
 - [Procedures Narrative](#)
 - [Procedural Consequences & Monitoring](#)
 - [Endpoint Method Information](#)
 - [Animal Numbers Requested](#)
- [Personnel List](#)
- [Protocol Attachments](#)
- [Amendment Reason](#)

Protocol Introduction

The questions on this page activate specific sections within the AUP form.

Note that species selection is part of this introductory page

Does this AUP involve teaching?

Yes No

Is the animal work on this project shared by another Animal Care Committee?

Yes No

Will you be using hazards?

Yes No

Will live animals be moved outside of their housing facility?

Yes No

Will field studies be conducted?

Yes No

Add/Update/Remove Species Used on this Protocol

Species	Agents	Drugs	Restraint	Breeding
Rat	No	Yes	No	No

Animal Use Protocol Overview

Curriculum Vitae

Name:

Andrea Wang, BMSc

Citizenship:

Canadian

Education:

Masters of Science, Medical Biophysics, University of Western Ontario, 2019-present
Supervisor: Dr. John McGuire

Bachelor of Medical Science, Honours Specialization in Pathology, University of Western Ontario, 2015-2019

Research experience:

Graduate Student Research Assistant, University of Western Ontario, 2019-2021
Supervisor: Dr. John McGuire

Fourth year thesis student, University of Western Ontario, 2018-2019

Project: Identifying Wrong Blood in Tube in Hematology and Chemistry Samples
Using the Delta HMR on Sysmex XN Analyzer

Supervisor(s): Dr. Ian Chin-Yee, Dr. Vipin Bhayana, Dr. Michael Knauer

Undergraduate student researcher, London Health Sciences Centre, 2016-2018

Supervisor(s): Dr. Jacob McGee

Teaching experience:

Graduate Teaching Assistant, Department of Medical Biophysics

MEDBIO 3501A, Biophysics of Transport Systems (2020)

MEDBIO 4700B, Case Studies in Medical Biophysics (2020, 2021)

Graduate student activities

Graduate Student Association member, Department of Medical Biophysics, 2019-2021

Council on Reforming Equity, Diversity, and Inclusion for Grads & Postdocs, Schulich School of Medicine and Dentistry, 2020-2021

Professional society membership:

Diabetes Canada (2019-2020)

Academic Honors:

Western Research Graduate Scholarship, \$5000 per year (2019-2021)

In-Course Scholarship, Faculty of Science, \$700, one-time award (2016)

PUBLICATIONS

Abstracts

Andrea Wang, Graham Fraser, John McGuire. The effects of ageing on endothelium function in isolated hindlimb arteries from Sprague Dawley rats. *Pharmacology 2020*, selected for oral presentation (British Pharmacology Society, DOI: 10.1111/bph.15316).

Manuscript in Review

Andrea Wang, Joselia Carlos, Graham Fraser, and John McGuire. Zucker Diabetic Sprague Dawley rat (ZDSD): type 2 diabetes translational research model. EP-REV-2020-089947.

Poster and Oral Presentation

Andrea Wang, Graham Fraser, John McGuire. The effects of ageing on endothelium function in isolated hindlimb arteries from Sprague Dawley rats. London Health Research Day, 2021.

Andrea Nienthu Wang, Jason Arnold, Michael Knauer, Vipin Bhayana, Gary Lam, Ian Chin-Yee. Identifying Wrong Blood in Tube in Hematology Samples Using the Sysmex XN Analyzer. International Society for Laboratory Hematology 2020 (ISLH), selected for oral presentation.